ABSTRACT

Title of Dissertation:	AQUEOUS PHOTOCHEMISTRY OF 1,4-BENZOQUINONES AND THEIR POSSIBLE ROLE IN THE PHOTOCHEMISTRY OF NATURAL ORGANIC MATTER
	Daqing Gan, Doctor of Philosophy, 2005
Dissertation Directed By:	Professor Neil V. Blough Department of Chemistry and Biochemistry

Past research implicated the presence of an organic species as a photochemical source of OH radical in natural waters. Quinones were postulated to be one of the possible OH sources due to 1) the ubiquitous occurence of quinonoid compounds in natural systems, and 2) prior work indicating that OH was produced in the photolysis of benzoquinones. However, more recent work indicated that photolysis of 1,4-benzoquinones does not give rise to OH, but instead proceeds through an oxidizing intermediate.

To further examine these two possibilities, radical trapping experiments, electron paramagnetic resonance measurements, product analysis of the reactions of benzoic acid, and optical studies were performed for a series of quinones with differing substituents.

OH was shown not to be a major product in the photolysis of methyl-1,4-benzoquinone in aqueous solution. Instead, an oxidizing intermediate arising from, but distinct from the triplet quinone was implicated in the photolysis of low

concentrations of mBQ. This intermediate is believed to be a triplet quinone-H_2O exciplex. In the absence of electron donors, the intermediate collapses to benzene-1,2,4-triol, ultimately to form hydroquinone and hydroxybenzoquinone. At high concentrations of mBQ, however, these products are formed through a reaction of triplet quinone with ground state quinone. A complete kinetic scheme consistent with experimental results is presented.

The formation of an intermediate exciplex between triplet state quinone and water was consistent with the results obtained in the photolysis of aqueous solutions of dimethyl- and dichloro-1,4-benzoquinones. Leakage of small amounts of OH from this intermediate was observed for dichloro-1,4-benzoquinones, which are much better electron acceptors than dimethyl-1,4-benzoquinones. In the case of tetrachloro-1,4-benzoquinone, which is an extremely good electron acceptor, a substantial amount of OH was produced.

The investigation of isolated natural organic matter (Suwannee River fulvic acid) revealed that either OH radical or a strong oxidant was produced upon UV irradiation. Several natural waters collected from Atlantic Ocean and Chesapeake Bay were studied. In these waters, nitrite and nitrate photolysis appears to be significant source of OH.

AQUEOUS PHOTOCHEMISTRY OF 1,4-BENZOQUINONES AND THEIR
POSSIBLE ROLE IN THE PHOTOCHEMISTRY OF NATURAL ORGANIC
MATTER

By

Daqing Gan

Dissertation submitted to the Faculty of the Graduate School of the
University of Maryland, College Park, in partial fulfillment
of the requirements for the degree of
Doctor of Philosophy
2005

Advisory Committee:
Professor Neil V. Blough, Chair/Advisor
Professor George R. Helz
Professor Daniel E. Falvey
Professor Alice C. Mignerey
Professor Robert Walker
Professor Elisabeth Gantt

Acknowledgements

I would like to thank my advisor, Professor Neil V. Blough for his guidance, patience, encouragement, and support through my graduate career. From him, I have learned not only science and knowledge, but also methods of thinking, patience, and many other things needed for future academic advancement. His kindness, consideration, and help are greatly appreciated.

Thanks to my committee Professor Daniel E. Falvey, Professor Robert Walker, Professor George R. Helz, Professor Alice C. Mignerey, and Professor Elisabeth Gantt for their assistance and guidance.

Thanks to members of Blough group (Rossana, Trudy, Matt, Nixon, Yu, Marjon, Pramila, and Qing) for their friendship and help.

I thank my family for their love and support. This Ph. D is as much as theirs as it is mine. Thank you, mother and father, your love and encouragement are my driving forces. Thank you, my brother and sister, thank you for your love and help. To my wife, thank you for supporting me these years. Thank you for letting me concentrate on my research and study.

I owe everything to my daughter Mary. I did not have time to play with her these five years and she is now five and half years old. Thank you, Mary, thank you for your understanding.

Table of Contents

List of Table

List of Scheme

List of Figures

List of Abbreviations

3ap	3-amino-2,2,5,5-tetramethyl-1-pyrrolidinyloxy
BA	benzoic acid
BQ	1,4-benzoquinone
$BQ^{\bullet-}$	1,4-benzoqiuinone semiquinone anion radical
CDOM	colored dissolved organic matters
$\bullet CH_3$	methyl radical
$2,5\text{-}Cl_2BQ$	2,5-dichloro-1,4-benzoquinone
$2,6\text{-}Cl_2BQ$	2,6-dichloro-1,4-benzoquinone
Cl_4BQ	tetrachloro-1,4-benzoquinone
3-CP	3-carbamoyl-proxyl free radical
DMPO	5,5-dimethyl-1-pyrroline-N-oxide
DMPO-OH	DMPO spin adduct
DMSO	dimethyl sulfoxide
$[DMSO]_{1/2}$	DMSO concentration at half saturation
DOM	dissolved organic matters
E_A	electron affinity
EDTA	ethylenediaminetetraacetic acid
Eox	oxidation potential
EPR	electron paramagnetic resonance
Ered	reduction potential

E_T	triplet energy
EtOH	ethanol
ε	Extinction coefficient
ΔG	free energy change
ΔG_{eT}	free energy change of electron transfer reaction
HPLC	high performance liquid chromatography
IHSS	International Humic Substance Society
IP	ionization potential
k_F	triplet formation rate
k_f	intermediate formation rate
k_T	triplet decay rate
LFP	laser flash photolysis
LMCT	ligand to metal charge transfer
MeCN	acetonitrile
MeOH	methanol
$2,5\text{-Me}_2\text{BQ}$	2,5-dimethyl-1,4-benzoquinone
$2,6\text{-Me}_2\text{BQ}$	2,6-dimethyl-1,4-benzoquinone
MS	mass spectrometer
NMR	nuclear magnetic resonance
NOM	natural organic matter
OH	hydroxyl radical
OX	oxidizing intermediate
2-OH-BA	2-hydroxy-benzoic acid

3-OH-BA	3-hydroxy-benzoic acid
4-OH-BA	4-hydroxy-benzoic acid
$Ph(OH)_3$	1,2,4-benzene-triol
$Q^{\bullet-}$	semiquinone anion radical
QH_2	hydroquinone
$^1Q^*$	excited singlet state quinone
$^3Q^*$	excited triplet state quinone
Q-OH	hydroxylated quinone
ROS	reactive oxygen species
SRFA	Suwannee River fulvic acid
τ_T	triplet lifetime
UV	ultraviolet radiation

Chapter I   Introduction

Aqueous Quinone Photochemistry

Quinones are found widely in both biological and environmental systems. Possible quinone sources in environment may be through degradation of lignin or microbial organic matter. Polyphenols synthesized by microorganisms are another possible source of quinone moieties, especially in environments in which there is little vascular plant input (Stevenson 1994). The existence of quinones in natural organic matter (NOM) in environment has been indicated by nuclear magnetic resonance (NMR) (Thorn et al. 1992) and electron paramagnetic resonance (EPR) studies (Senesi and Steelink 1989). It was also reported that quinones within humic substances acted as electron acceptors and mediated microbial Fe (III) – reduction (Lovley et al. 1996; Scott et al. 1998). In biological systems, quinones play a basic role as electron carriers in electron transport chains in both photosynthetic and respiratory processes (Patai, S. 1974).

Prior work suggested that hydroxyl radical (OH) could be photochemically produced in low yield upon UV irradiation of dissolved organic matter (DOM) in natural waters (Mopper and Zhou 1990; Vaughan and Blough 1998). However, the nature of the organic species responsible for this production has yet to be identified. Based on the previous work of Ononye and Bolton (Ononye and Bolton 1986) and Alegría et al. (Alegría et al. 1997; Alegría et al. 1999), who reported that the photolysis of quinones in aqueous solution produced OH radicals, it was postulated

1

that quinone moieties within the dissolved organic matter might be responsible for this production.

Considering that the OH radical is a highly reactive species, the photochemical production of OH by quinones in biological and environmental systems could have a significant impact. Further, as quinoid moieties have been implicated as important components of dissolved organic matter in aquatic systems, an understanding of their aqueous photochemistry represents an important potential step in revealing the photochemical reactivity of dissolved organic matter in natural waters. This thesis thus addresses the aqueous photochemistry of 1,4-benzoquinones and their possible role in the photochemistry of natural organic matter.

The UV spectra of 1,4-benzoquinones in aqueous solution have three absorption bands corresponding to $\pi \rightarrow \pi^*$, $\pi \rightarrow \pi^*$, and $n \rightarrow \pi^*$ transitions (**Figure I –1**). The wavelengths of these transitions depend on the solvent and substitution on the quinone ring. Upon UV irradiation, ground state quinone molecules are first excited to a singlet state. Following relaxation to the lowest excited singlet state, most quinones undergo rapid intersystem crossing to the excited triplet state (Turro 1991; Marquardt et al. 1992). Due to the high intersystem crossing efficiency, it is generally accepted that quinone photochemistry originates from triplet state. The formation of triplet state quinone was reported to be less than 20 ps (Lewis et al 2000). Although the singlet – triplet transition is spin forbidden, strong spin-orbit coupling facilitates the intersystem crossing with an efficiency close to unity (Turro 1991).
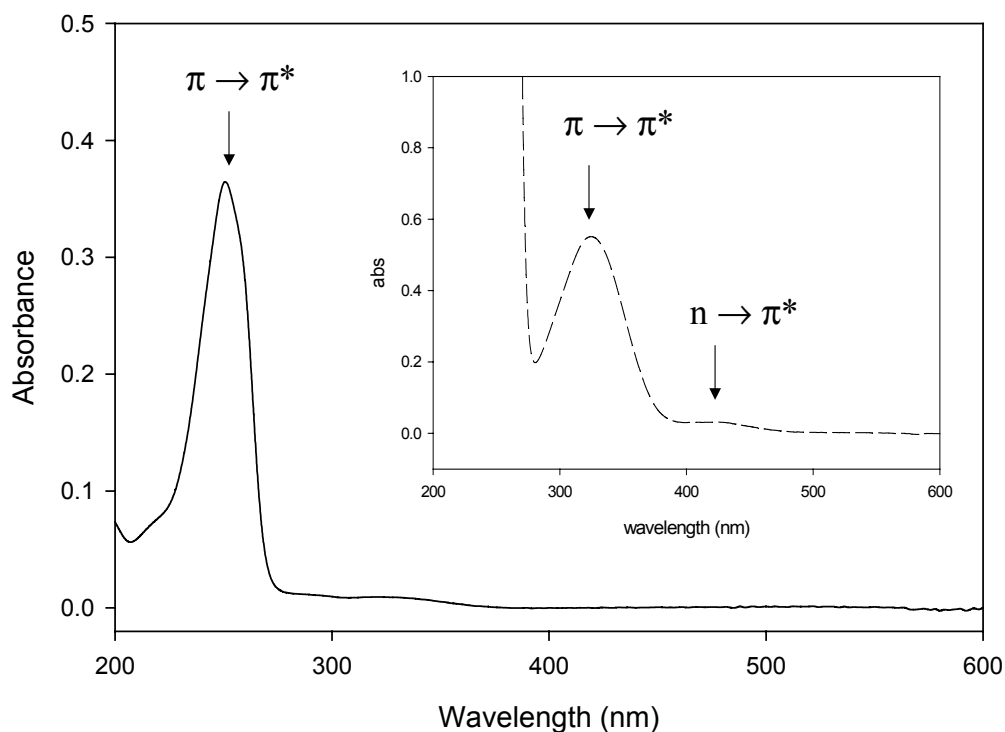
Figure I - 1. Electronic transitions and corresponding absorption wavelengths of 2-methyl-1,4-benzoquinone in aqueous solution.

Products of the photolysis of 1,4-benzoquinones in aqueous solution have previously been identified by a number of means such as spectrophotometric and chromatographic methods and include the semiquinone, benzene-1,2,4-triol $(Ph(OH)_3)$, hydroquinone, and hydroxylated quinone **(Scheme I-1)** (Leighton and Forbes 1929; Poupe 1947; Joschek and Miller 1966; Kurien and Robins 1970; Bishop and Tong 1965).
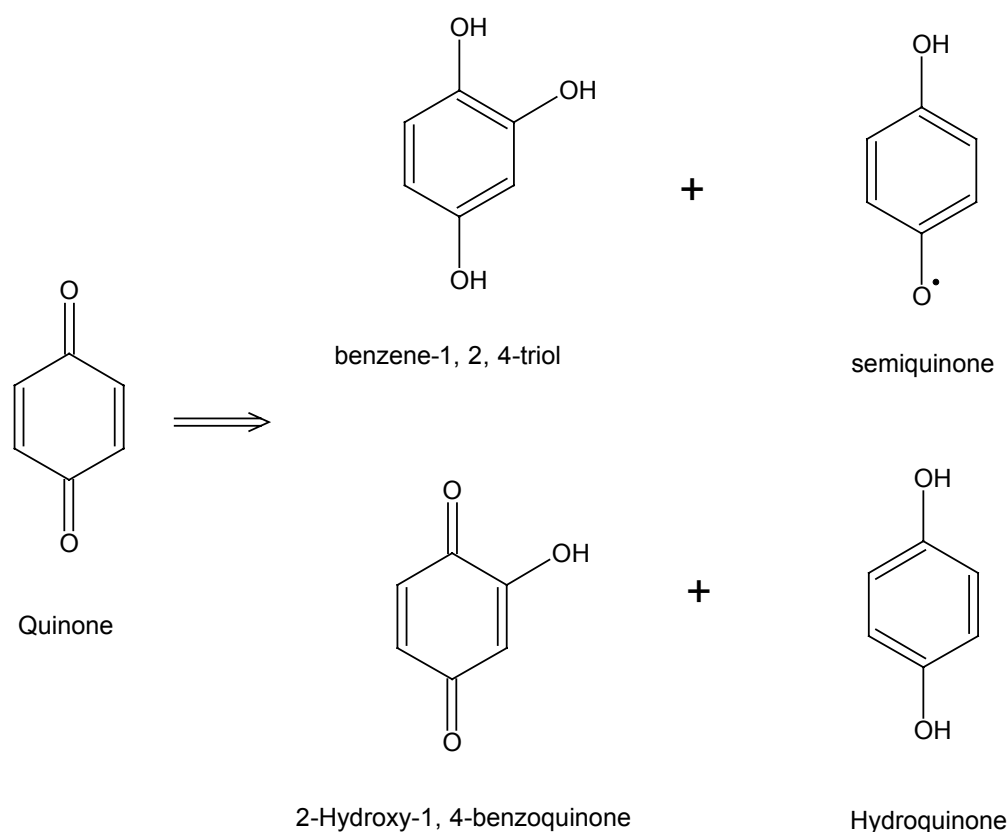
Scheme I - 1.   Quinone and quinone photoproducts

The hydroquinone of 1,4-benzoquinone is stable in acidic and neutral solutions but can be oxidized by O_2 to regenerate the quinone in basic solution (Kurien and Robins, 1970). The hydroquinone has an absorption maxima at ~ 290 nm which overlaps that of benzene-1,2,4-triol and causes difficulty in spectral identification. Benzene-1,2,4-triol reacts rapidly with dioxygen to form 2-hydroxy-1,4-benzoquinone. Benzene-1,2,4-triol can also be oxidized by quinone to form the

hydroquinone and hydroxylated quinone in equal amounts (Kurien and Robins, 1970). 2-hydroxy-1,4-benzoquinone is acidic (pKa = 4.2) and at low pH exhibits two absorption bands at 256 nm and 380 nm. Upon deprotonation, the 380 nm band shifts to 480 nm, and this shift may be used to identify this species (Schuchmann et al., 1998).

Although the final photoproducts of aqueous 1,4-benzoquinone photolysis have been identified as the hydroquinone and hydroxylated quinone under both aerobic and anaerobic conditions, the mechanism(s) that leads to the formation of these products is still a matter of debate. In principle, there are four distinct mechanisms that could produce these same products. These mechanisms are named as the OH, direct triplet, intermediate, and quinone-quinone or electron transfer (at high Q concentrations) mechanisms.

In the OH mechanism (**Scheme I -2**), the triplet quinone abstracts an H atom from water, resulting in the formation of an OH radical and semiquinone radical. The OH radical can then react with quinone to form the hydroxylated quinone (Schuchmann et al., 1998). Two semiquinone molecules disproportionate to form hydroquinone and quinone.
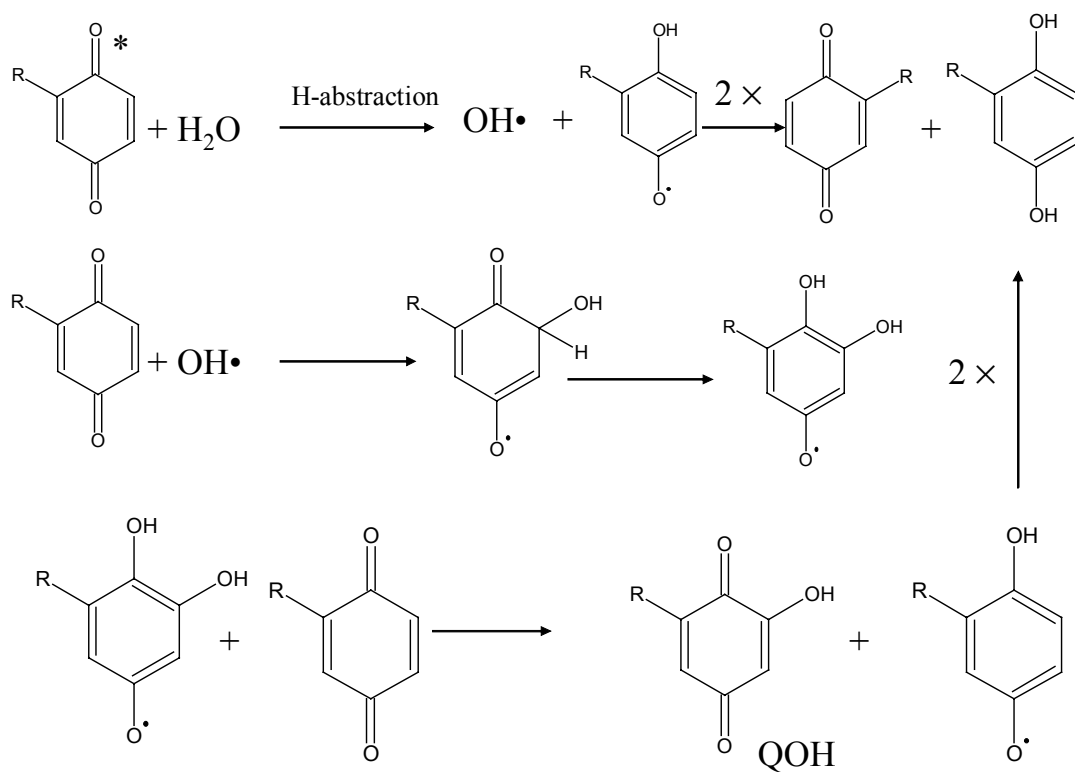
Scheme I - 2.   OH mechanism

(Ononye and Bolton, 1986; Alegría et al*.,* 1997)

In the direct triplet mechanism (**Scheme I -3**), triplet quinone reacts with water to form benzene-1,2,4-triol directly through a polar mechanism, which then rearranges to form the final products. (Shirai 1975; von Sonntag et al 2004; Gorner 2003)
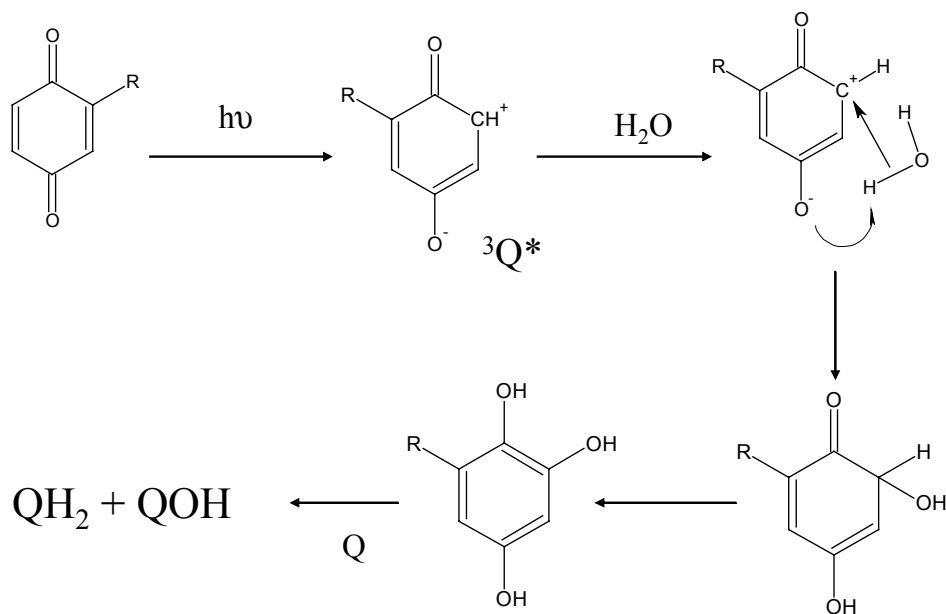
Scheme I - 3.   Direct triplet mechanism

(Shirai 1975)

In the intermediate mechanism (**Scheme I -4**), an intermediate with a finite lifetime is produced through reaction of triplet quinone with water. The lifetime, structure, and reactivity of this intermediate, proposed to be an exciplex, appears distinct from that of triplet quinone ($^3Q^*$). (Pochon et al. 2002).
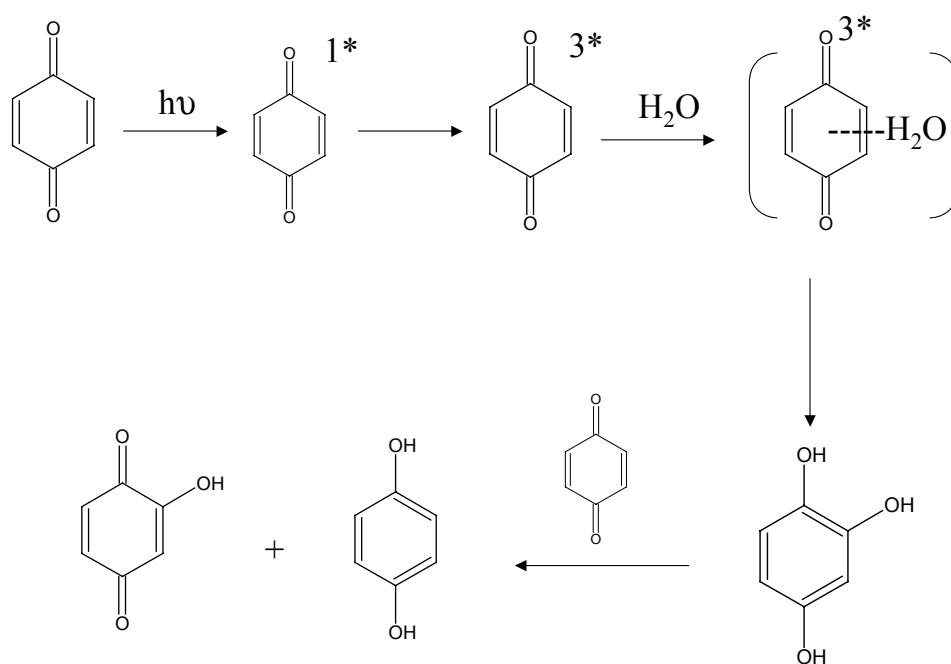
Scheme I - 4.   Intermediate mechanism

At high concentrations of quinone, an electron transfer mechanism, in which $^3Q^*$ oxidizes Q by one electron transfer, has been proposed by a number of workers (Gorner 2003; von Sonntag et al. 2004) (**Scheme I-5**).

$$^3Q^* \xrightarrow{+\,Q} \left[\; Q^{+\bullet}Q^{\bullet-} \quad \leftrightarrow \quad {}^3Q^*Q \; \right]$$

(b)

H_2O $-H^+$

(a) $+ H_2O$

QH$_2$ QOH
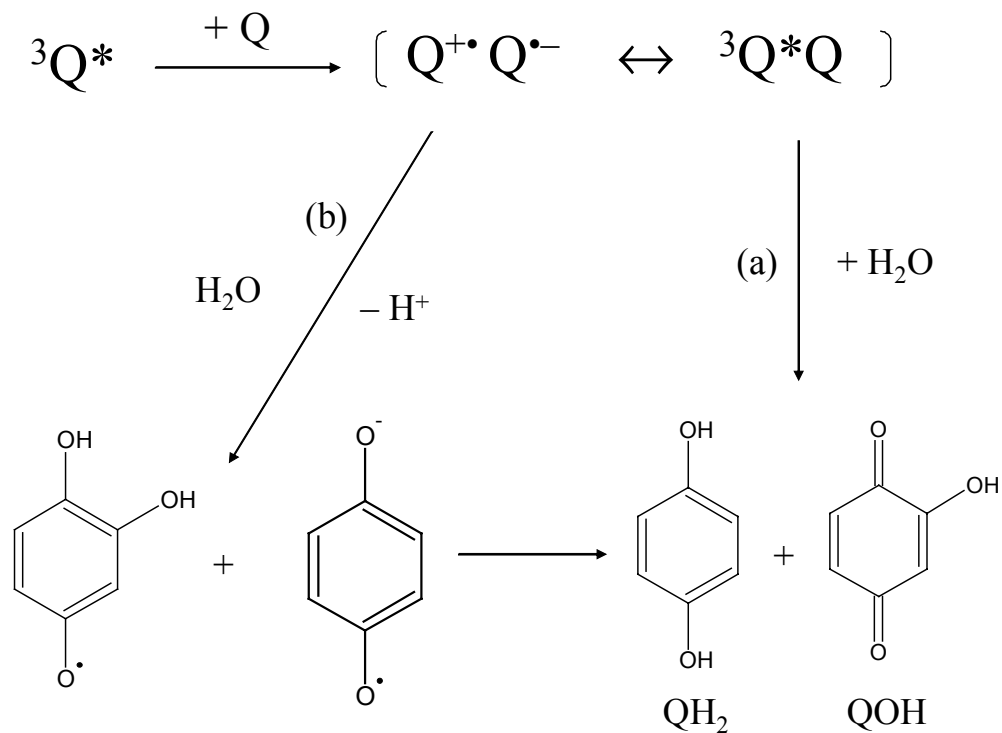
Scheme I - 5.   Quinone-Quinone or electron transfer mechanism

(Gorner 2003)

Because the final products are identical, product analysis cannot be used to differentiate these reaction mechanisms; the most obvious way to distinguish the mechanisms is to test for the presence of a reaction intermediates, either OH radical or another strong oxidant distinct from the excited triplet. If there is no OH or other strong oxidant detected in the system, then the preferred mechanism is the direct reaction of the triplet with water to form the products directly.

Because OH radical is extremely reactive, the steady state concentration of this species is far below the detection limit of electron paramagnetic resonance (EPR) spectroscopy (10^{-6} ~10^{-7} M) and optical spectroscopy. Instead, spin trapping combined with EPR detection and product analysis has been the most widely used method for indirect detection of reactive radicals such as OH [Weil et al. 1994]. In this method, a spin trap such as 5,5-dimethyl-1-pyrroline N-oxide (DMPO) (**Figure I-2**) reacts with OH to form a persistent paramagnetic spin adduct (DMPO-OH) that can be detected by EPR. DMPO is a diamagnetic species and has no spin. However, when OH radical reacts with DMPO, DMPO + OH $\rightarrow$ DMPO-OH, the product DMPO-OH has four-line EPR signal (**Figure I –2**) (Buettner 1987; Janzen and Haire 1990).

Ononye et al (Ononye et al 1986; Ononye and Bolton 1986) used DMPO to investigate the photochemistry of 1,4-benzoquinone in aqueous solutions**.** Based on the detection of the four-line DMPO-OH EPR signal, combined with a competition experiment employing formate at single concentration, they concluded that OH was produced in the photolysis of 1,4-benzoquinone aqueous solution. It was proposed

that excited triplet quinone abstracted an H atom from water to produce a hydroxyl radical and a semiquinone radical QH• (or anion radical Q•⁻ depending on the pH).

Alegría and co-workers further used DMPO spin trap method to investigate water-soluble quinones and concluded that 1,4-benzoquinone and 2-methyl-1,4-benzoquinone were able to oxidize water with the consequent production of OH radical, whereas 9,10-anthraquinone-1,5-disulfonate was not (Alegría et al. 1997; Alegría et al. 1999).

OH• +   5,5-Dimethyl-1-pyrroline N-oxide
(DMPO)   →   DMPO-OH

DMPO-OH EPR
spectrum

15 G
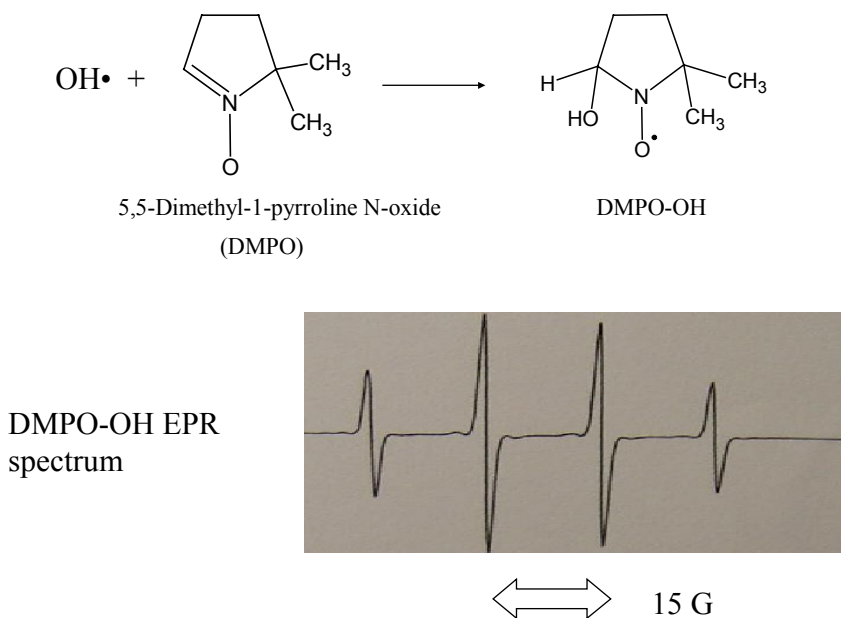
Figure I - 2.   The reaction of OH radical with DMPO spin trap and the formation of DMPO-OH spin adduct.

However, the DMPO-OH spin adduct can be easily produced from sources other than OH radical. Under aerobic condition, the superoxide radical can add to DMPO and subsequently decompose to generate DMPO-OH (Pou et al 1989). Oxidation of DMPO by excited state quinone could also lead to the formation of DMPO-OH even under anaerobic condition as shown in **Scheme I – 6** (Eberson and Persson 1997; von Sonntag 2004). The observation of DMPO-OH EPR signal, therefore, does not provide unequivocal evidence of the production of OH in aqueous quinone solutions, but does suggest the presence of a relatively strong oxidant, either the excited triplet or another oxidizing species.
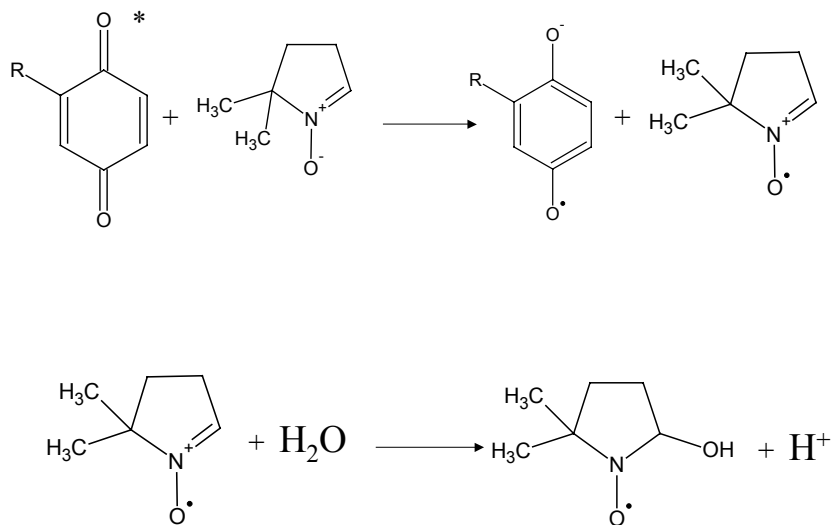
Scheme I - 6.   The oxidation of DMPO by excited quinone and the production of DMPO-OH.

Recently, the OH mechanism was questioned by Pochon et al. (2002) based on experiments employing laser flash photolysis and a new radical trapping technique illustrating in Scheme I-7.
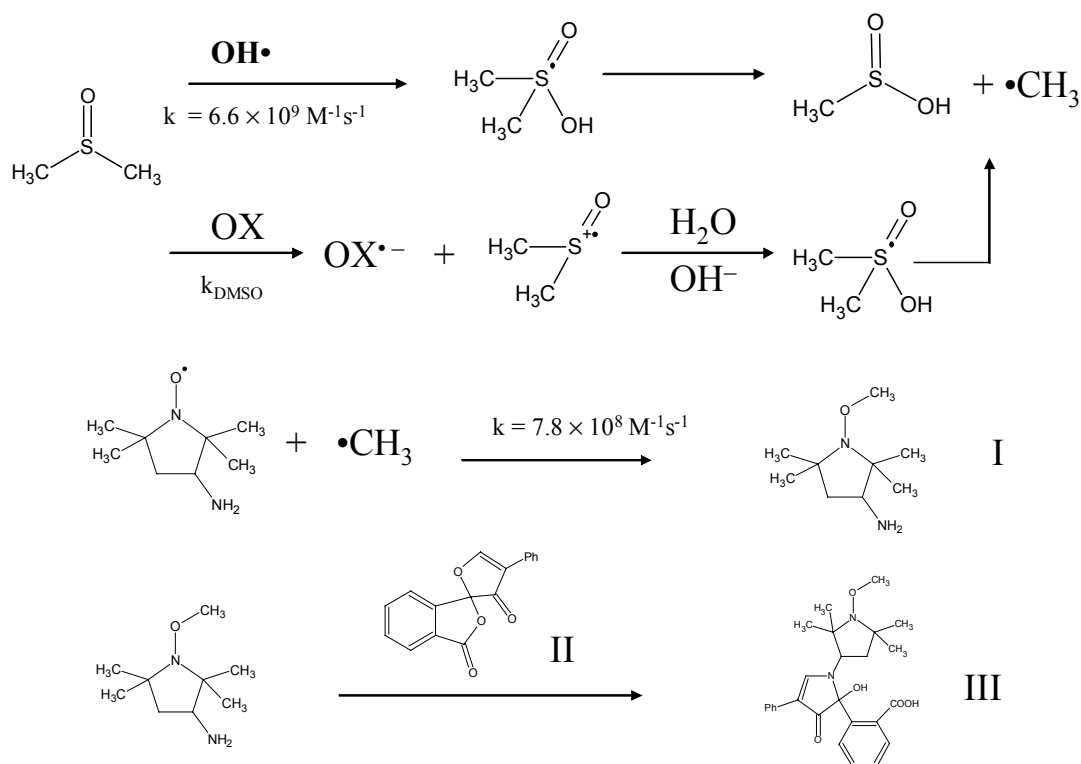
Scheme I - 7. The radical trapping method using 3ap and DMSO

As shown in **Scheme I-7**, the hydroxyl radical or other strong oxidant (OX) can react with DMSO to create a methyl radical, which is then trapped by a stable nitroxide radical 3-amino-2,2,5,5-tetramethyl-1-pyrrolidinyloxy (3ap) to form a methyl adduct (I). The methyl adduct can be converted to a highly fluorescent product III by derivatization with fluorescamine II (Kieber and Blough 1990). III is then separated from other components by reversed-phase HPLC and detected

fluorimetrically. The identity of III was previously established by low and high-resolution mass spectrometery (EI). (Li et al 1997; Johnson et al 1996; Kieber et al 1992)

This radical trapping method can be readily applied to the quinone system (**Scheme I-8**). Following excitation to the singlet state and subsequent intersystem crossing to the triplet state, the excited triplet quinone, being a relatively strong oxidant, could react directly with the DMSO. Alternatively, the triplet quinone could react with water to form either an OH radical or a exciplex, which could also act as a strongly oxidizing intermediate. Reaction of DMSO with OH or an oxidizing intermediate will generate the CH_3 radical, which then could be trapped by 3ap, and subsequently analyzed as described above.

$$Q \xrightarrow{\text{h}\upsilon} {}^1Q^* \xrightarrow{\text{k}_F} {}^3Q^* \xrightarrow[\text{k}_f]{+\text{H}_2\text{O}} \begin{array}{c} \text{OH}\bullet \text{ or} \\ \text{intermediate} \end{array} \longrightarrow QH_2 + Q\text{-}OH$$
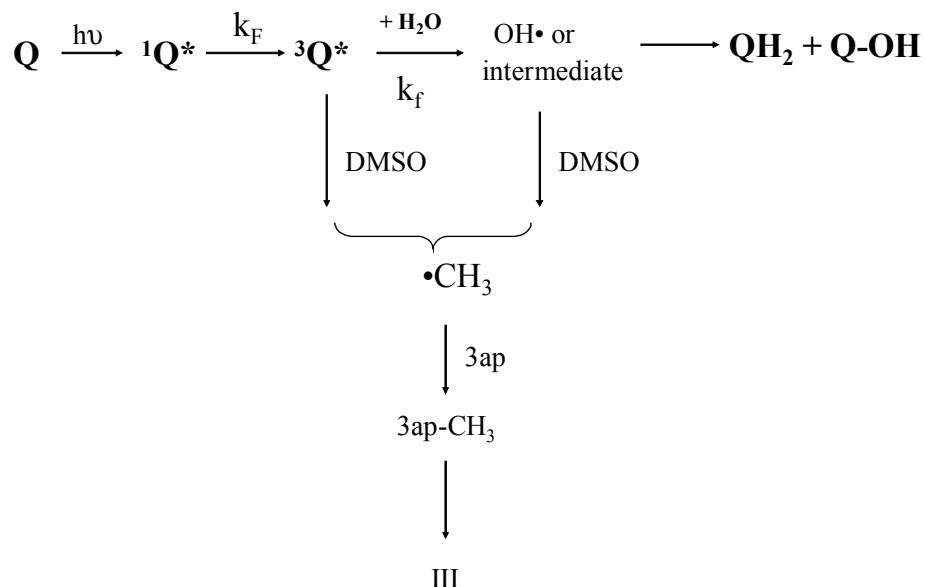
Scheme I - 8. The application of the radical trapping method to detect intermediates produced by quinone photolysis

Although both the OH radical and strong oxidants could produce the same fluorescent product (III), the reaction rate constant between the oxidant, OX, and DMSO is expected to differ from that between OH and DMSO.

To distinguish the OH mechanism from the intermediate mechanism, Pochon et al (2002) employed this technique and showed that the reaction rate constant between DMSO and the species generated in mBQ photolysis was about 2 orders of magnitude lower than the reported rate constant for the reaction of free OH with DMSO (6.6×10^9 M^{-1} s^{-1}), thus indicating that OH radical was not a major product of

the 2-methyl-1,4-benzoquinone photolysis in aqueous solution. The production of III, however, indicated the presence of a strong oxidant, either the $^3Q^*$ or another strong oxidant, as a photolysis intermediate in aqueous mBQ solution. A series of competition experiments employing nitrite, formate, and salicylate showed non-competitive inhibition of III formation, indicating the presence of an intermediate distinct from the triplet.

Based on these results as well as additional results from laser flash photolysis, Pochon et al. concluded that OH was not produced as a major product of 2-methyl-1,4-benzoquinone photolysis in aqueous solution, but instead, an oxidizing intermediate distinct from the triplet, was responsible for hydroxylation or oxidation of DMSO.

Three possible intermediate structures were proposed in Pochon et al. (2002), but, the semiquinone and OH π-complex structure (2) (**Scheme I–9)** was preferred based on the capability of hydroxyl group transferring and the detection of semiquinone radical anion from laser flash photolysis experiment.
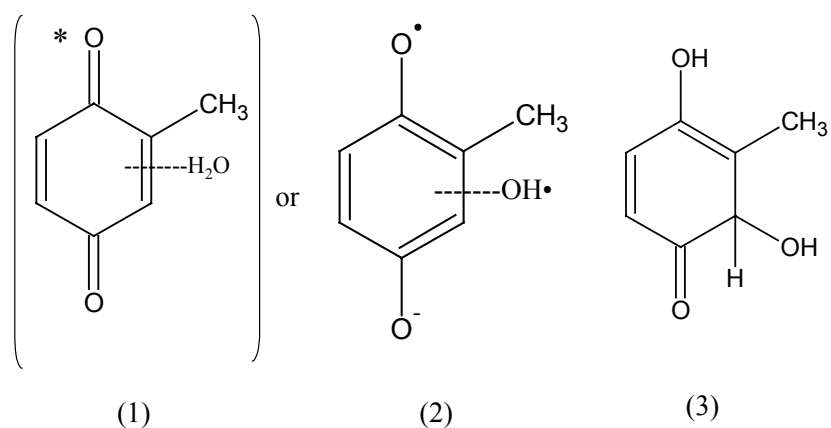
Scheme I - 9. The three possible intermediate structures proposed by Pochon et al. (2002)

While agreeing with Pochon et al (2002) that the OH radical was not a major product and that DMSO reacted with an oxidant to produce radicals in the photolysis of aqueous solutions of 1,4-benzoquinones, Gorner disputed the existence of an oxidizing intermediate distinct from the triplet quinone (Gorner 2003). Instead, Gorner claimed that the triplet state and semiquinone radicals were spectroscopically and kinetically distinct. He excluded the presence of an oxidizing intermediate based on the absence of spectroscopic evidence for an intermediate other than the triplet. Further, based on previous work that suggested chloride anion quenched the triplet by a purely physical mechanism (Loeff et al 1983 A; Loeff et al 1983 B; Loeff et al

1992; Loeff et al 1993), Gorner examined the relationship between the quinone decomposition quantum yield (Φ_d) and the concentration of chloride anion. Due to the agreement between experimental and theoretical half-chloride concentrations ($[Cl]_{1/2}$), which were calculated based on the assumption of purely physical quenching of the triplet, a direct triplet mechanism was concluded for the photolysis of 1,4-benzoquinone in aqueous solution. The implication from Gorner's work was that DMSO reacted directly with the triplet quinone.

In contrast to both Pochon et al (2002) and Gorner (2003), however, von Sonntag et al.(2004) claimed that there was no chemical reaction between DMSO and any intermediate produced in the photolysis of aqueous 1,4-benzoquinone solutions. DMSO was proposed to act as a purely physical quencher to the triplet quinone with a rate constant of $2.7 \times 10^9 \text{ M}^{-1} \text{ s}^{-1}$.

The dependence of triplet lifetime on the concentrations of quinone was examined by both Gorner and von Sonntag et al. At low concentrations of quinones, both Gorner (2003) and von Sonntag et al (2004) suggested a direct triplet mechanism, which includes a charge separation in the lowest triplet state followed by the water addition and formation of benzene-1,2,4 –triol (**Scheme I-3**). This water – mediated triplet reaction was reported to involve no radicals based on low semiquinone radical yield at pH 5 – 9.

At elevated quinone concentration, the triplet quinone was thought to react with ground state quinone to form a charge separated state ($Q^{\bullet+}Q^{\bullet-}$) followed by reaction with water to form hydroquinone and hydroxylated quinone. The charge

separation state ($Q^{\bullet+}Q^{\bullet-}$) could form the final photoproducts via non –free radical (a) and free radical (b) pathways as shown in **Scheme I – 5**.

Because only a very low yield of semiquinone radical was detected by laser flash photolysis a non-free radical pathway was proposed by Gorner for the photolysis of BQs in aqueous solution at both low and high concentrations. Overall, a direct triplet mechanism in which triplet reacts with water (at low Q concentration) and excited quinone -ground quinone mechanism (at high concentrations of quinone), were concluded for the photolysis of benzoquinones in aqueous solution (Gorner, 2003).

In contrast to Gorner's non – radical mechanism for the photolysis of BQ at high quinone concentrations in aqueous solutions, von Sonntag et al. (2004) proposed a free radical pathway (**Scheme I –11**) to account for the increase in free radical yields with increasing quinone concentration. It was claimed that the monomer – dimer equilibrium followed by electron – transfer within the dimer triplet could account for the formation of radical $Q^{\bullet-}$ and $Q^{\bullet+}$ as illustrated in **Scheme I – 11**.
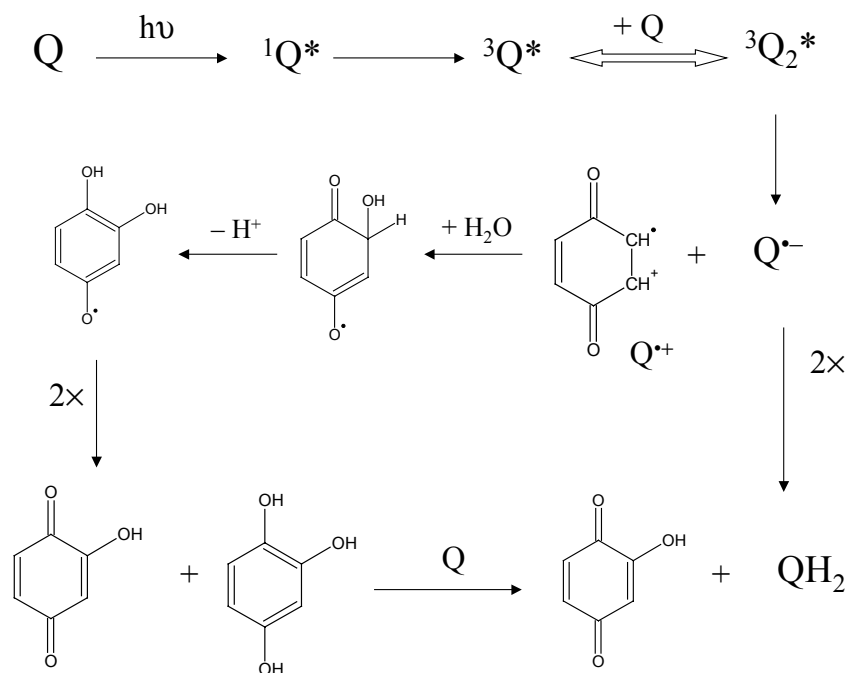
Scheme I - 10. The free-radical mechanism for the photolysis of quinones at high concentrations

von Sonntag et al also disputed that a π-complex of strongly oxidizing radical such as OH with a strongly reducing radical such as $\bullet QH/Q^{\bullet-}$, which was proposed by Pochon et al. (2002) as the oxidizing intermediate, would exist because it would immediately collapse either by electron transfer or by recombination. Instead of the semiquinone – OH intermediate mechanism, a polar mechanism modified from Shirai et al (Shirai 1975) with the production of benzene-1,2,4-triol and its precursor

(**Q(H$_2$O)**) (**Scheme I – 11**), which was identical to one of the structures proposed by Pochon et al. (2002) was presented at low concentrations of BQ.

Mechanism proposed by von Sonntag et al
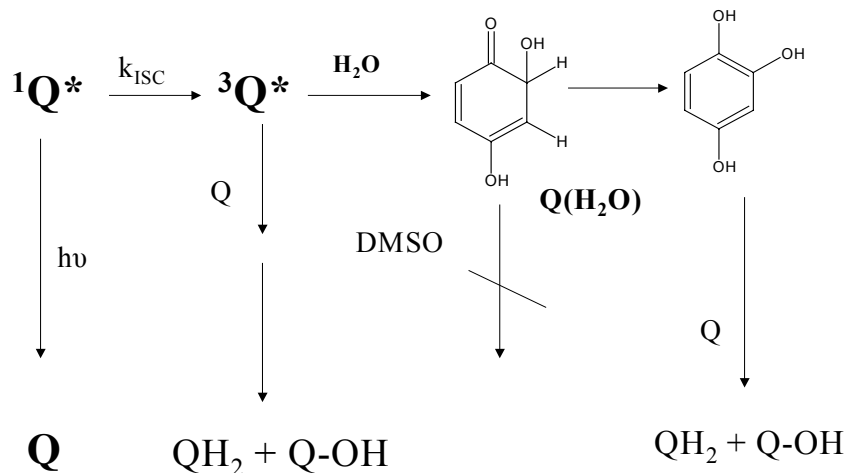
Scheme I - 11. The mechanism of BQ photolysis proposed by von Sonntag et al.

It is evident from previous research that a number of questions concerning quinone photolysis are still unclear. First, although there is strong evidence that 1,4-benzoquinone and 2-methyl-1,4-benzoquinone do not produce OH, it remains uncertain whether OH could be a major product in the photolysis of other 1,4-bezoquinones in aqueous solutions. Second, does DMSO react with an intermediate produced in the photolysis of quinone solution? Third, if so, is this intermediate the

excited triplet state or a species derived from the triplet? Fourth, does the mechanism of quinone photolysis change with quinone concentration?

The purpose of this research was therefore to clarify the mechanisms of aqueous quinone photochemistrys, as well as the possible role of quinones in the photochemistry of organic matter in natural waters.

In Chapter II, a variety of techniques are employed including radical trapping, optical studies, and EPR measurements to examine these questions for 2-methyl-1,4-benzoquinone (mBQ). These results established that 1) OH is not a major product; 2) DMSO reacts with an intermediate generated in the photolysis of aqueous solution of mBQ; 3) this intermediate arises from the excited triplet state, but is distinct from this species; 4) the mechanism of quinone photolysis changes with quinone concentration. A general photochemical mechanism for the photolysis of mBQ in aqueous solution is presented.

The photochemistry of a series of 1,4-benzoquinones including dimethyl-, dichloro-, and tetrachloro-substituted 1,4-benzoquinones was investigated with the techniques developed in Chapter II. A non-OH mechanism, similar to that of mBQ, is suggested for the dimethyl- and dichloro-1,4-benzoquinones. A OH mechanism is proposed for the photolysis of tetrachloro-1,4-benzoquinone in aqueous solution.

A study of the photochemistry of Suwannee River fulvic acid (SRFA) and natural waters is then presented in Chapter IV. The reason for this study is that OH was reported to be produced from the photolysis of natural organic matter (Mopper and Zhou 1990). However, based on the quinone photochemistry study, the previously reported OH might be an oxidizing intermediate instead of OH. To clarify

this possibility, an isolated organic source (SRFA) is first studied and the results are compared with those of natural waters. Based on the results obtained from radical trapping experiments employing DMSO, organic matter in SRFA does produce a strong oxidant. The identity of this strong oxidant is not known for certain. However, based on the quinone photochemistry study, this strong oxidant may not be OH.

A strong oxidizing intermediate is also observed in the photolysis of natural waters. Because of the agreement in OH production between nitrite and natural water photolysis, the intermediate produced in the photolysis of natural waters is believed to be OH, resulting from nitrite and nitrate photolysis.

Chapter II   Method Establishment and Results for 2-Methyl-1,4-Benzoquinone

Introduction

In this chapter, a detailed mechanistic investigation was conducted for the photolysis of mBQ in aqueous solution with emphasis on answering the questions posed in Chapter I. Optical and EPR measurements, and radical trapping methods were employed in this work. Chloride was employed in radical trapping experiments in the presence of DMSO to distinguish the nature of the oxidizing intermediate. Additional probes were used to test for the production of OH in quinone photolysis. The influence of quinone concentration on the photolysis mechanism was investigated independently by radical trapping and EPR measurements.

Radical Trapping Experiments with DMSO and CH_4

As shown in Chapter I, the radical trapping method employing DMSO was applied to detect the production of OH radical or other oxidizing intermediates during the photolysis of 1,4-benzoquinones. However, radical trapping with DMSO is not specific for the OH radical. To further test for the presence of OH, the production of III in the presence of CH_4 was examined. While both OH and some strong oxidants (OX) can react with DMSO, only OH is likely to react facilely with methane to generate methyl radicals (**Scheme II −1**). Thus the detection of III in the presence of DMSO could indicate that either a strong oxidant or OH is generated in the system. The detection of III in the presence of CH_4, however, is almost certainly from OH.

$$CH_4 \xrightarrow[k = 1.2 \times 10^8 \text{ M}^{-1}\text{s}^{-1}]{\text{OH•}} H_2O + \text{•}CH_3$$
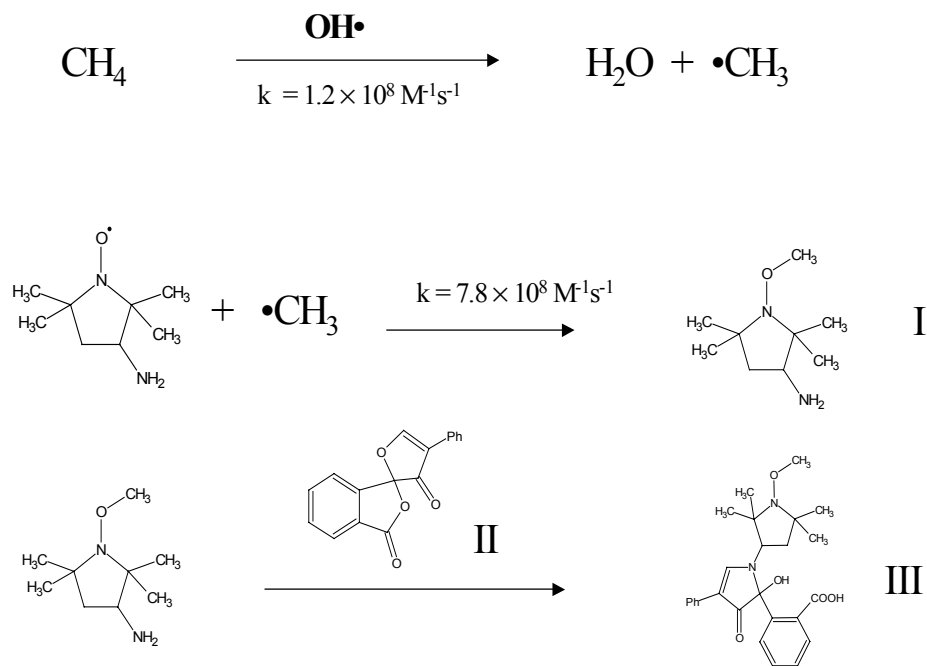
Scheme II - 1.   The radical trapping with 3ap in the presence of CH_4

Kinetics is another important way to differentiate the identity of a reactive intermediate. As indicated in equations II-1 and II-2, DMSO or methane can be employed in these trapping experiments in the presence of competitors with known rate constants k_C for the reaction with OH.

$$\xrightarrow{k_f} OX + DMSO \xrightarrow{k_{DMSO}} CH_3 \text{•} + 3ap \rightarrow I + II \rightarrow III \qquad (II\text{-}1)$$

$$+ CH_4 \quad \xrightarrow{k_{CH4}} \quad CH_3 \bullet + 3ap \; \rightarrow \; I \; + \; II \; \rightarrow \; III$$

$$+ Competitor \; \xrightarrow{k_C} \; Other \; products \qquad\qquad (II\text{-}2)$$
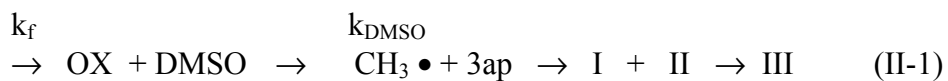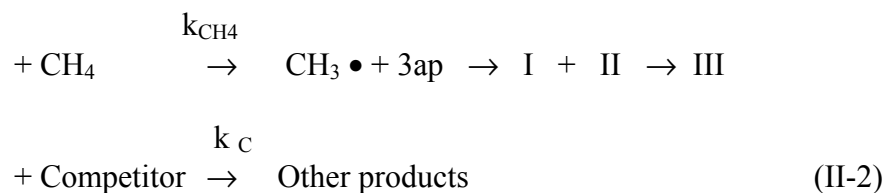
where, OX represents either free OH or another oxidizing species. The initial

formation rate of III (P_{DMSO}) is determined by equation II-3, where C represents the

sum of all compounds that can compete with DMSO for OH or a strong oxidant.

$$P_{DMSO} = \cfrac{k_f k_{DMSO}\,[DMSO]}{k_{DMSO}\,[DMSO] + \Sigma\, k_{Ci}[C]_i} \qquad\qquad (II\text{-}3)$$

According to equation II-3, a hyperbolic dependence of the initial production

rate of III on the DMSO concentration is predicted. At very high [DMSO],

$k_{DMSO}[DMSO] \gg k_C[C]$, P_{DMSO} reaches its maximum value $^{max}P_{DMSO}$. At half

saturation value where $P_{DMSO} = 1/2 \; ^{max}P_{DMSO}$, the concentration of DMSO is defined

as $[DMSO]_{1/2}$.

The experimental value of $^{EX}[DMSO]_{1/2}$ can be obtained from the plot of

P_{DMSO} versus [DMSO] and compared with theoretical value predicted for OH on the

basis of known rate constants for reaction with this species (equation II-4).

$$[DMSO]_{1/2} = \Sigma k_{Ci}[C]_i \,/\, k_{DMSO} \qquad\qquad (II\text{-}4)$$

If the experimentally measured $[DMSO]_{1/2}$ is consistent with theoretical value,

the intermediate is likely OH. On the other hand, if the experimental $[DMSO]_{1/2}$ value

is significantly different from the theoretical value, an intermediate other than OH

would then be implied.

A linear relationship (equation II –5) between the initial production rate of III and DMSO concentrations can be obtained by taking the reciprocal of equation II – 3.

$$1/P_{DMSO} = 1/k_f + (\sum k_{Ci}[C]_i /k_f k_{DMSO}) / [DMSO] \qquad (II-5)$$

with the slope (S) and intercept (In) of the reciprocal plot given by

$$S = \sum k_{Ci}[C]_i /k_f k_{DMSO} \qquad (II-6)$$

$$In = 1/k_f \qquad (II-7)$$

The reaction rate constant of this species with DMSO, k_{DMSO}, can be obtained from double-reciprocal plots of the experimental data and compared with literature values to characterize the intermediate oxidant.

Under the same experimental conditions, the initial rate of III production in the CH4 experiment (P_{CH4}) can be compared with that of DMSO experiment (P_{DMSO}). If OH is the major product, then $R = P_{DMSO}/ P_{CH4}$ should be close to theoretical value predicted for OH. Assuming that 3ap and quinone are the only other OH sinks, $R = P_{DMSO}/ P_{CH4}$ can be calculated using equation II-8.

$$R= P_{DMSO}/ P_{CH4} = 1 + \{k_{3ap}[3ap]+k_Q[Q]\}/ k_{CH4}[CH_4] \qquad (II-8)$$

where k_{3ap}, k_Q, and k_{CH4} are reaction rate constants between OH radical and 3ap, the quinone, and CH4, respectively [$k_{3ap} = 3 \sim 4\times10^9$ $M^{-1}s^{-1}$ (this group), $k_Q =1.2 \sim 6\times10^9$ $M^{-1}s^{-1}$ (Adams and Michael 1967; Scheuchmann et al. 1998), $k_{CH4} =1.2\times10^8$ $M^{-1}s^{-1}$ (Stevens et al. 1972)]. In a system not producing OH, P_{DMSO}/ P_{CH4} should be much greater than the theoretical value.

By this method, not only the production of III but also the loss of reactant (3ap) can be monitored. 3ap is a stable nitroxide radical and exhibits a three-line EPR

spectrum. The loss of this EPR signal can be used to quantitate total loss of 3ap, which can be compared to the extent of III production.

Benzoic Acid Product Analysis

The reaction of benzoic acid with OH radical can also be employed as a relatively specific method to detect the production of OH radicals. As shown in the **Scheme II-2**, addition of OH to benzoic acid ring gives rise to three mono-hydroxylated benzoic acid isomers.

The initial step of this reaction is a fast addition of OH radical to the aromatic ring resulting in the formation of an intermediate radical. In the presence of electron acceptors such as dioxygen, the intermediate radical will be oxidized to produce the hydroxylated benzoic acid. The ratio of these three isomers including 2-OH-BA, 3-OH-BA, and 4-OH-BA is close to 1: 1: 1 for reaction with authentic OH (Oturan and Pinson 1995).
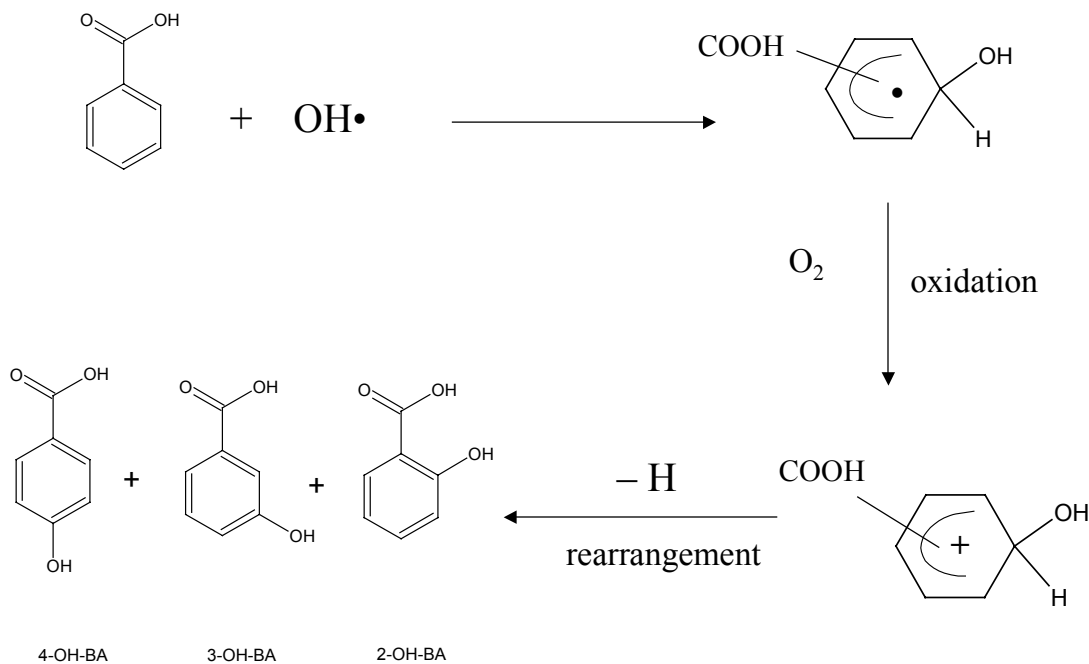
Scheme II - 2. The mechanism of OH radical addition to benzoic acid.

Analysis for these hydroxylated products provides an independent means for identifying the involvement of OH radical under aerobic conditions. 2-hydroxy-benzoic acid absorbs at 300 nm ($\varepsilon_{300} = 3.1 \times 10^3$ M^{-1} cm^{-1}) and has very strong fluorescence emission at 410 nm, and can thus be detected fluorimetrically with high sensitivity. 4-hydroxy-benzoic acid has strong absorption peak at 255 nm ($\varepsilon_{255} = 9.05 \times 10^3$ M^{-1} cm^{-1}) and 3-hydroxy-benzoic acid absorbs moderately at 300 nm ($\varepsilon_{300} = 1.88 \times 10^3$ M^{-1} cm^{-1}). The results obtained from benzoic acid product analysis can be

compared with those from nitroxide trapping employing DMSO and methane. If OH is the main product, the initial production rate of three hydroxylated benzoic acids (P_{BA}) should be comparable to the production of III (P_{DMSO}) in the presence of DMSO. However, if another oxidant is involved, yield of III should be much greater than P_{BA}. P_{BA}/P_{CH4} is also valuable in the determination of the reaction mechanism.

Employing these techniques we find that (1) OH radical is not a major product in the photolysis of 2-methyl-1,4-benzoquinone aqueous solution. Instead, an oxidant is generated that is shown to react with DMSO. This intermediate is demonstrated to be distinct from the excited triplet state quinone. Finally, photochemical mechanism is found to depend on the concentration of quinone, with the quinone-quinone mechanism dominating at high Q concentration.

Experimental Section

Materials

Salicylic acid 99+%, 3-hydroxybenzoic acid 99+%, 4-hydroxybenzoic acid 99+%, HPLC grade dimethyl sulfoxide 99% (DMSO), HPLC grade acetonitrile 99.93+%, phosphoric acid 85 wt% (99.999%), boric acid 99.999%, sodium dihydrogen phosphate 99.999%, sodium hydrogen phosphate 99.995%, sodium hydroxide 99.98%, fluorescamine (>97% TLC powder), 3-carbamoyl-proxyl free radical 97% (3-CP), activated carbon (decolorizing), KCl, $FeSO_4$, ethylenediaminetetraacetic acid (EDTA), and methyl-1,4-benzoquinone 98% (mBQ) were obtained from Aldrich. 3-amino-2,2,5,5-tetramethyl-1-pyrrolidinyloxy 99% (3ap) was obtained from Acros. Reagent grade $NaNO_3$, $NaNO_2$, HPLC grade methanol, 30% H_2O_2, 2-propanol, and chloroform were obtained from Fisher. Glacial acetic acid (99.9%) was purchased from J.T. Baker. Ultra-pure (99.99%) grade nitrogen and methane were purchased from Airgas. Methyl-1,4-benzoquinone was purified by sublimation and stored at 4°C in the dark.

A Millipore Milli-Q system provided water for all the experiments. Benzoic acid was recrystalized from water and store at room temperature in the dark.

31

Apparatus

The monochromatic irradiation system consisted of a 1000-W Hg-Xe arc lamp combined with a Spectral Energy GM 252 monochromator, which was set to a band-pass of 10 nm. The broadband irradiation system consisted of a 300 W Xe arc lamp housed in an ILC Technology R400-2 and powered by an ILC technology PS300-1 power supply. The lamp irradiance was measured with an IL-1700 radiometer. Schott WG305, WG 325, WG 355, and KV 399 long-wavelength pass filters, where the number indicates the wavelength of 50% transmission, were used for irradiation in different wavelength ranges. A 1.0-cm quartz cuvette was used for all sample irradiations and optical measurements.

A Hewlett-Packard 8452A diode array and Shimadzu 2401 UV-PC spectrophotometers were used for absorption measurements. A Bruker/IBM ER 200D-SRC EPR spectrometer was employed in all EPR measurements. Samples were drawn into 50 µL capillary tubes, which were then sealed at the top and bottom and placed in standard 3 mm i.d. quartz EPR tubes. Standard EPR instrument settings were as follows: frequency 9.7 GHz; power, 10 mW; modulation amplitude 1.0 G, and time constant 80 ms.

The EPR spectrometer was calibrated daily with a standard 3ap solution. The concentrations of 3ap were calibrated with 3-carbamoyl-proxyl (3-CP) and confirmed by UV absorbance before use. To calibrate 3ap concentration and EPR signal, a 10 mM 3-CP stock solution was prepared in water. After serial dilution, the EPR peak heights or area obtained by double integration and UV/vis absorbance of different concentrations of 3-CP were measured and a linear relationship between 3-CP

concentration and EPR signal was obtained. Based on this calibration curve, the concentration of 3ap was thus obtained. The extinction coefficient of 3ap at 236 nm was found to be $\varepsilon_{236} = 2850 \text{ M}^{-1} \text{ cm}^{-1}$, which is almost identical to that of 3-CP.

The high-performance liquid chromatograph consisted of an Eldex Model B-100-S single piston pump, E-lab gradient controller (OMS Tech, Miami, FL), a 0-5000 psi pressure gauge, a Valco Model C10W injection valve, and a RCM 8×10 cm Waters radial compression module containing a 5×100 mm Nova – PAK C_{18} 4 -μm reversed phased column. 0.5-μm filters from Upchurch were placed after the pump and before the column. A Perkin Elmer 785A UV/Vis detector and a L-7480 Hitachi fluorescence detector were connected to the Elab PC-based data collection system (OMS Tech). The loop sizes were 50 μL and 600 μL depending on the experiment. The chromatographic separations were at 27°C. A BUCHI B-481 water bath was employed to provide a constant column temperature. The flow rate was of 1 ml/min. Isocratic elution with mobile phase composition of 65% MeOH and 35% acetate buffer at pH 4.0 was used for the separation and identification of III from other components in the system. The excitation and emission wavelengths of the fluorescence detector were set to 390 nm and 490 nm, respectively.

Fluorescent detection of 2-hydroxy-benzoic acid was achieved by setting the excitation and emission wavelengths to 310 nm and 410 nm, respectively.

A Mettler AT261 Delta Range electronic balance was used for all mass measurements. An ORION model 720A pH meter was used to measure the pH of all solutions.

Experiment Protocols

Optical Measurements

An optical absorption study of 2-methyl-1,4-benzoquinone was performed in water and in 1:1 aqueous 2-propanol solutions in the presence of different substrates including DMSO, 3ap, or other competitors under aerobic and anaerobic conditions at low and high concentrations. For aerobic samples, the 1 cm cuvette was open to air during irradiation (either monochromatic or polychromatic light) and for the absorption measurements. Anaerobic samples were degassed with N_2 for 5 to 10 min and then continuously purged with N_2 during irradiation. The irradiation wavelengths were chosen from the longest detectable absorption bands generally assigned to n $\rightarrow$ π^* (430 nm) and $\pi \rightarrow \pi^*$ (320 nm) transitions.

Radical Trapping Using 3ap

Samples containing appropriate concentrations of DMSO, quinone, and 3ap, with or without other competitors, were prepared in water or phosphate buffer solutions. For anaerobic experiments, the sample was degassed with N_2 for 5 to 10 minute and then continuously purged with N_2 during irradiation. Aerobic experiments were performed with the sample cuvette open to air. Generally, the samples were irradiated with UV-vis light for a period of time during which 10% or less of quinone was reacted. After irradiation, the sample solution was mixed with an equal volume of 0.2 M pH 8.5 borate buffer. The pH of the resultant solution was above 8. To a one

ml aliquot of this solution, 200 µl of 5 mM fluorescamine in acetonitrile was added, with the sample then mixed and placed in dark for 2 or 3 min to produce III. The resultant solution was then loaded onto HPLC for separation and quantification.

In experiments where CH_4 was used in place of DMSO, the sample solution was first degassed with N_2 for 3 min and then bubbled with CH_4 for 5 min. The solubility of CH_4 in water is 1.5 mM. The derivatization procedure was the same as that in DMSO trapping experiment.

Synthesis of Fluorescent Compound III (Standard) from Fenton's Reaction

III was synthesized independently using the Fenton reaction to generate OH as described previously (Li et al 1997; Li et al. 1998). Three mM of 3ap, 5% DMSO, and 3 mM H_2O_2 were mixed in 100 mM pH 7.5 phosphate buffer. 3 mM Fe (II) – EDTA was prepared by dissolving 4 mM EDTA and 3 mM ferrous sulfate in 100 mM of pH 4.3 phosphate buffer. 2 ml Fe (II) – EDTA was then added to 2 ml of the mixed solution and the reaction was allowed to proceed in dark for 35 min. Anaerobic conditions were maintained during entire reaction course by bubbling with N_2. After reaction, the solution was derivatized as described above. III was isolated either with solid-phase or liquid extraction, following pH adjustment to 4 with dilute HCl or acetic acid.

Solid-phase extraction was performed with a Waters C_{18} Sep-Pak to enrich III. The Sep-Pak was rinsed sequentially with 30 ml of Milli-Q water, 20 ml of HPLC grade methanol, and 30 ml of Milli-Q water to activate the stationary phase. A 10-ml

aliquot of reaction mixture was then loaded onto the Sep-Pak and rinsed with 30-40 ml of Milli-Q water. A deep yellow band was observed on the Sep-Pak; this band was then eluted with a minimum volume of acetonitrile or methanol. The volume of acetonitrile or methanol was reduced by flushing with dry N_2.

The remaining yellow solid was dissolved in minimum volume of HPLC mobile phase (35% acetate buffer and 65% MeOH) and the solution was injected into the HPLC for separation. Collected directly from the column upon elution, III was extracted in 2 ml of chloroform. After evaporation of chloroform by flushing with dry N_2, a bright yellow oil remained that was subsequently stored at -20° C.

Calibration and Identification of the Fluorescent Compound

III (ε_{386} = 5225 $M^{-1}.cm^{-1}$), synthesized via the Fenton reaction as described above was used to calibrate the response of fluorescence detector. A linear range between 5 nM and 600 nM was obtained. For routine analyses, an analytical trial using III was always run to find the retention time and concentration. Co-elution with this standard was performed as a test of the identity of the product produced by quinone photolysis.

Relative Quantum Yields and 3ap Consumption Measurements

The dependence of the initial rate of III production (P_{DMSO}) on the concentration of mBQ was determined employing concentrations of mBQ ranging from 10 μM to 10 mM under anaerobic conditions and with sufficiently high concentrations of DMSO and 3ap to obtain III production that was independent of

DMSO and 3ap concentrations. The quinone solutions were prepared by serial dilution of a 20 mM stock solution of mBQ. The absorbance of quinone solutions were monitored at 420 nm and 320 nm and used for the calculation of relative quantum yields (see below). The irradiance of the lamp was kept identical or normalization was conducted to ensure quantum yield was calculated based on the identical irradiance. To normalize the irradiance in relative quantum yield calculation, the irradiance obtained from radiometer reading in different trials can be calculated with respect to the irradiance of one trial. Because the experiment was performed within one or two days, the variation in lamp output was negligible for most of the time.

The dependence of 3ap loss on mBQ concentrations was determined by EPR spectroscopy under anaerobic condition employing concentrations of mBQ ranging from 10 μM to 10 mM. The reaction was driven to completion as indicated by no further optical or EPR spectral change. The amount of 3ap loss was determined based on the 3-CP calibration and the difference between the initial and remaining 3ap EPR signal. Control experiments employing identical mBQ concentration but varying concentrations of 3ap and DMSO were performed. 3ap loss was found to be independent of DMSO concentrations over the range from 50 mM to 200 mM and 3ap concentrations over the range from 10 μM to 75 μM.

Product Analysis of the Reactions with Benzoic Acid

Benzoic acid, at concentrations ranging from 100 μM to 2 mM, was added to solutions containing 10 to 20 μM of quinone. The resultant solution was then

irradiated aerobically at the same wavelength as those for DMSO or CH_4 in the nitroxide trapping experiments. After irradiation, salicylic acid, 3-hydroxybenzoic acid, and 4-hydroxybenzoic acids were separated and identified by HPLC. Salicylic acid was detected fluorimetrically with an excitation wavelength of 305 nm and an emission wavelength of 410 nm. 3-hydroxybenzoic acid and 4-hydroxybenzoic acids were detected spectrophotometrically at 300 nm and 252 nm, respectively (Jankowski et al 1999).

The mobile phase composition for the elution of 2-OH-BA was 35 % MeOH and 65 % pH 2.0 phosphate buffer. 3-hydroxybenzoic acid and 4-hydroxybenzoic acid were eluted with a mobile phase consisting of 95% sodium acetate buffer (pH 4.0) and 5% MeOH and detected using absorbance detector at 300 nm and 252 nm, respectively.

Calibration curves were obtained for salicylic acid, 3-hydroxybenzoic acid, and 4-hydroxybenzoic acids by serial dilution of known concentration of stock solutions. The detection limit for 2-hydroxybenzoic acid was 2 nM. For 3-hydroxybenzoic acid and 4-hydroxybenzoic acids the detection limits were 2.5 µM and 0.2 µM, respectively employing 600 µL injection loop.

Results and Discussion

Does DMSO React with an Intermediate?

von Sonntag et al (2004) previously disputed the involvement of DMSO in a chemical reaction with intermediate(s) produced during photolysis of 1,4-benzoquinones (Pochon et al. 2002). In order to clarify this issue, additional studies were performed to test for the reaction of DMSO during photolysis of mBQ.

Irradiation of mBQ (< 30 µM) in the presence of 50 µM 3ap and 50 mM DMSO produced a product that increased linearly with irradiation time under conditions in which < 10% of the quinone was reacted (**Figure II-1**). This product was shown to be III by co-elution with III synthesized independently via the Fenton reaction (equation II-9) and nitrite photolysis (equations II-10 and II-11), which are authentic OH sources. This product was previously identified by both low and high-resolution mass spectrometry (**Figure II – 2**). [Johnson et al 1996; Li et al 1998]

$$[Fe(II) - EDTA\ ]^{2-} + H_2O_2 \rightarrow [Fe(III) - EDTA\ ]^{-} + OH\bullet + OH^{-} \qquad (II\text{-}9)$$

$$NO_2^- + h\upsilon \rightarrow NO + O^- \tag{II-10}$$

$$O^- + H_2O \rightarrow OH + OH^- \tag{II-11}$$
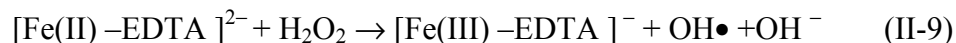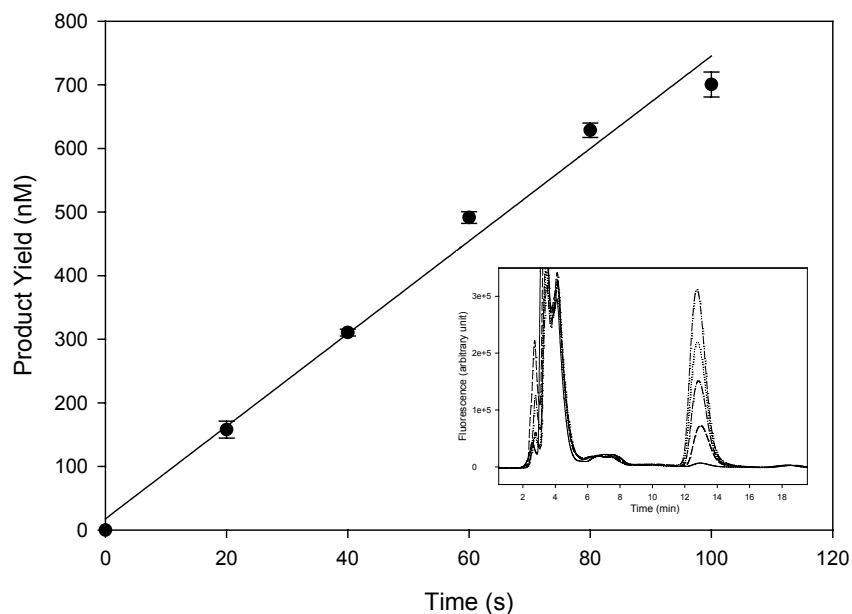
Figure II- 1.   Cumulative production of III with irradiation time for samples containing 20 µM mBQ, 50 µM 3ap, and 50 mM DMSO in aqueous solution.

Samples were irradiated at 320 nm using monochromatic light for 20 sec (– – –), 40 sec (–··–··–), 60 sec (······), 100 sec (··—··–) under anaerobic conditions

Inset: chromatogram illustrated the increase in III (13 min) with increasing irradiation time. The blank contained 20 µM mBQ + 50 µM 3ap (——) and was irradiated 100 second under the same condition. The lamp intensity was 7.1×10^{-4} W/cm^2.
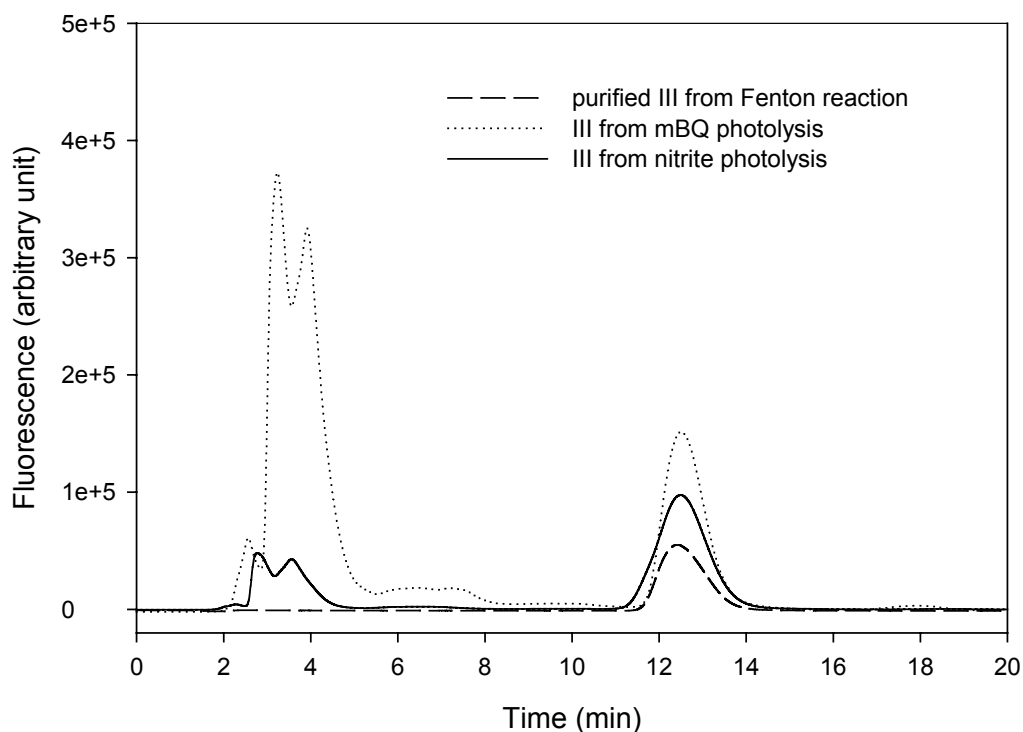
Figure II-2   Chromatogram of III obtained from mBQ photolysis, the Fenton reaction, and nitrite photolysis.

The fluorescent product III (peak at 13 min) obtained from quinone photolysis (dotted line) was separated using HPLC with Waters C18 reversed-phase column and compared with purified III synthesized via Fenton reaction (dashed line) and nitrite photolysis (solid line). The mobile phase was 65% Me OH and 35% acetate buffer at pH 4.0. The fluorescence detector was set to an excitation wavelength of 390 nm and emission wavelength of 490 nm.

For this product (III) to be formed, there must be a methyl radical source and formation of 3ap-CH$_3$ adduct (I) as shown in **Scheme I –7**. The only reasonable source of methyl radical in the reaction system is DMSO. Therefore the formation of III in radical trapping experiments employing DMSO indicated that DMSO must be involved in the reaction.

The relationship between the initial rate of III formation (P_{DMSO}) and DMSO concentration was examined. At constant concentrations of quinone and 3ap, P_{DMSO} increased with increasing concentrations of DMSO until the maximum value $^{max}P_{DMSO}$ was reached, consistent with DMSO reacting with an intermediate produced during quinone photolysis.
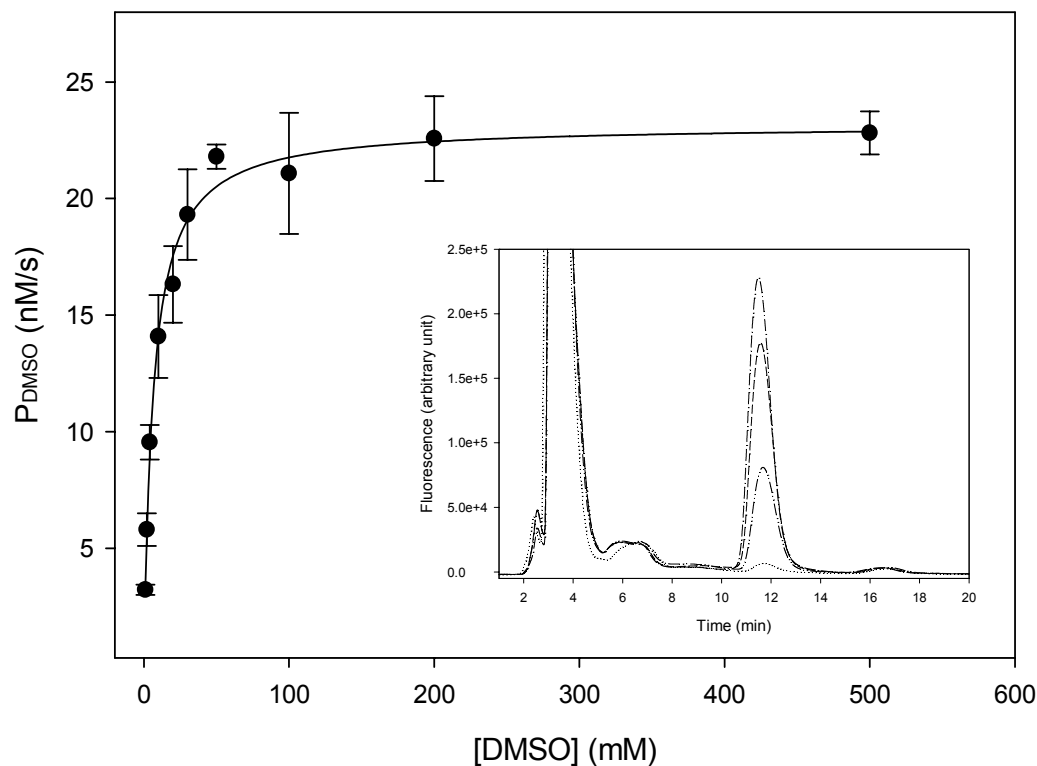
Figure II- 3. The initial rate of III production (P_{DMSO}) on the concentration of DMSO in initial rate period.

20 μM mBQ + 50 μM 3ap + DMSO was irradiated at 320 nm for 1 min under anaerobic conditions. The lamp intensity was 6.0×10^{-4} W/cm^2. Inset: Peak at 11.8 min was the fluorescent product (III). Blank 20 μM mBQ + 50 μM 3ap ($\cdots$), 20 μM mBQ + 50 μM 3ap + 5 mM DMSO (–··–··), 20 μM mBQ + 50 μM 3ap + 20 mM DMSO (– – –), 20 μM mBQ + 50 μM 3ap + 50 mM DMSO (–·–·–·).

The nitroxide (3ap) used in this method is a stable radical and has a characteristic three-line EPR signal. Thus EPR can also be employed to monitor the spin loss of 3ap. 3ap spin loss was only observed in the presence of both mBQ and DMSO (**Figure II-4**). No appreciable 3ap spin loss was observed when samples containing only mBQ or DMSO with 3ap were irradiated. However, when 3ap was

irradiated in the presence of both DMSO and mBQ, 3ap spin loss was observed at different concentrations of mBQ and 3ap over the entire course of reaction. It is worth noting that the relative 3ap consumption ratio (reacted 3ap/[mBQ]) decreased with increasing concentrations of mBQ, although the absolute 3ap consumption increased with increasing mBQ concentration over the range from 10 μM to 5 mM (see below).

The spin loss of 3ap in the presence of mBQ and DMSO was consistent with chromatographic results. The product yield of III as determined chromatographically was proportional to 3ap spin loss as determined by EPR measurement (**Figure II-5**). The cumulative III production yield detected by HPLC and the reacted 3ap as measured by EPR showed a linear relationship with a slope of 0.77.

As there was no chromatographic evidence for the formation of other products and further, as 3-ap spin levels did not increase upon addition of 3 μM Cu^{2+} under aerobic conditions following irradiation (through hydroxylamine oxidation), it is likely that 3-ap is quantitatively converted to III, and that the discrepancy in slop (0.77 versus 1.0) is due to a systematic bias in LC calibration.
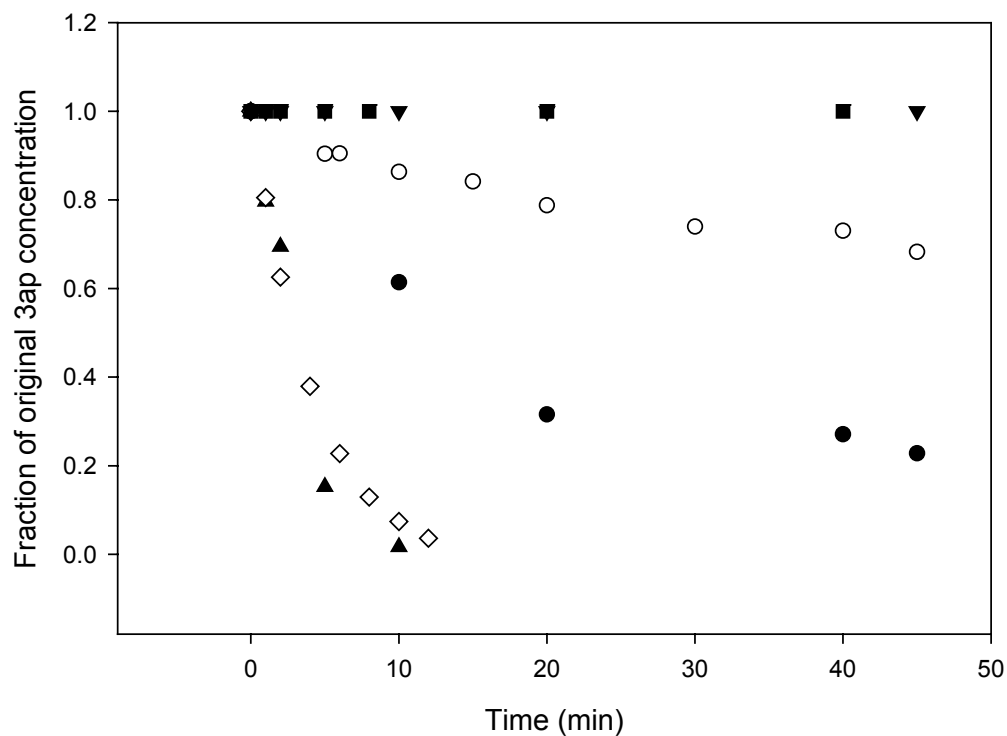
Figure II- 4.   Loss of 3ap with irradiation time as determined by EPR.

Samples containing 20 µM mBQ + 50 µM 3ap (▼), 50 µM 3ap + 50 mM DMSO (■), 20 µM mBQ + 50 µM 3ap + 50 mM DMSO (○), 500 µM mBQ + 100 µM 3ap + 50 mM DMSO (●), and 500 µM mBQ + 50 µM 3ap + 50 mM DMSO (◊) were irradiated under anaerobic and 500 µM mBQ + 50 µM 3ap + 50 mM DMSO (▲) was irradiated under aerobic conditions @ 320 nm using monochromatic light in aqueous solution. The light intensity was 5×10^{-4} W/cm^2.
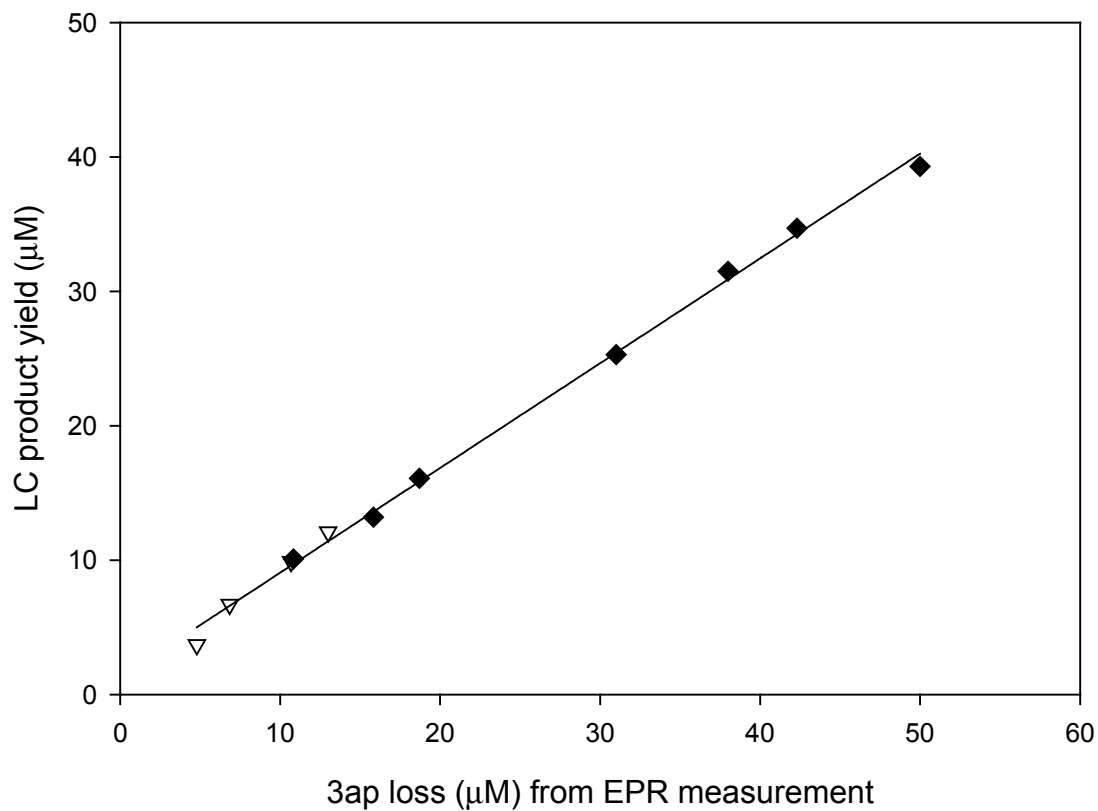
Figure II- 5. The relationship between yield of III determined chromatographically and the loss of 3ap determined by EPR on identical samples.

20 µM (∇) or 500 µM ($\blacklozenge$) of mBQ aqueous solution in the presence of 50 µM 3ap and 50 mM DMSO were irradiated at 320 nm with monochromatic light under anaerobic conditions for 1 to 40 min and 1 to 20 min, respectively.

These experiments unequivocally demonstrate that DMSO is involved in the reaction and produces methyl radical during the photolysis of mBQ. From the control experiments (**Figure II-4**), it is evident that although semiquinone radicals and trace amount of OH radicals might exist in the system, the only species that could cause 3ap spin loss to a measurable extent was the methyl radical, produced by DMSO reaction with an intermediate.

An optical absorption study further supports this conclusion. When mBQ was photolyzed in the absence of DMSO both hydroquinone and hydroxylated quinone were formed (**Figure II-6**).
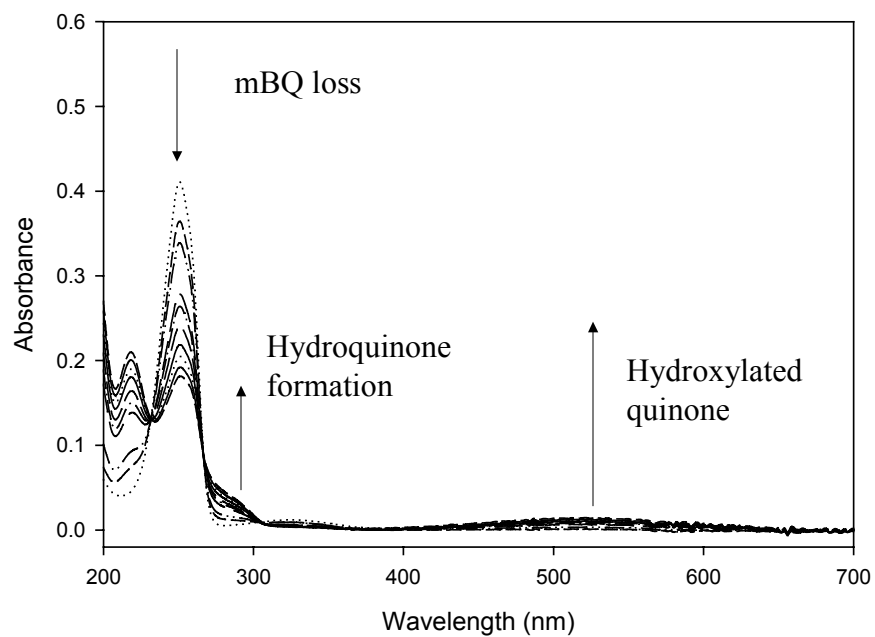
Figure II- 6. Ultraviolet/visible absorption spectra of 20 µM mBQ and its photoproducts in aqueous solution upon irradiation with 320 nm monochromatic light.

The absorption spectrum of the hydroquinone can be obtained by photolysis of mBQ in the presence of 1:1 (vol) 2-propanol (**Figure II –7**).
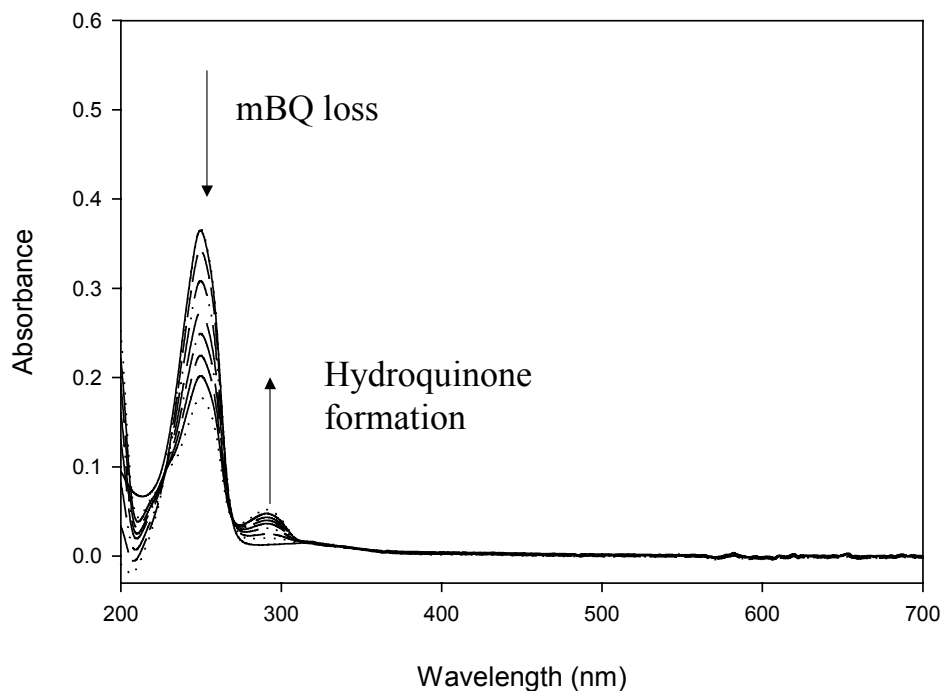
Figure II- 7.   Change of mBQ absorption spectrum upon irradiation with 320 nm light in 1:1 (v/v) H_2O and 2-propanol.

In the presence of 2-propanol, which is a good hydrogen atom donor, the formation of hydroquinone results from H-atom transfer from 2-propanol to excited triplet state quinone, followed by an electron transfer from 2-propanol radical to ground state quinone (ref). Two molecules of semiquinone are thus formed, which then disproportionate to form the hydroquinone and mBQ (**Scheme II-3)**.

H atom abstraction

Q*   2-propanol alcohol   semiquinone radical

e - transfer
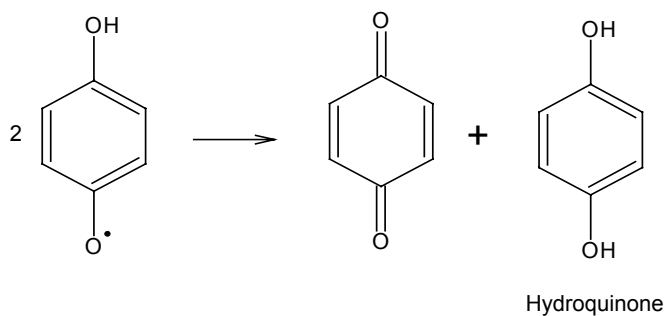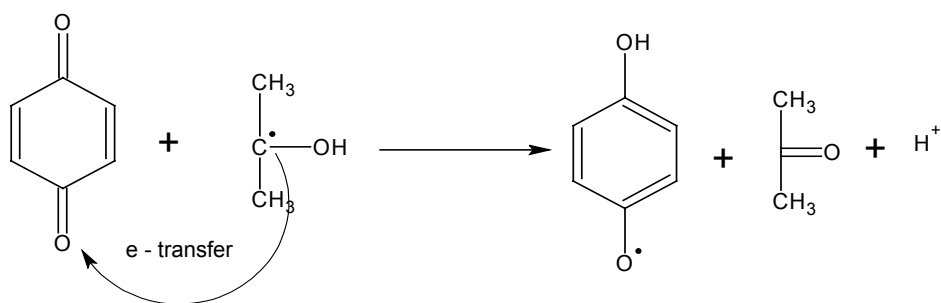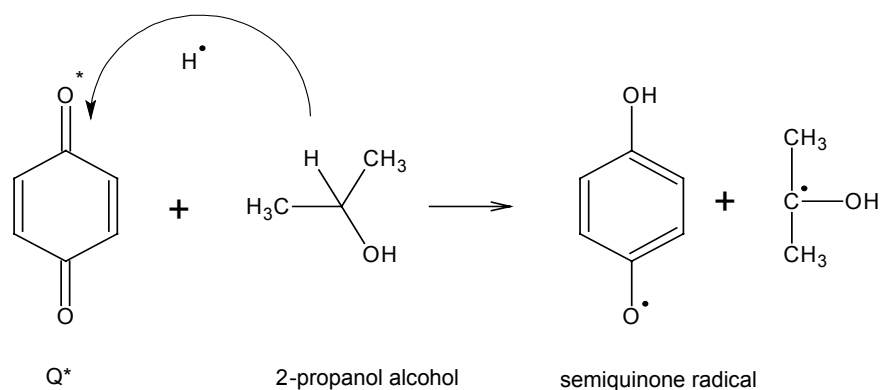
Hydroquinone

Scheme II - 3.   The mechanism of quinone photolysis in the presence of 2-propanol

     The hydroxylated quinone was identified by comparison of spectral peak position with that of literature and also the change in peak position at different pH values (Kurien and Robins 1970; von Sonntag et al 2004). At neutral and basic pH the

hydroxylated benzoquinone has a broad absorption peak centered at 520 nm. In acidic solutions, the absorption of hydroxylated methyl-1,4-benzoquinone shifts to about 410 nm.

As shown in **Figure II-8**, the loss of mBQ and the production of hydroquinone were observed when a low concentration of mBQ was photolyzed in the presence of a high concentration of DMSO.
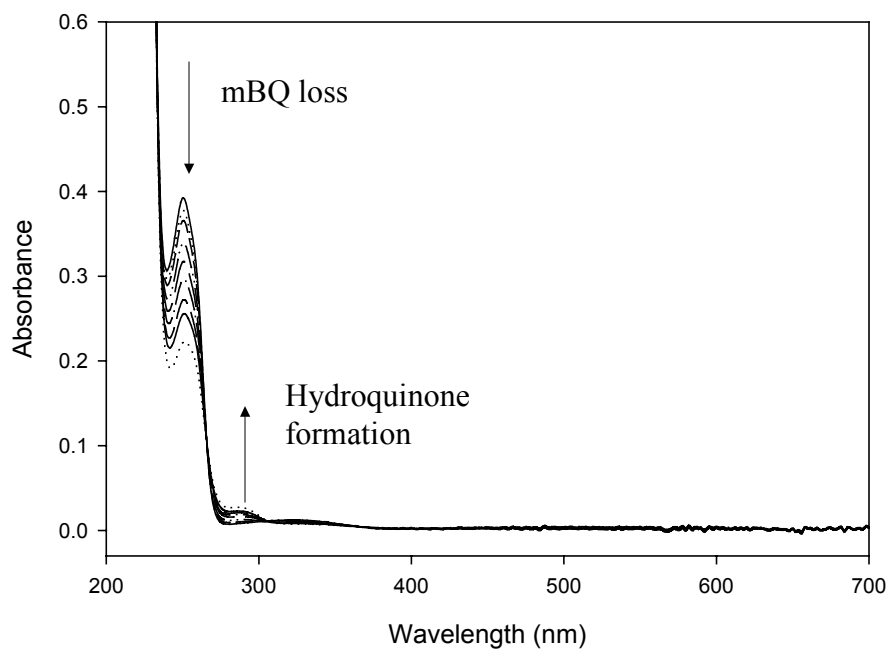
Figure II- 8.   Changes in the absorption spectrum of 20 µM mBQ upon irradiation with 320 nm light in aqueous solution in the presence of 50 mM DMSO.

It is evident from **Figure II-8** that DMSO does not physically quench the excited triplet state. If DMSO only acted as physical quencher to the triplet with high quenching rate constant (2.7×10^9 $M^{-1}s^{-1}$) (von Sonntag et al. 2004), no quinone loss or hydroquinone formation should be observed when mBQ is photolyzed in the presence of high concentrations of DMSO. The results obtained in this optical study also directly contradict the conclusion of von Sonntag et al (2004).

The above experiments unequivocally establish that 1) DMSO reacts with an intermediate produced during the irradiation of aqueous mBQ and 2) the product of this reaction is the methyl radical, which is trapped by 3ap to produce III following derivatization.

Additional Tests for the Formation of OH

Evidence against the formation of OH in the photolysis of aqueous 2- methyl-1,4-benzoquinone was provided by Pochon et al (2002). using 3ap as a radical trap in the presence of DMSO (Pochon et al 2002). In this work, in addition to DMSO, CH_4 as well as benzoic acid were used to further test for the formation of OH in the photolysis of aqueous solution of 2-methyl-1,4 –benzoquinone.

Radical trapping using 3ap in the presence of saturated CH_4 (1.5 mM) and 20 µM mBQ showed that at best, only trace amounts of III ($\leq$ 5 nm) were produced (**Figure II – 9)**. As a further test for the formation of OH, mBQ was irradiated in the presence of benzoic acid. Similarly, only trace amounts of 2-OH-BA ($\leq$ 8 nm) were detected (**Figure II-10)**.
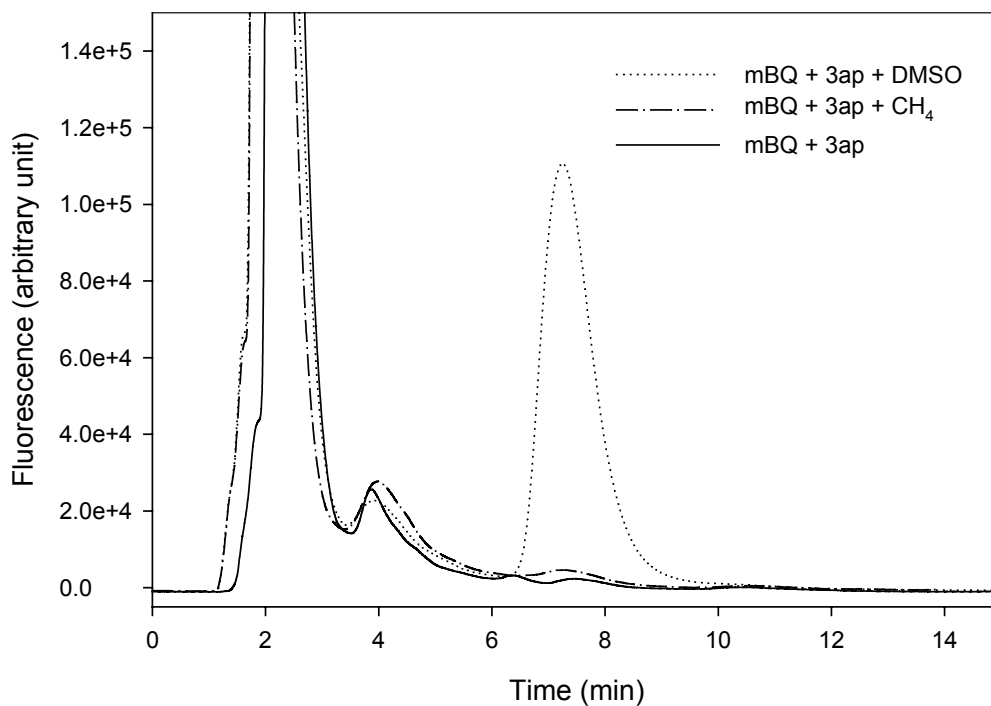
Figure II- 9. The chromatogram of III (peak at 7.5) obtained from radical trapping with DMSO and CH₄, respectively.

20 µM mBQ in the presence of 30 µM 3ap and 50 µM DMSO or saturated (1.5 mM) CH_4 in aqueous solution were irradiated at 320 nm for 2 min. The light intensity at 320 nm was 5.0×10^{-4} W/cm^2.
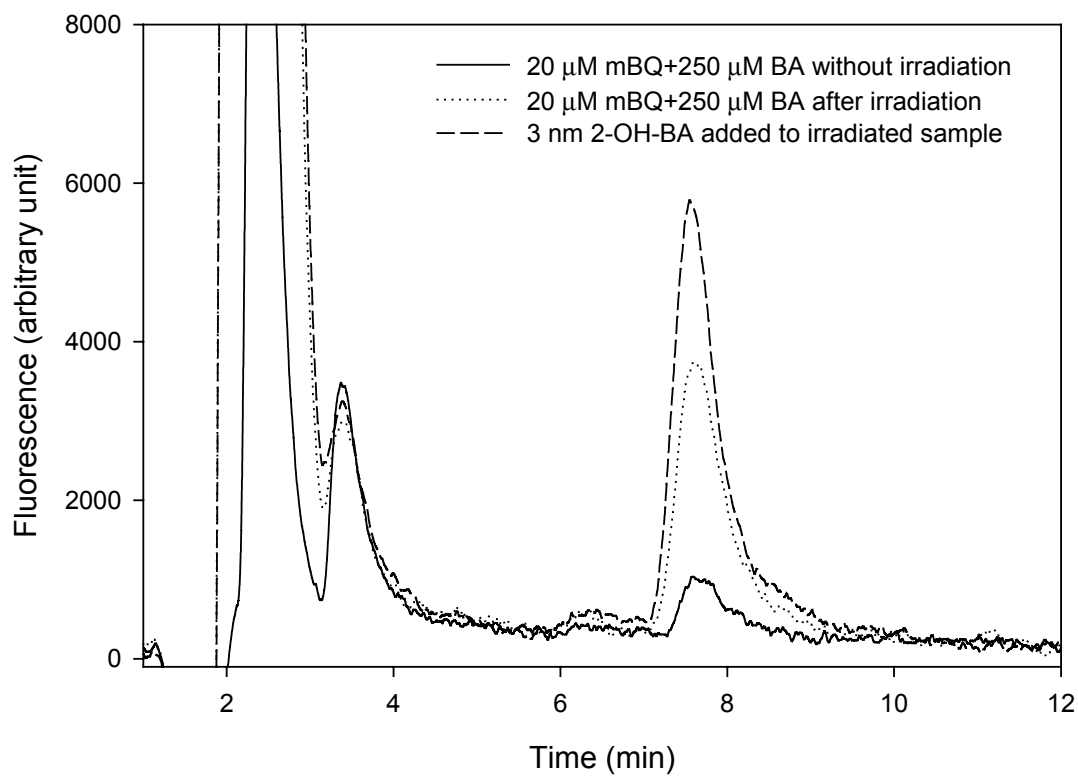
Figure II-10. The chromatogram of 2-OH-BA (peak at 7.8 min) obtained from benzoic acid production analysis.

Samples: 20 μM mBQ + 250 μM BA (........) was irradiated at 320 nm using monochromatic light for 3 min. 3 nM of 2-OH-BA addition to the irradiated sample (– – – –). 20 μM mBQ + 250 μM BA (——) without irradiation.

The results of Figure II-3, II-9, and II-10 are summarized in **Table II-1**.

Table II- 1. mBQ kinetics and product analysis data

[DMSO]½ (μM)	[DMSO]½ (μM)	k_{DMSO} / k_{DMSO}	P_{DMSO}/P_{CH4}	P_{DMSO}/P_{BA}
5690 ± 510	51.5	1.13×10^{-2}	≥ 100	52 ± 5

[Th][DMSO]$_{1/2}$: the theoretical [DMSO]$_{1/2}$, which is calculated on the basis of OH reactions.

[EX]k_{DMSO}: the rate constant of the reaction between DMSO and the species produced in quinone photolysis.

[Th]k_{DMSO} : the rate constant of OH and DMSO reaction, which equals to $6.6 \times 10^9 M^{-1}.s^{-1}$. (Veltwisch and Asmus 1982)

With the value of [DMSO]$_{1/2}$ obtained from the experimental data (**Figure II-3**), [EX]k_{DMSO} was calculated to be 7.1×10^7 $M^{-1}s^{-1}$ using **equation II-4** assuming that 3ap and mBQ are only other competitors with reaction rate constants of 4×10^9 $M^{-1}s^{-1}$ and 5×10^9 $M^{-1}s^{-1}$, respectively. This result is in reasonable agreement with the value reported by Pochon and co-worker (2.1×10^7 $M^{-1}s^{-1}$) (Pochon et al. 2002) and two orders of magnitude lower than the reported rate constant for the reaction of OH radical with DMSO (6.6×10^9 $M^{-1}s^{-1}$).

Based on the results from DMSO and CH$_4$ radical trapping as well as the benzoic acid product analysis, unequivocal evidence has been obtained to conclude that OH is not produced substantially during the photolysis of mBQ in aqueous solution, consistent with previous work of Pochon et al (2002), and subsequently Gorner (2003) and von Sonntag et al (2004).

Is the Intermediate the Triplet State or a Species that is Distinct from the Triplet?

The existence of an oxidizing intermediate that is distinct from excited triplet state was proposed by Pochon et al (2002) based on non-competitive kinetic behavior observed between DMSO and salicylate, formate, and nitrite in radical trapping experiments employing 3ap. However, the existence of this intermediate was strongly disputed by Gorner (2003) and subsequently von Sonntag et al (2004).

As noted in Chapter I, Gorner excluded the existence of such an intermediate based on 1) no spectral indication of the formation of such an intermediate and, 2) the quenching effect of chloride on the triplet state quinone. Chloride anion was reported to physically quench the triplet state quinone (Loeff et al. 1984; Loeff et al. 1993). Gorner examined the effects of KCl on triplet decay rate and decomposition quantum yield of quinone. Based on the linear relationship between triplet decay rate ($1/\tau_T$) and chloride concentration, as well as the $[Cl]_{1/2}$ at which the decomposition quantum yield of quinone is 50% of the maximum value, a direct triplet state mechanism was proposed (Scheme I-3). In this mechanism, the triplet quinone reacts with water directly to form benzene-1,2,4-triol, which is then oxidized by ground state quinone to produce the hydroquinone and hydroxylated quinone. Chloride anion was reported to quench the triplet state of 2-methyl-1,4-benzoquinone with a rate constant of $2.4 \times 10^9 \, M^{-1} \, s^{-1}$ (Görner 2003).

However, a single triplet state quenching experiment with chloride was not adequate for mechanism assignment even though the $[Cl]_{1/2}$ obtained from the

experiment was consistent with the value calculated based on the assumption that only triplet state was present as intermediate. In order to further test the effect of chloride on the triplet state and the existence of a species other than the triplet, radical trapping using 3ap in the presence of DMSO and chloride was performed.

In the previous section, DMSO was demonstrated to react with an intermediate, either the triplet state quinone or another species distinct from the triplet, to produce methyl radical. Logically, if there is no other intermediate except the triplet in the system then it must be the triplet that reacts with DMSO to produce the methyl radical. Because both DMSO and chloride anions would interact with the same species, strictly competitive kinetics should be observed (**Scheme II-4**).

$$Q^{\cdot -} + CH_3SOO + CH_3 \longrightarrow \longrightarrow III$$

DMSO $\quad k_{DMSO}$

$$Q \xrightarrow{h\upsilon} {}^1Q^* \xrightarrow{k_F} {}^3Q^* \xrightarrow[k_{H2O}]{H_2O} Ph(OH)_3$$

Cl⁻ $\quad k_{Cl}$

Competitive
between
DMSO and Cl⁻ $\qquad$ **Q**

$$QH_2 + Q\text{-}OH$$
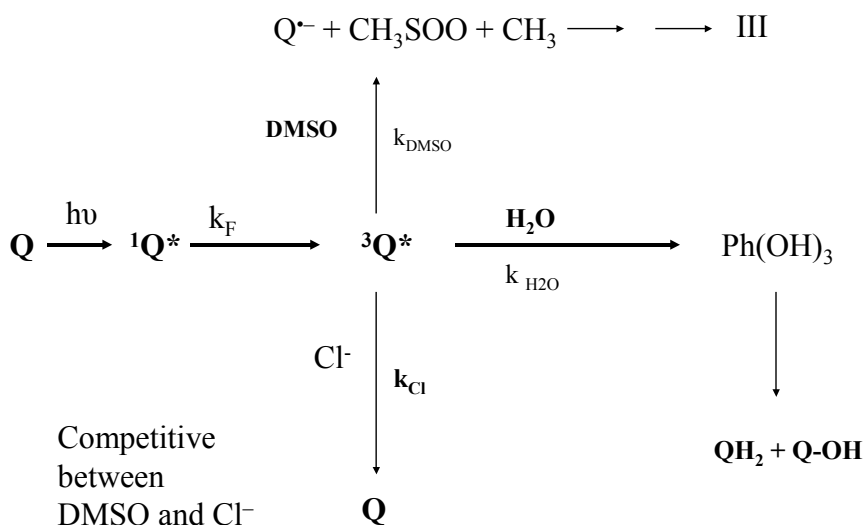
Scheme II - 4. The competition between chloride and DMSO towards triplet quinone

On the other hand, if there is another species that is distinct from triplet, but arises from triplet and reacts with DMSO, strictly non-competitive kinetics should be observed as illustrated in **Scheme II-5**.

$$QH_2 + Q\text{-}OH$$

$$Q \xrightarrow{h\upsilon} {}^1Q^* \xrightarrow{k_F} {}^3Q^* \xrightarrow[k_{H2O}]{H_2O} \text{intermediate} \longrightarrow Ph(OH)_3$$

$$Cl^- \Big| k_{Cl} \qquad\qquad DMSO \Big| k_{DMSO}$$

Non-competitive between DMSO and Cl^- 　　　 **Q** 　　　　 $Q^{\bullet-} + CH_3SOO + CH_3$

$$III$$
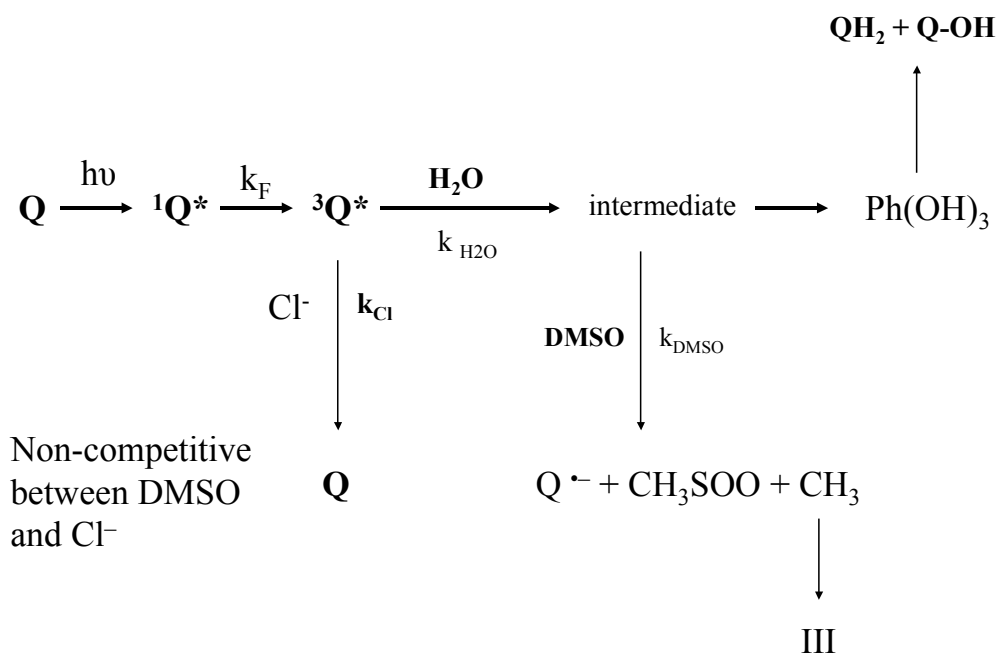
Scheme II - 5.　Scheme giving rise to non-competitive kinetics between chloride and DMSO.

The relationship between initial formation rate of III and the concentration of DMSO in the presence of different concentrations of chloride was examined. As shown in **Figure II-11**, the initial III production rate (P_{DMSO}) decreased with increasing chloride concentration and $[DMSO]_{1/2}$ increased with increasing $[Cl^-]$.

From **Figure II-12**, which is the double reciprocal plot of the curves in **Figure II-11**, it is evident that the presence of increasing amounts of chloride affects the production rate of III in both competitive and non-competitive fashions. The slope change in the presence of different concentrations of chloride indicates competitive and the intercept change indicates non-competitive kinetics. The observation of slope and intercept changes indicated both competitive and non-competitive kinetics.

The non-competitive kinetics can only be explained by a kinetic scheme (**Scheme II-6**) in which chloride quenches the triplet state and DMSO reacts with an intermediate that arises from the triplet state quinone. Chloride anion quenches the triplet state quinone and thus removes the precursor of the species (intermediate) with which DMSO reacts. Therefore, at high concentrations of DMSO, the initial formation rate of III decreases with increasing concentrations of chloride. In contrast the $[DMSO]_{1/2}$ shift indicates a competition between DMSO and chloride towards an intermediate arising from the triplet. These results are consistent with those previously reported by Pochon et al. (2002) for the photolysis of mBQ in aqueous solution.
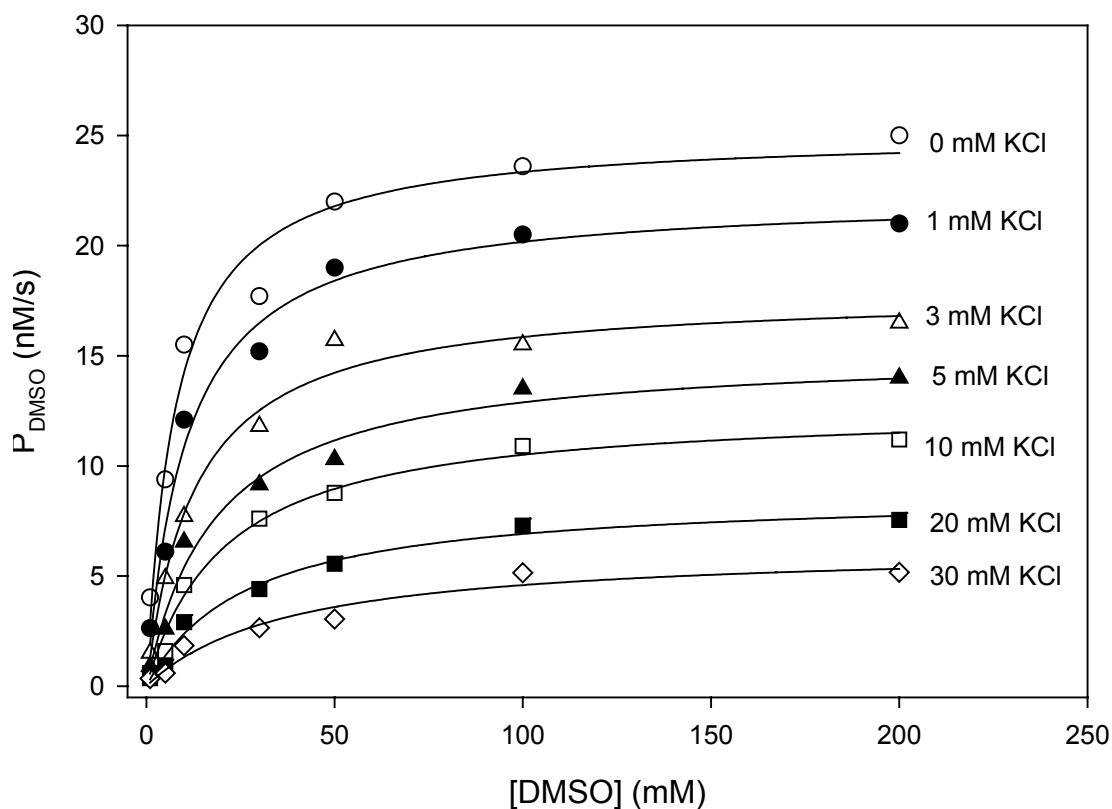
Figure II- 11.   The dependence of initial III production rates (P_{DMSO}) on chloride concentrations.

20 μM mBQ + 50 μM 3ap + DMSO + [KCl] was irradiated using broadband light with 350 nm cutoff filter for 30 sec under anaerobic condition. The lamp intensity was 2.5×10^{-3} W/cm^2 at 350 nm. Without KCl (0.0 mM KCl ○), the maximum production rate was 25.3 nM/s. Increased KCl concentrations the maximum production rates decreased accordingly from 21.2 nM/s (1 mM KCl ●), 17.1 nM/s (3.0 mM KCl Δ), 15.2 nM/s (5.0 mM KCl ▲) 12.6 nM/s (10.0 mM KCl □), to 8.8 nM/s (20.0 mM KCl■) and 6.3 nM/s (30 mM KCl ◊).
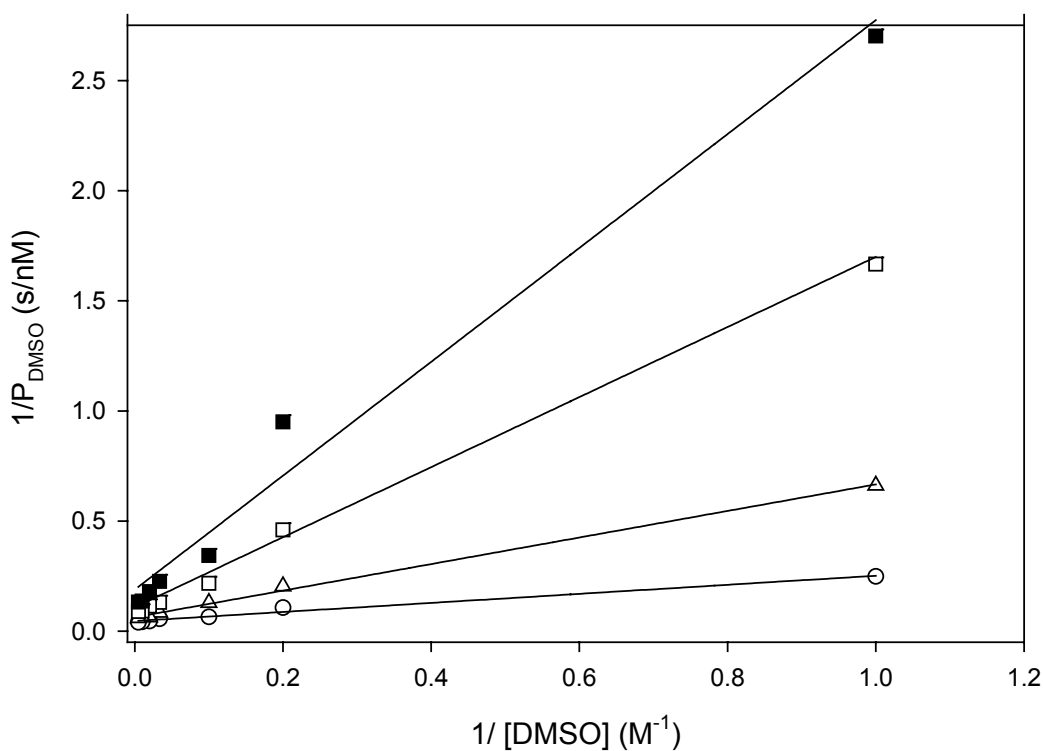
Figure II- 12. Double reciprocal plot of initial III production rate ($1/P_{DMSO}$) versus $1/[DMSO]$ in the presence of different concentrations of KCl.

20 μM mBQ + 50 μM 3ap + DMSO + [KCl] was irradiated using broadband light with 350 nm cutoff filter for 30 sec under anaerobic conditions. The lamp intensity was 2.5×10^{-3} W/cm^2 at 350 nm. Without KCl (○), 3.0 mM KCl (Δ), 10.0 mM KCl (□), and 20.0 mM KCl (■)
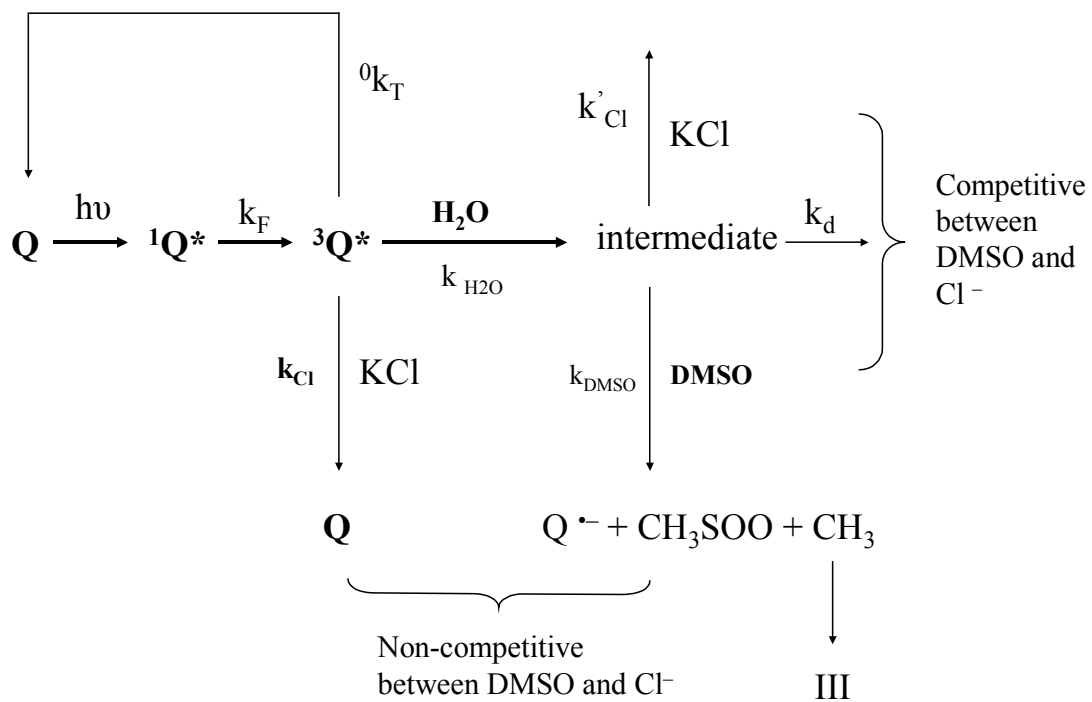
Scheme II - 6. The overall reaction of triplet quinone and intermediate in the presence of chloride and DMSO.

The competitive and non-competitive effects of chloride can also be separated and quantified by the following equations **(II-12)**.

$$P_{DMSO} = \left(\frac{k_F \, k_{H2O}[H_2O]}{k_{H2O}[H_2O] + \,^0k_T + k_{Cl}[Cl]} \right) \left(\frac{k_{DMSO}[DMSO]}{k_{DMSO}[DMSO] + k_d + k'_{Cl}[Cl]} \right)$$

$$= \frac{C_1[DMSO]}{C_2 + [DMSO]} \qquad \qquad \textbf{(II-12)}$$

$$\frac{C_1}{^0C_1} = \frac{k_{H2O}[H_2O] + \,^0k_T}{k_{H2O}[H_2O] + \,^0k_T + k_{Cl}[Cl]} \qquad \begin{cases} C_1 = \dfrac{k_F k_{H2O}[H_2O]}{k_{H2O}[H_2O] + \,^0k_T + k_{Cl}[Cl]} \\[2em] ^0C_1 = \dfrac{k_F k_{H2O}[H_2O]}{k_{H2O}[H_2O] + \,^0k_T} \end{cases}$$

$$C_2 - \,^0C_2 = \frac{k'_{Cl}[Cl]}{k_{DMSO}} \quad ; \quad C_2 = \frac{k_d + k'_{Cl}[Cl]}{k_{DMSO}} \quad ; \quad ^0C_2 = \frac{k_d}{k_{DMSO}}$$

P_{DMSO} is the initial formation rate of III. C_1 and $^0C_1$ are the maximal initial formation rates of III ($^{max}P_{DMSO}$) in the presence and absence of triplet quencher (Cl$^-$), respectively. The C_1 / $^0C_1$ evaluates the quenching effect of chloride on the triplet state. C_2 and $^0C_2$ provide the values of $[DMSO]_{1/2}$ in the presence and absence of chloride, respectively. C_2 - $^0C_2$ is the change in $[DMSO]_{1/2}$ due to competition effect of chloride with DMSO towards the intermediate.

The effects of chloride on the initial formation rate of III and $[DMSO]_{1/2}$ are summarized in Table II-2.

Table II- 2.   The competitive and non-competitive effects of chloride on the initial formation rate of III and $[DMSO]_{1/2}$

	0 mM KCl	1 mM KCl	3 mM KCl	5 mM KCl	10 mM KCl	20 mM KCl	30 mM KCl
$C_1 / {}^0C_1$	1	0.84	0.68	0.60	0.43	0.35	0.25
C_2 (mM)	7.67	10.61	13.86	18.3	23.26	28.9	39.52

With $C_1 / {}^0C_1$ vs. [KCl] data, $[Cl^-]_{1/2}$, the concentration of chloride at which the initial formation rate of III is 50% of that in the absence of chloride, is found to be 7.0 mM from this experiment ($C_1 / {}^0C_1 = 0.5$).

Similar kinetic analysis can be performed using double reciprocal plot. As shown in **Figure II-13**, the reciprocal of initial III production rate (1/P) at high DMSO concentration (200 mM) versus concentrations of KCl showed a linear relationship with a slope of 5×10^9 and an intercept of 4.2×10^7 (s/M). Analysis of the slope and intercept according to **equation II-13**, which can be deduced from **Scheme II-6**, reveals that k_{Cl} / k_{H2O} equals to 6.6×10^3.

$$1/P = \left[{}^0k_T + k_{H2O}[H_2O] / k_F k_{H2O}[H_2O] \right] + \left[k_{Cl}[Cl] / k_F k_{H2O}[H_2O] \right] \qquad \text{(II-13)}$$
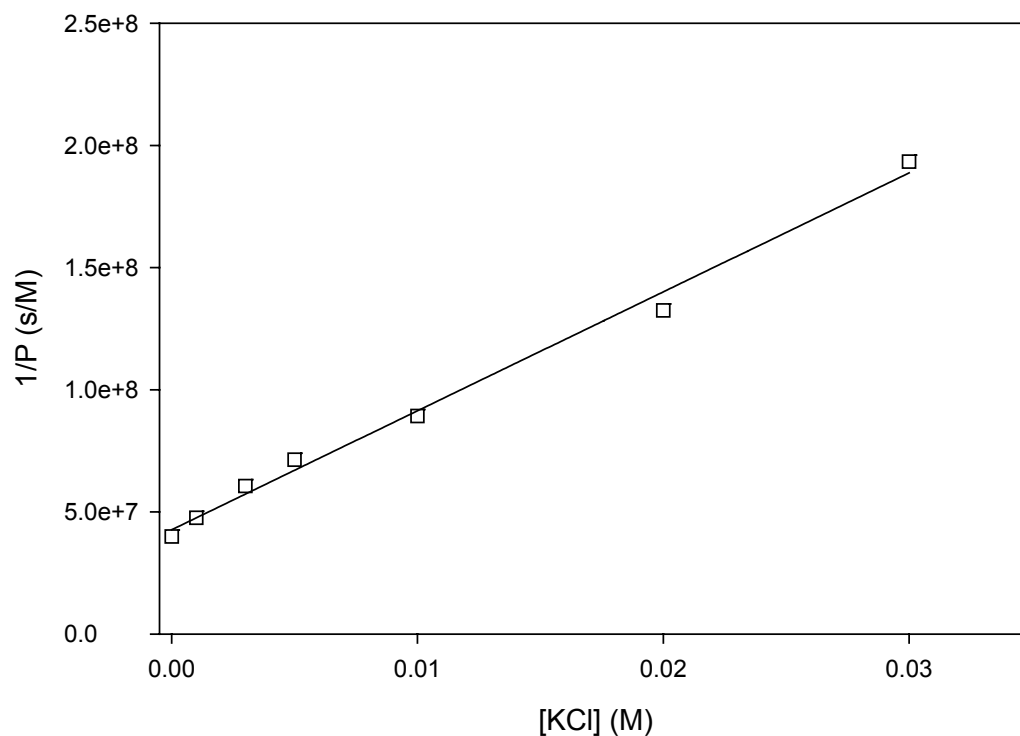
Figure II- 13.   The double reciprocal of III formation rates versus KCl concentration in chloride competition experiment.

20 μM mBQ + 50 μM 3ap + 200 mM DMSO + [KCl] was irradiated using broadband light with 350 nm 50% transmittance short-wavelength cutoff filter for 30 sec under anaerobic condition. The reciprocal of III formation rates P was plotted vs. concentrations of KCl.

These experiments established that 1) another species distinct from the triplet exists in the photolyzed quinone system, 2) DMSO does not quench or react with triplet state quinone to a significant extent in the concentration range employed in these experiments. If DMSO reacted with the triplet then a purely competitive

66

kinetics would be observed in chloride vs. DMSO experiment. If DMSO quenches the triplet state, the formation rates of III should decrease with increasing concentrations of DMSO. A detailed mechanism consistent with the observed kinetics is presented in a subsequent section.

Does the Mechanism Change with Quinone Concentration?

Suggested by the initial work of Clark and Stonehill (Clark and Stonehill 1972) and subsequently Gorner (Gorner 2003) and von Sonntag et al (von Sonntag et al 2004), the mechanism of quinone photolysis was proposed to change with increasing quinone concentration.

As shown in **Scheme II-7**, if quinone itself competes with water for the triplet state quinone, the relative quantum yield of III is expected to decrease with increasing concentration of mBQ. The relative quantum yield of III, which measures the branching ratio of triplet quinone towards quinone - water and Q reactions, was measured as a function of quinone concentration
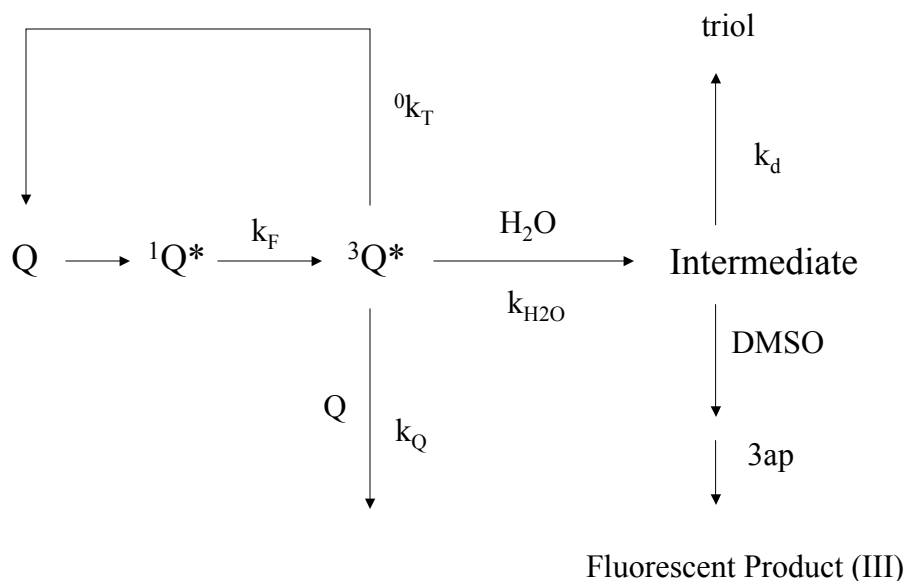
Scheme II - 7. The competitive triplet state decay pathways at high concentrations of Q.

Quinone will not compete significantly with water for the triplet at exceedingly low concentration. Therefore, the relative quantum yield of III (Φ_R) at higher concentration can be obtained with respect to that of 10 µM mBQ, at which the competition of quinone is believed to be minimum. The initial production rate of III and initial absorption of quinone solutions were measured for all concentrations of quinone reaction and relative III quantum yields were calculated with respect to that of 10 µM mBQ as shown in **equation II-14**.

$$\Phi_R = \Phi_{[mBQ]} / \Phi_{10\,\mu M} = P_{[mBQ]} (1-10^{-A_{10\mu M}}) / P_{10\,\mu M} (1-10^{-A_{[mBQ]}}) \qquad (II-14)$$

where $\Phi_{[mBQ]}$ and $\Phi_{10\,\mu M}$ are quantum yields of III production at higher concentration of mBQ and at 10 µM, respectively. $A_{[mBQ]}$ and $A_{10\,\mu M}$ were the initial absorbance of mBQ at high concentrations and at 10 µM. $P_{[mBQ]}$ and $P_{10\,\mu M}$ were initial III formation rates at high concentrations and 10 µM of mBQ, respectively. The absorbance of the quinone was obtained either at 320 nm or 420 nm.

In the absence of a reaction between Q and $^3Q^*$, the initial rate of III production would be expected to increase linearly with concentration of Q under optically thin conditions. Instead, the initial production rate of III obtained from experiment increases with increasing quinone concentration at low concentrations, then levels off at high quinone concentrations (above 5 mM) as shown in **Figure II-14**. This clearly demonstrates that quinone concentration affects the initial formation rate of III and thus suggests a reaction between the ground state and excited triplet

state quinone. The result further implies that the product of the quinone-quinone

reaction does not react with DMSO to produce a CH3 radical.
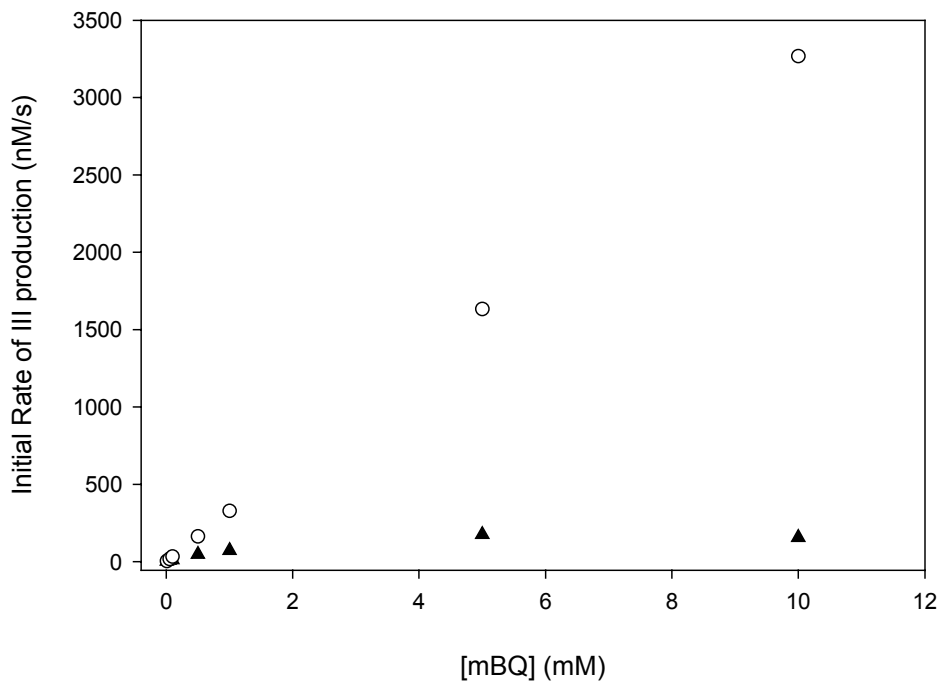
Figure II- 14. Comparison between theoretical (O) and experimental (Δ) initial rates of III production as a function of quinone concentrations.

(10 μM to 10 mM) mBQ + (50 μM to 500 μM) 3ap + 100 mM DMSO were irradiated for 1 min with polychromatic light (300 W Xe arc lamp) passed through a 420 nm (50% transmittance) low pass filter and an 0.5 neutral density filter.

The relative quantum yield of III formation at different quinone concentrations was shown to decrease with increasing quinone concentration (**Figure II-15**).
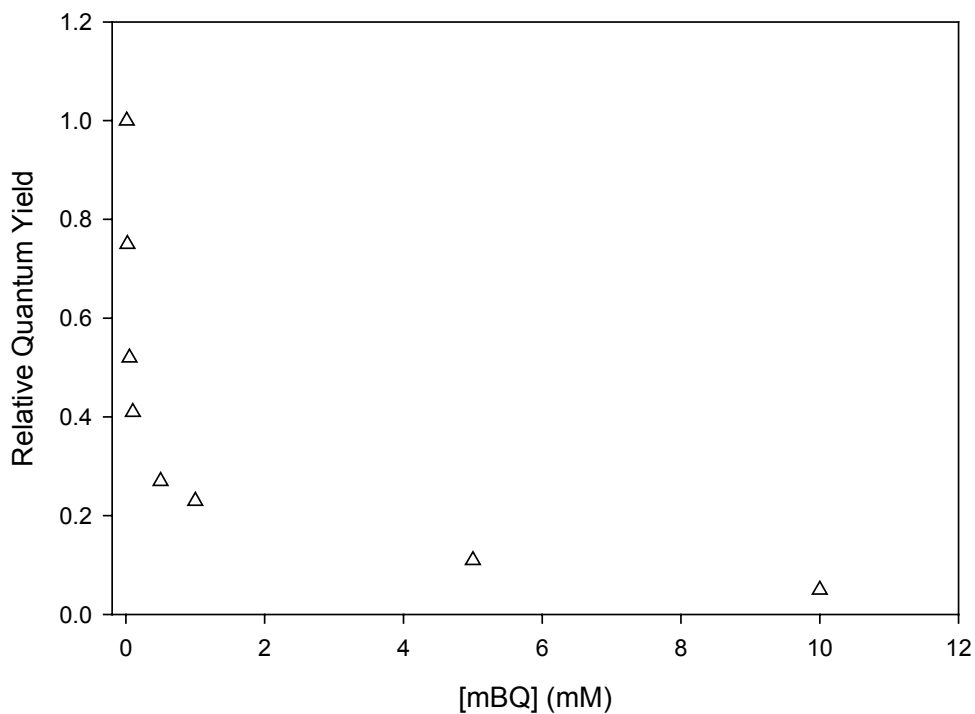
Figure II- 15.   The relative quantum yield of III as a function of mBQ concentration.

(10 μM ~ 10 mM) mBQ + (50 μM to 500 μM) 3ap + 100 mM DMSO were irradiated for 1 min with polychromatic light (300 W Xe arc lamp) passed through a 420 nm (50% transmittance) low pass filter and an 0.5 neutral density filter.

As a further test for the relationship between relative III quantum yield and the concentration of mBQ, relative 3ap consumption ratios [reacted 3ap]/[mBQ] were measured by EPR for increasing concentrations of mBQ. If quinone concentration affects the relative quantum yield of III formation, and based on the correlation between 3ap loss and III formation (**Figure II-5**), the relative 3ap consumption ratios [reacted 3ap]/[mBQ] should decrease with increasing mBQ concentration in the radical trapping experiments.

As shown in **Figure II-16**, consistent with the relative quantum yield measurements (**Figure II-15**), the relative 3ap consumption ratio decreases with increasing mBQ concentration. This 3ap consumption versus total mBQ concentration experiment provides additional evidence to support the dependence of III quantum yield on quinone concentration.

From these experimental data, it is evident that the relative quantum yield of III decreased with increasing concentrations of quinone. This clearly showed that, with increasing concentrations of mBQ, the triplet quinone-water reaction became less important; instead the triplet quinone–ground state quinone reaction became more significant, and at high mBQ concentration this becomes the major pathway. The results are consistent with those of previous workers (Gorner 2003; von Sonntag et al. 2004).
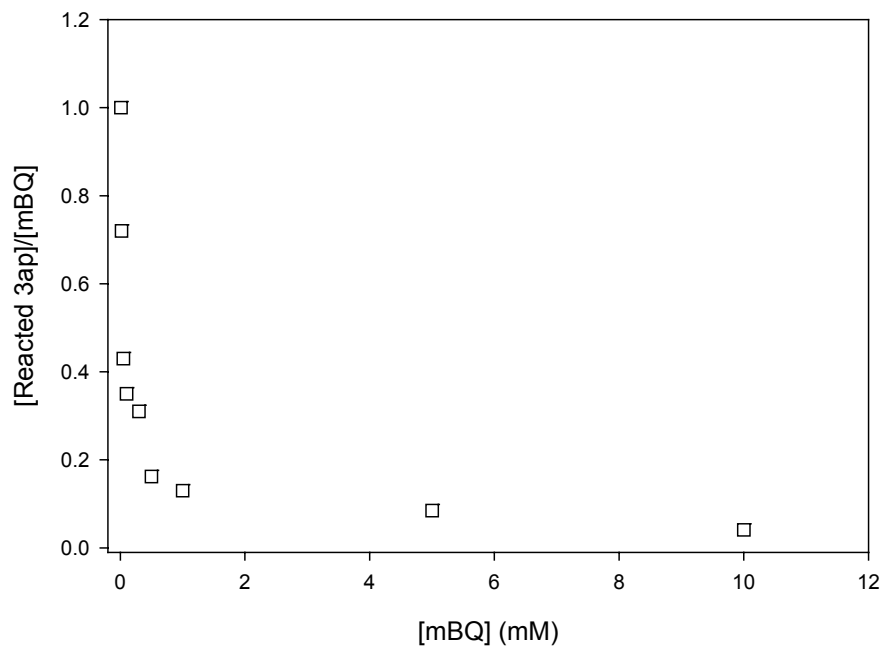
Figure II- 16. The dependence of relative 3ap consumption on the concentrations of mBQ.

(10 μM ~ 10 mM) mBQ + (50 μM ~ 500 μM) 3ap + 100 mM DMSO were irradiated until complete consumption of mBQ with polychromatic light (300 W Xe arc lamp) passed through a 420 nm (50% transmittance) low pass filter and an 0.5 neutral density filter.

The initial absorbances of different concentrations of quinone at 320 nm and 420 nm and corresponding relative quantum yields as well as relative 3ap consumption rates are summarized in Table II-3.

Table II- 3.   The initial absorbance, relative quantum yield, and relative 3ap consumption rate of different concentrations of mBQ

Q (mM)	0.01	0.02	0.05	0.1	0.3	0.5	1.0	5.0	10.0
A_{320}	0.0055	0.0110	0.0279	0.0535	0.162	0.2701	0.5301	2.4591	2.8599
A_{420}	~	~	~	~	0.0097	0.0158	0.0307	0.1536	0.3197
Φ_R	1	0.75	0.52	0.41		0.27	0.23	0.11	0.05
$[3ap]_R$	1	0.72	0.43	0.33	0.30	0.20	0.17	0.085	0.04

A_{320} and A_{420} are initial absorbance of different concentrations of quinone at 320 nm and 420 nm, respectively.
Φ_R is the relative quantum yield calculated from **equation II-14**.
$[3ap]_R$ is the relative 3ap consumption rate calculated from [reacted 3ap]/[mBQ]total.

According to **Scheme II-7**, the relative quantum yield of III production at low versus high Q concentrations can also be calculated by **equation II-15**.

$$\Phi_R = k_{H2O}[H_2O]/ (k_{H2O}[H_2O]+k_Q[Q]+ {}^0k_T) \qquad \text{(II-15)}$$

Taking the reciprocal of equation II-15 produces **equation II-16;** the relationship between $1/\Phi_R$ and quinone concentration is shown in **Figure II-17**.

$$1/\Phi_R =\left[1 + {}^0k_T / k_{H2O}[H_2O]\right] + \left[k_Q[Q] / k_{H2O}[H_2O]\right] \qquad \text{(II-16)}$$
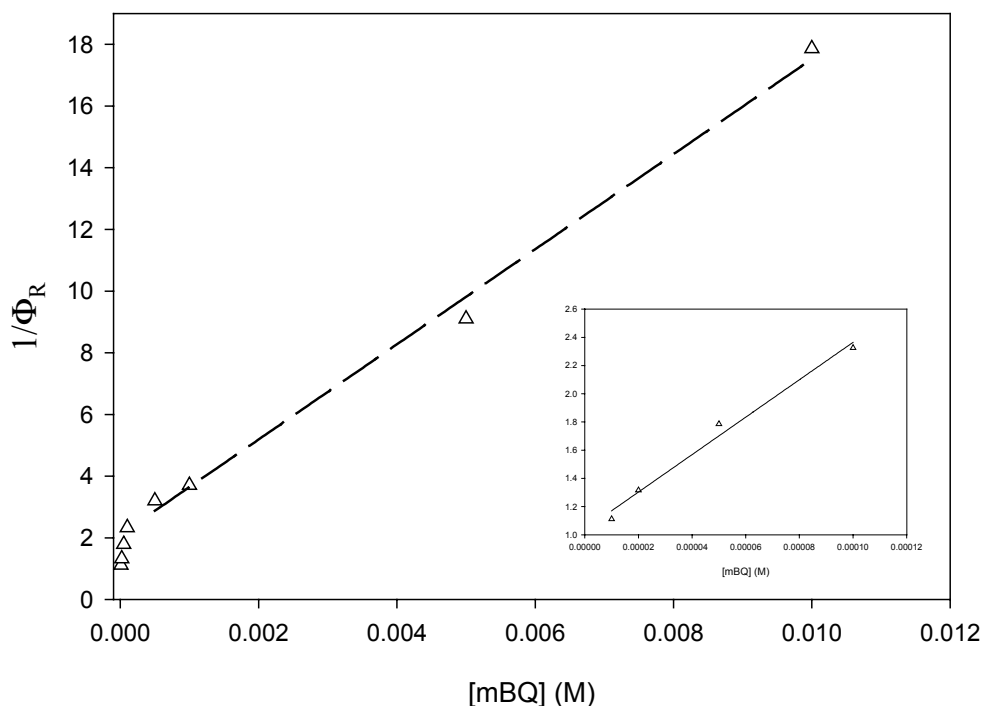
Figure II- 17. The relationship between the reciprocal of relative quantum yield $1/\Phi_R$ and mBQ concentration

Inset: the double reciprocal plot for high concentrations of mBQ in the presence of DMSO and 3ap.

The slope of this double reciprocal plot represents $k_Q/k_{H2O}[H_2O]$ value. At low concentrations of quinone, the slope ($k_Q/k_{H2O}[H_2O]$) equals to 1.0×10^4. At high concentrations of mBQ, the slope is (3×10^3). A similarly slope change at different concentrations of quinone, was also observed in both Gorner (Gorner 2003) and von Sonntag et al (von Sonntag et al 2004). The kinetics obtained in this experiment will be discussed with results obtained from chloride experiment in next section.

An optical absorption study was performed for high concentrations of mBQ in the presence and absence of DMSO. As shown in **Figure II-18 and Figure II-19**, for a solution of 500 µM mBQ, with or without DMSO, both hydroquinone and hydroxylated quinone are formed upon irradiation. This result indicates that DMSO has no obvious effects on aqueous quinone photolysis and product formation when the quinone concentration is very high.
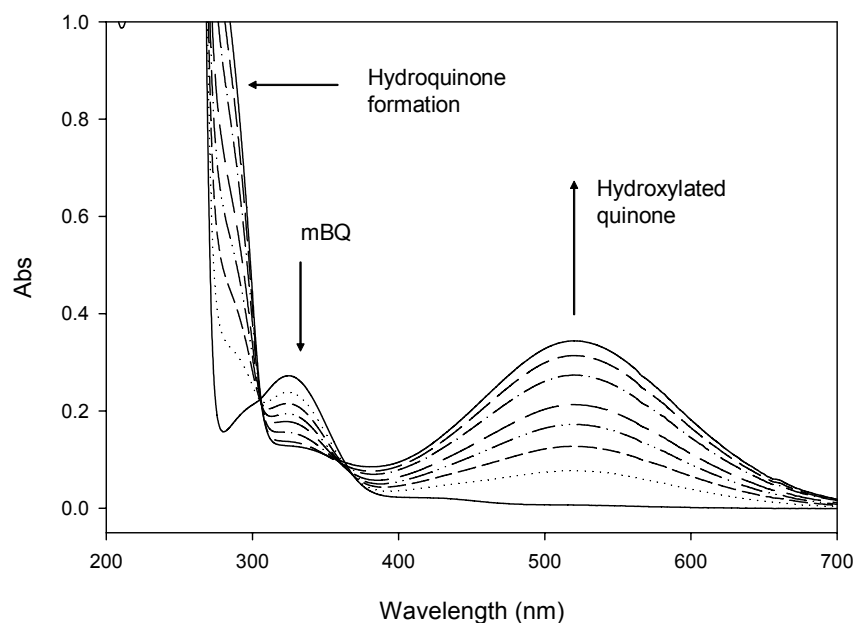
Figure II- 18.   The UV spectrum of 500 µM mBQ in 12 mM pH 7.0 phosphate buffer upon irradiation with 320 nm light.
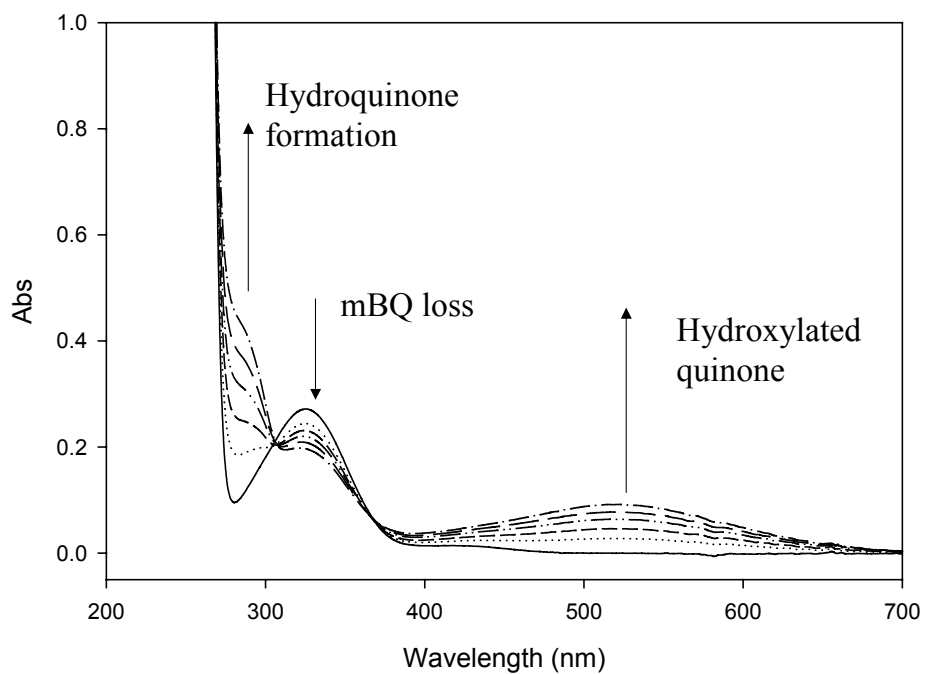
Figure II- 19.   The UV spectrum of 500 µM mBQ in 12 mM pH 7.0 phosphate buffer upon irradiation with 320 nm light in the presence of 50 mM DMSO.

Kinetics Analysis

The overall reaction scheme is depicted in **Scheme II-8**.
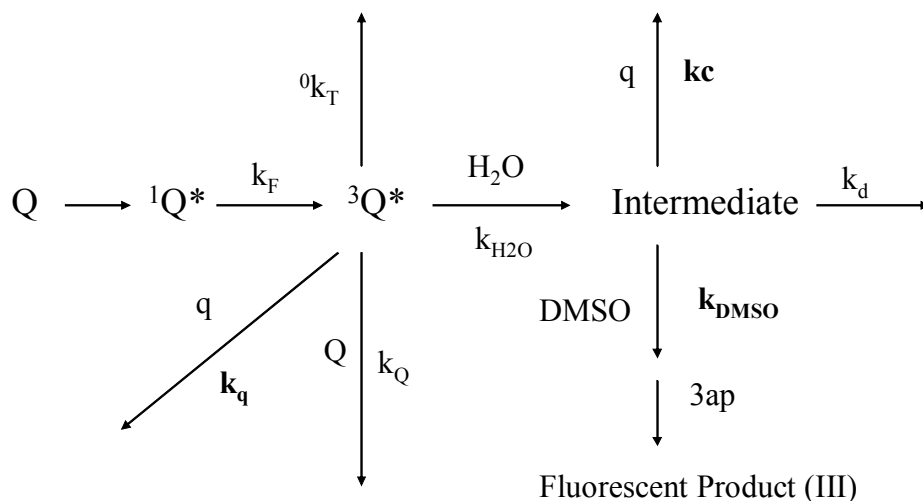
q (triplet quencher or intermediate):
Cl^-, NO_2^-, formate, salicylate, DMPO
k_q is the triplet quenching rate constant
k_c is the intermediate quenching rate constant

Scheme II - 8. The overall triplet decay and intermediate reaction pathways.

Scheme II-8 can be parameterized by use of the data obtained in chloride experiments and quinone concentration dependence experiments.

Triplet decay rate and lifetime

A key issue in the quantitative kinetic analysis of the data is the triplet lifetime in a completely inert solvent as compared to water. The triplet decay rate (k_T) or corresponding triplet lifetime (τ_T) of mBQ has been determined in different solutions by different research groups (Rondard 1980; Gorner 2003; Pochon et al 2002). However, there is no reported natural mBQ triplet decay rate, ^0k_T, the triplet decay rate in completely inert solvent in the absence of any quencher. This may partially result from the use of different organic solvents, which are not completely inert. But the most important reason is the difference in mBQ concentration employed in the triplet lifetime determinations. Generally, high mBQ concentrations were employed in the triplet decay rate measurements. Depending on the excitation wavelength in laser flash photolysis experiment, 200 to 500 μM and 3 to 10 mM of mBQ could be used in LFP experiment at excitation wavelength of 266 nm or 355 nm. Although Gorner attempted to investigate the concentration dependence of quinone triplet lifetime, his results are internally inconsistent in the case of mBQ.

The previously reported triplet decay rate (k_T) (Rondard 1980; Gorner 2003; Pochon et al 2002) was re-calculated using the equation ($k_T = {^0k_T} + k_Q[Q]$) to account for the quenching effects of quinone on the triplet state. Based on the ^0k_T obtained from the re-calculation as well as comparison with the triplet lifetimes of those quinones with similar substituents and structure, a natural triplet lifetime ($^0\tau_T$) of **2.0 ~ 2.5 μs** is estimated for mBQ in inert organic solvents.

The rate constant for triplet quinone and water reaction, k_{H2O}

According to the triplet lifetime (~ 0.7 μs) in MeCN-H_2O reported by Gorner (2003) and the estimated natural triplet lifetime of mBQ, the rate constant for reaction between triplet mBQ and water (k_{H2O}) can be calculated from **equation II-17**.

$$k_T = {}^0k_T + k_{H2O} [H_2O] \qquad\qquad (II\text{-}17)$$

where k_T is the triplet decay rate in aqueous solution, which can be obtained from the reciprocal of reported triplet lifetime (τ_T). ${}^0k_T$ is the natural triplet decay rate, which can be obtained from natural triplet lifetime (${}^0\tau_T$). For mBQ, the natural triplet lifetime (${}^0\tau_T$) is estimated to be 2.0 ~ 2.5 μs (see previous section).

The rate constant for reaction between triplet quinone and water is then calculated to be $k_{H2O} = 1.6 \sim 2.0 \times 10^4 \text{ M}^{-1}\text{s}^{-1}$. This value is close to the rate constant for reaction of ${}^3BQ^*$ and water ($1 \times 10^4 \text{ M}^{-1}\text{s}^{-1}$) reported by Gorner (2003).

The rate constant for triplet quinone and quinone reaction k_Q

The $k_Q / k_{H2O}[H_2O]$ and thus k_Q / k_{H2O} values can be obtained experimentally from the slope of double reciprocal plot in **Figure II-17**.

At low concentration of mBQ, the slope of the double reciprocal plot is 1.0 $\times 10^4$, which equals to $k_Q / k_{H2O}[H_2O]$. Use the value $k_{H2O} = 1.6 \times 10^4 \text{ M}^{-1}\text{s}^{-1}$, at low quinone concentration, k_Q equals to $8.5 \times 10^9 \text{ M}^{-1}\text{s}^{-1}$ can be calculated. This value agrees with the reported k_Q value ($> 5 \times 10^9 \text{ M}^{-1}\text{s}^{-1}$) for BQ very well (von Sonntag 2004).

At high concentrations of mBQ, however, a different slope (3×10^3) was revealed as shown in **Figure II-17**. Use the value $\mathbf{k_{H2O} = 1.6 \times 10^4 \ M^{-1}s^{-1}}$, at high quinone concentration, k_Q can be calculated as $\mathbf{2.7 \times 10^9 \ M^{-1}s^{-1}}$.

A possible explanation for the decrease of k_Q value is the reduction of effective quinone concentration due to the formation of ground state dimer (Clark and Stonehill, 1972; Gorner 2003). This result was consistent with that found by von Sonntag et al. (2004) and an equilibrium between monomeric triplet $^3Q^*$ and an exciplex dimer $^3Q_2^*$ was suggested there. A k_Q of $2.8 \times 10^8 \ M^{-1}s^{-1}$ was observed for 1,4-benzoquinone at high concentrations of quinone compared to that of $k_Q > 5 \times 10^9$ $M^{-1}s^{-1}$ at low concentrations of quinone. Similar k_Q change was observed in Gorner's work (Gorner 2003).

The rate constant for triplet and chloride reaction, k_{Cl}

The rate constant k_{Cl} can be calculated from chloride competition experiment using **equation II-18** with a $[Cl]_{1/2}$ of 7 mM at which $C_1/{}^0C_1 = 0.5$ (**see Scheme II-6 and equation II-12**).

$$C_1/{}^0C_1 = k_{H2O} [H_2O] + {}^0k_T \ / \ k_{H2O} [H_2O] + {}^0k_T + k_{Cl}[Cl]_{1/2} \quad \text{(II-18)}$$

k_{Cl} is calculated to be $\mathbf{1.2 \sim 1.5 \times 10^8 \ M^{-1}s^{-1}}$. This value agrees with the value obtained from double reciprocal plot (**Figure II-13**) very well. There, a slope of 5 $\times 10^9$ and an intercept of 4.2×10^7 (s/M) were obtained and the rate constant ratio $k_{Cl}/k_{H2O} = 6.6 \times 10^3$ was calculated.

A similar value of $[Cl]_{1/2}$ (2.3 mM) with slightly different definition was reported by Gorner. The $[Cl]_{1/2}$ was defined as the concentration of chloride at which the decomposition quantum yield of quinone was 50% of the maximum value and could be calculated as $[Cl]_{1/2} = 1/(k_{Cl} \times \tau)$, where k_{Cl} was the triplet quenching rate of chloride and τ is the triplet lifetime in the presence of chloride in aqueous solution. In contrast to the result obtained in this work ($k_{Cl} = \mathbf{1.2 \sim 1.5 \times 10^8 \ M^{-1}s^{-1}}$), a substantially greater chloride - triplet quinone reaction rate constant ($k_{Cl} = \mathbf{2.4 \times 10^9 \ M^{-1}s^{-1}}$) was reported in Gorner's paper. Detailed investigation, however, showed that triplet lifetime and other rate constants reported there were internally contradictory and the Stern-Volmer relationship was violated.

The rate constant k_{Cl} was reported to be $\mathbf{2.4 \times 10^9 \ M^{-1}s^{-1}}$ which was problematic due to the use of a questionable triplet decay time ($< 0.2 \ \mu s$). Gorner defined $[Cl]_{1/2}$ (= $1/k_{Cl}\tau_T$), where k_{Cl} is the quenching rate constant of chloride to triplet quinone. With the reported $[Cl]_{1/2}$ (2.3 mM) and triplet lifetime ($< 0.2 \ \mu s$), the k_{Cl} can be calculated exactly as $\mathbf{2.4 \times 10^9 \ M^{-1}s^{-1}}$.

The quenching effects of different substrates on the triplet state and corresponding rate constants obtained in this work and Vaughan (1999) was summarized in **Table II-4.**

Table II- 4. **The triplet quenching rate constants and rate constant ratios of different substrates in aqueous mBQ photolysis**

substrate	$C_1/{}^0C_1$	$C_2-{}^0C_2$ $(\times 10^{-3}\ M)$	k_q $(M^{-1}s^{-1})$	kc/k_{DMSO} observed	kc/k_{DMSO} predicted
5.0 mM † KCl	0.6	10.63	$1.2 \sim 1.5$ $\times 10^8$	2.1	0.5
0.48 mM nitrite	0.48	4.4	* 3.6×10^9	9.2	1.7
24 mM formate	0.5	11	* 6.7×10^7	0.46	0.48
5 mM salicylate	0.13	38	* 2.1×10^9	8.0	4.1 (?)
10 mM DMPO	0.067	6.5	* 2.2×10^9	0.65	0.65

† KCl results were obtained from this work; results of other substrates were from Vaughan (1999).

* k_q: is the triplet quenching rate as shown in Scheme II-8, which can be calculated from equation II-12.

$$C_1/{}^0C_1 = k_{H2O}\ [H_2O] + {}^0k_T\ /\ k_{H2O}\ [H_2O] + {}^0k_T + k_q[q]_{1/2}$$

** Re-calculated rate constants using $C_1/{}^0C_1$ obtained in Vaughan (1999) and a revised triplet decay rate of $k_T = 1.6 \times 10^6\ M^{-1}s^{-1}$ from this work.

*** k_c: reaction rate constant of intermediate and q as shown in Scheme II-8. **k_c/k_{DMSO} observed** can be calculated from $C_2-{}^0C_2$ value using the following equation. $C_2-{}^0C_2 = k_c[q]/k_{DMSO}$

**** **k_c/k_{DMSO} predicated** is calculated using reaction rate constants of OH and substrates such as nitrite, formate, salicylate, DMPO, and DMSO.

$k_{NO2-} = 6.0 \times 10^9\ M^{-1}s^{-1}$ (Logager and Sehested, 1993).
$k_{Cl} = 3.0 \sim 4.3 \times 10^9\ M^{-1}s^{-1}$ (Grigor'ev et al. 1987; Jayson et al. 1973).
$k_{HCO2-} = 3.2 \times 10^9\ M^{-1}s^{-1}$ (Buxton and Greenstock 1988)
$k_{DMPO} = 4.3 \times 10^9\ M^{-1}s^{-1}$ (Buxton and Greenstock 1988)

Summary

At low mBQ concentrations and in the absence of DMSO or other competitors, the triplet quinone will react with water to form an intermediate, which subsequently collapses to the benzene-1,2,4-triol. Benzene-1,2,4-triol can be oxidized by quinone and/or atmospheric oxygen to produce the final photoproducts. In the presence of DMSO, however, the intermediate will react with DMSO and form methyl radicals as well as semiquinone. At high concentrations of DMSO, the rearrangement of the intermediate to benzene-1,2,4-triol was interrupted due to the competition of DMSO. The formation of semiquinone from DMSO and intermediate interaction was demonstrated in Pochon et al (2002) and supported by photolysis results from Gorner (2003).

Based on the evidence together with what was suggested in previous work (Pochon et al 2002; Kurien and Robins 1970), the mechanism for the photolysis of mBQ at low concentration is proposed in **Scheme II-9**.

In the absence of DMSO:

$$^3Q^* \xrightarrow{\;H_2O\;} \quad \longrightarrow \quad \longrightarrow QH_2 + QOH$$

In the presence of DMSO:

$$^3Q^* \xrightarrow{\;H_2O\;}$$

$$CH_3SOOH + {}^\bullet QH + {}^\bullet CH_3 \xrightarrow{\;3ap\;} \quad \longrightarrow \quad III$$
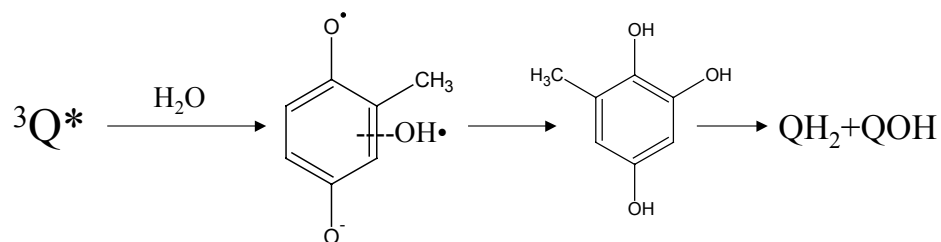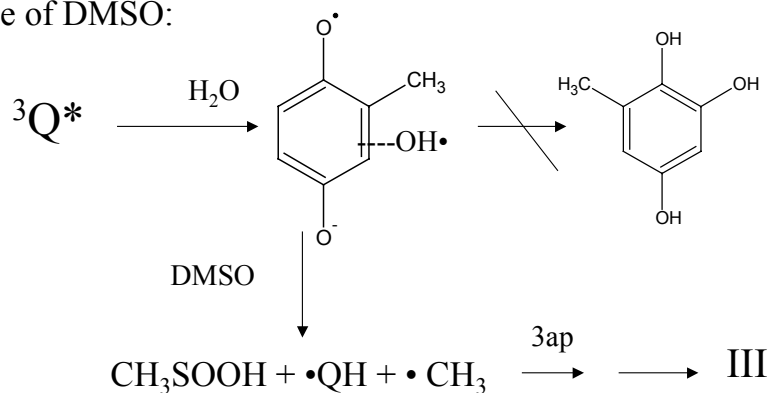
Scheme II - 9. The photochemical mechanism of mBQ photolysis at low quinone concentration in the absence and presence of DMSO.

The results of an optical absorption study supported the above mechanism. As shown in the **Figure II-6**, in the absence of DMSO both hydroquinone and hydroxylated quinone were formed. However, in the presence of DMSO, at low concentrations of 2-methyl-1,4-benzoquinone, only hydroquinone was formed (**Figure II – 8**). The disappearance of hydroxylated quinone was due to the switch of the reaction pathway in the presence of DMSO. Without DMSO, benzene-1,2,4-triol was formed from the rearrangement of the intermediate. In the presence of high concentrations of DMSO, no benzene-1,2,4-triol was produced and the intermediate

reacted with DMSO to produce semiquinone radical or radical anion accompanied with methyl radical. The semiquinone radicals could combine to form the hydroquinone. However, no hydroxylated quinone would be produced as seen in the spectrum.

At high concentrations of mBQ, according to both radical trapping and 3ap consumption experiments, the major reaction pathway was switched to triplet quinone and ground state quinone reaction.

Based on the above experiments, an overall mechanism for the photolysis of mBQ in aqueous solution at both low and high concentrations is presented as shown in **Scheme II-10**.

$$^3Q^* \xrightarrow[\text{Low [Q]}]{H_2O} [Q^*\!\!-\!\!H_2O] \longrightarrow Ph(OH)_3 \longrightarrow QH_2 + Q\text{-}OH$$

$[Q^{\bullet-} \; Q^{\bullet+}]$

$^1Q^*$

high [Q]

OH^-

$h\upsilon$

$\xrightarrow{+Q} QH_2 + Q\text{-}OH$

Q

DMSO

$CH_3SO(OH) + \bullet QH + \bullet CH_3$

3ap

Fluorescent product III
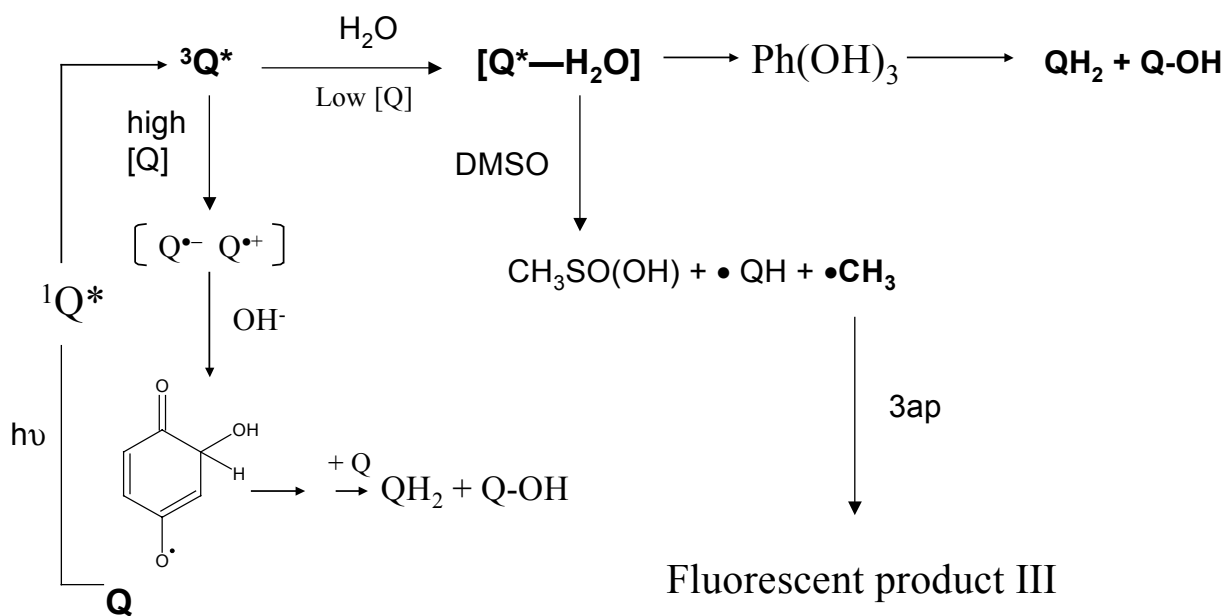
Scheme II - 10. The overall photochemical mechanism for mBQ at both low and high concentrations.

The optical absorption study at high concentrations of mBQ (**Figure II-18 and II-19**) provided further evidence to support the mechanism proposed in Scheme II-10. At high concentrations of mBQ, the major photolysis pathway was quinone-

quinone reaction. DMSO would not react with the intermediate produced from quinone-quinone interaction to a measurable extent and thus the product formation would not be affected by the presence of DMSO. Again, the argument that DMSO acted as a sole triplet state quencher was overturned.

The structure of the intermediate, if any, formed in high concentrations of quinone solutions could be separated cation and anion quinone radicals or a non – separated charge separated excited state of quinone dimer. No matter what the intermediate is, it does not react with DMSO. This may result from that the intermediate is too short live or not capable of reacting with DMSO. Contradictory descriptions have been provided in the literatures as previously discussed in Chapter I. Gorner claimed that neither free radical (semiquinone radical etc.) nor ground state and excited state dimer was produced in the photolysis of benzoquinones at both high and low concentrations. von Sonntag et al. (2004), on the other hand, proposed a free radical mechanism for the photolysis of benzoquinone at high concentration with the formation of exciplex dimer and subsequent generation of separated quinone cation and semiquinone anion radical. The quinone radical cation was then expected to react with water "immediately" and form the final products.

Chapter III   Aqueous Photochemistry of Dimethyl and Dichloro Benzoquinone

Introduction

In the previous chapters it was proposed that at low mBQ concentration, the reaction proceeds through a $^3Q^*$ - H_2O intermediate to form a trihydroxyybenzene, which proceeds to form the final products, while at high mBQ concentration, Q-$^3Q^*$ is the major pathway.

Here we examine how the mechanism might change as a function of substituents on the quinone ring. In particular, we want to examine whether the mechanism change with the thermodynamic driving force for electron transfer from water to the excited triplet state quinone. A series of quinones (**Scheme III–1)** with different substituents including dimethyl-, dichloro-, and tetrachloro-1,4-benzoquinones were employed for a systematic investigation. **Table III-1** summarizes the thermodynamic parameters for these compounds.

Aqueous quinone photochemistry is the reaction of excited triplet quinone with water. Because excited state electron donor has smaller ionization potential (IP*) and excited state electron acceptor has larger electron affinity (E_A*) than their respective ground state molecules, excited states are better electron donor and acceptors and thus are stronger reductants and/or oxidants (Kavarnos 1993).

For oxidation-reduction or electron transfer reactions to take place, the free energy change ΔG should be negative. For quinone and water reaction (**III-1)**, the free energy change can be calculated according to equation **III-2**.

$$^3Q^* + H_2O \rightarrow Q^{\bullet -} + OH + H^+ \qquad\qquad (III\text{-}1)$$

$$\Delta G_{eT} = E_{ox} - (E_{red} + E_T) \qquad\qquad\qquad \text{(III-2)}$$

where ΔG_{eT} is the free energy of electron transfer reaction. E_{ox} is the oxidation potential of the electron donor (water) and E_{red} is the reduction potential of ground state electron acceptor (quinone) (Green et al 1990). E_T is the excited triplet energy ($E_T = 2.2 \sim 2.7\text{eV}$) of quinone (Hubig and Kochi 1999).

The standard oxidation potential for the reaction of water (**III-3**) is 2.65 V with respect to NHE (Schwarz 1981). This potential would be 2.24 V at pH 7 using a correction factor of 0.05915 V per pH unit.

$$\bullet OH + H^+ + e^- \rightarrow H_2O \qquad\qquad\qquad \text{(III-3)}$$

The conversion between NHE and SCE reduction potentials can be obtained by equation **III-4**.

$$\text{Potential vs. NHE} - 0.2412\ V = \text{Potential vs. SCE} \qquad \text{(III-4)}$$
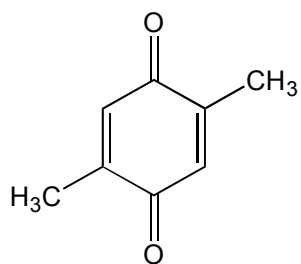
2,5-Me₂BQ   **2,6-Me₂BQ**

2,5-Cl₂BQ   **2,6-Cl₂BQ**   **Cl₄BQ**

Scheme III - 1. The structures of dimethyl-, dichloro-, and tetrachloro-1,4-benzoquinones.

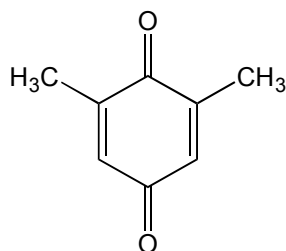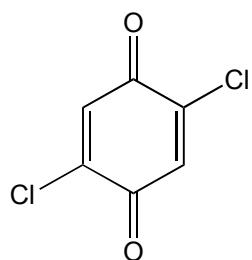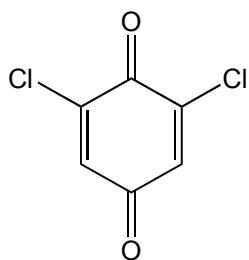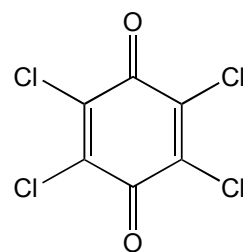**Table III- 1.   Reduction potentials and free energy change for different quinones**

Quinones	E_{red} (v)	E_T (ev)	pKa	ΔG_{eT} (V)
2,5-MeBQ	-0.067[a]	2.24[b]	4.6[c]	0.067
2,6-MeBQ	-0.08[d]	2.24[b]	4.75[c]	0.08
mBQ	0.023[a]	2.24[†]	4.45[c]	-0.023
BQ	0.078[d]	2.301[e]	4.0[i]	-0.139
2,5-ClBQ	0.21[f]	2.29[g]		-0.26
2,6-ClBQ	0.21[f]	2.27[g]		-0.24
Cl_4BQ	> 0.43[†]	2.70[h]		-0.89

This table was modified from that in Vaughan (1999).

a = Ilan, Y., Czapski, G. and D. Meisel *Biochim. Biophys. Acta.* 430, 209-224.

b = Bruce, J. M. Photochemistry of quinones. *The chemistry of quinonoid compounds.* S.Patai. New York, John Wiley and Sons. 1. 465 – 538.

c = Patel, K. B. and Willson, R.L. J. Chem. Soc., Farad. Trans. I.1973, 69, 814 – 825.

d = Meisel, D. and Fessenden, R. W. *J. Am. Chem. Soc.* 1976, 98, 7505-7510.

e = Beck, S.M. and Brus, L.E. *J. Am. Chem. Soc*. 1982, 104, 1103-1104.

f = Raymond, K.S., Grafton, A. K. and Wheeler, R.A. *J. Phys. Chem. B*. 1997, 101, 623-631.

g = Trommsdorff, H.P., Sahy, P. and Kahane-Paillous, J. *Spectrochimica Acta (A),* 1970, 26, 1135.

h = Hubig, S. M. and Kochi, J. K. *J. Am. Chem. Soc.* 1999, 121, 1688 –1694.

i = Adams, G. E. and Michael, B. D. *Trans. of the Farad. Soc.*1967, 63,1171-1180.

[†]Estimated value: The E_{red} value for Cl_4BQ in aqueous solution was estimated based on the difference between E_{red} values of 2,5-, 2,6-Cl_2BQ (*E_{red} =1.76 V) and Cl_4BQ (*E_{red} =2.15 V) in organic solvents (Hubig and Kochi, 1999). The difference in electron affinities calculated by Raymond et al (1997) also supported this estimation, where the calculated electron affinity of 2,5-, 2,6- and tetrachloro-1,4-benzoquinone are 2.48 eV, 2.48 eV, and 2.83 eV, respectively.

Although the photolysis of 1,4-benzoquinone in aqueous solution was shown to be incapable of producing OH radical (Gorner 2003; von Sonntag et al 2004) and similar result was obtained from our experiments for the photolysis of methyl-1,4-benzoquinone in aqueous solution as shown in Chapter II, with the substitution of electron withdrawing Cl-groups complete electron transfer could take place and consequently produce OH radicals.

Substituents have a significant effect on the redox potentials and thus could significantly alter the photochemical mechanism of different quinones. Methyl groups are electron donors and the incorporation of electron donating group to quinone ring will lower the reduction potential of the substituted quinone and result in a more positive free energy change. Cl-groups, on the other hand, are electron withdrawing and will make the quinones better electron acceptors. Since the oxidation potential of H_2O remains unchanged, but the reduction potential of the electron acceptor (quinone) will increase with increasing numbers of Cl substituent. When the reduction potential of the electron acceptor is sufficiently high, electron transfer between water (donor) and quinone (electron acceptor) could take place.

Experimental

Chemicals

2,6-dimethyl-benzoquinone 99%, 2,6-dichloro-1,4-benzoquinone 98%, 2,5-dichloro-1,4-benzoquinone 98%, tetrachloro-1,4-benzoquinone, salicylic acid 99+%, 3-hydroxybenzoic acid 99+%, 4-hydroxybenzoic acid 99+%, HPLC grade dimethyl sulfoxide 99% (DMSO), HPLC grade acetonitrile 99.93+%, phosphoric acid 85 wt% (99.999%), boric acid 99.999%, sodium dihydrogen phosphate 99.999%, sodium hydrogen phosphate 99.995%, sodium hydroxide 99.98%, fluorescamine (>97% TLC powder), and 3-carbamoyl-proxyl free radical 97% (3-CP) were obtained from Aldrich. 2,5-dimethyl-p-benzoquinone and 3-amino-2,2,5,5-tetramethyl-1-pyrrolidinyloxy 99% (3ap) were purchased from Arcos. Reagent grade $NaNO_3$, $NaNO_2$, HPLC grade methanol, 30% H_2O_2, 2-propanol, and chloroform were obtained from Fisher. Glacial acetic acid (99.9%) was purchased from J.T. Baker. Ultra pure grade nitrogen and methane were purchased from Airgas.

2,5-dichloro1,4-benzoquinone was recrystallized from ether. Tetrachloro-1,4-benzoquinone was recrystallized from acetic acid or acetone. All other quinones were purified by sublimation and stored at 4°C protected from light. Benzoic acid was recrystallized from water and store at room temperature in dark. A Millipore Milli-Q system provided water for all the experiments.

2,5-Me_2BQ and 2,6-Me_2BQ are very soluble in water. 2,5-Cl_2BQ and 2,6-Cl_2BQ are soluble and 2,6-Cl_2BQ aqueous solutions will turn brown when stored at room temperature in dark after several hours. Tetrachloro-1,4-benzoquinone is least

soluble and the concentration of saturated Cl_4BQ aqueous solution can only be determined approximately from the extinction coefficient of this quinone (ε_{296} = 1.906×10^4) in organic solvents, assuming that the extinction coefficient will not change significantly in aqueous solution.

Instrument and Techniques

VWR model 150T sonicator was used to assistant dissolve dichlorobenzoquinone and especially tetrachlorobenzoquinone due to its extremely low solubility in aqueous solution.

The HPLC, irradiation systems, spectrophotometer, electronic balance, and pH meter were the same as described in Chapter II.

Identical protocols for radical trapping and benzoic acid product analysis were employed in this work.

Results

Radical Trapping Experiments with DMSO

Identical experimental protocols for radical trapping using 3ap and DMSO were applied to 2,5-Me$_2$BQ, 2,6-Me$_2$BQ, 2,5-Cl$_2$BQ, 2,6-Cl$_2$BQ, and Cl$_4$BQ.

Solutions contained quinone, 3ap, and various concentrations of DMSO were irradiated under anaerobic condition. The production of III was observed in the presence of 3ap and DMSO in radical trapping experiment for all quinones.

As shown in **Figure III-1,** the initial rate of III production increases with DMSO at low concentrations and reaches saturation value at high concentration of DMSO. [DMSO]$_{1/2}$ values obtained from experimental were summarized in **Table III-2**.
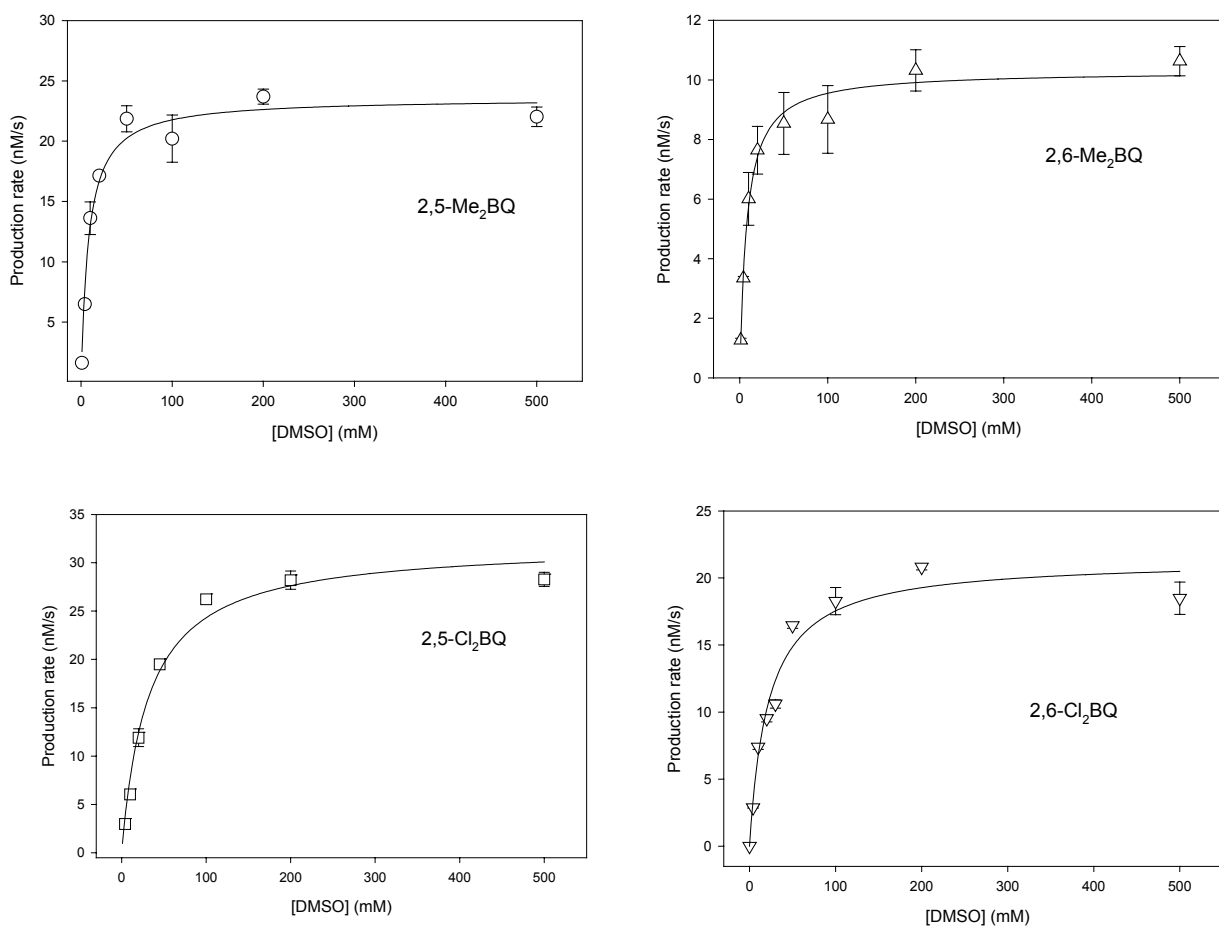
Figure III- 1. Dependence of initial III production rate on DMSO concentrations for different quinones.

20 μM 2,5-Me$_2$BQ (○) or 2,6-Me$_2$BQ (Δ), 50 μM 3ap, and DMSO was irradiated at 325 nm for 2 min. LP =5.53 ×10^{-4} W/cm^2. 10 μM 2,5-Cl$_2$BQ ( ) or 2,6-Cl$_2$BQ (∇), 50 μM 3ap, and DMSO was irradiated at 334 nm for 2 min. LP =8.87 ×10^{-4} W/cm^2.

Table III- 2. [DMSO]$_{1/2}$ and ^{EX}k$_{DMSO}$ values for different quinones in the absence of competitor

quinone	^{Ex}[DMSO]$_{1/2}$	Th[DMSO]$_{1/2}$	^{EX}k$_{DMSO}$	^{EX}k$_{DMSO}$/k$_{DMSO}$
mBQ	5.6 ± 0.5mM	51.5 µM	7.43×10^7	1.13×10^{-2}
2,5-MeBQ	8.2 ± 1.4 mM	66.7 µM	5.17×10^7	7.83×10^{-3}
2,6-MeBQ	7.6 ± 1.2 mM	66.7 µM	5.58×10^7	8.43×10^{-3}
2,5-ClBQ	25.9 ± 6.5 mM	51.5 µM	1.37×10^7	2.07×10^{-3}
2,6-ClBQ	21.9 ± 3.7 mM	51.5 µM	1.88×10^7	2.85×10^{-3}

k$_{DMSO}$ = 6.6×10^9 M^{-1} s^{-1} , k$_{3ap}$ = $3.6 \sim 7.8 \times 10^9$ M^{-1} s^{-1} (from this lab)

As shown in Table III-2, the [DMSO]$_{1/2}$ values obtained from experiments are much greater than those calculated on the basis of OH radical and thus indicate a mechanism that does not involve OH. It is interesting to note that the [DMSO]$_{1/2}$ values of dichloro-1,4-benzoquinones are about 5 times greater than those of dimethyl and methyl benzoquinones.

In contrast to the other quinones, the [DMSO]$_{1/2}$ value obtained for Cl$_4$BQ was substantially smaller than those of other quinones and consistent with the reaction with OH.

To additionally test for the formation of OH by Cl$_4$BQ, different competitors such as MeCN and benzoic acid were employed to examine the kinetics of reaction with DMSO. As shown in **Figure III-2**, in the presence of 100 mM MeCN and 5 mM

benzoic acid, [DMSO]$_{1/2}$ values were 0.3 mM and 4.31 mM, respectively. These values are consistent with the reaction with OH based on the known rate constants for reactions of OH with these competitors (**Table III-3**).

Table III- 3.   [DMSO]$_{1/2}$ and ^{EX}k$_{DMSO}$ values for tetrachloro-benzoquinone in the presence of competitors

Competitors	Experimental [DMSO]$_{1/2}$	Calculated [DMSO]$_{1/2}$	^{EX}k$_{DMSO}$	^{EX}k$_{DMSO}$ /k$_{DMSO}$
100 mM MeCN	0.26 ± 0.1mM	0.30 mM	8.32×10^9	1.25
5 mM EtOH	1.52 ± 0.26 mM	1.83 mM	7.96×10^9	1.2
5 mM Benzoic acid	4.31 ± 1.6mM	3.66 mM	5.61×10^9	0.85

- k$_{EtOH}$ = $1.9 \times 10^9\,M^{-1}.s^{-1}$,
- k$_{BA}$ = $4.3 \times 10^9\,M^{-1}.s^{-1}$,
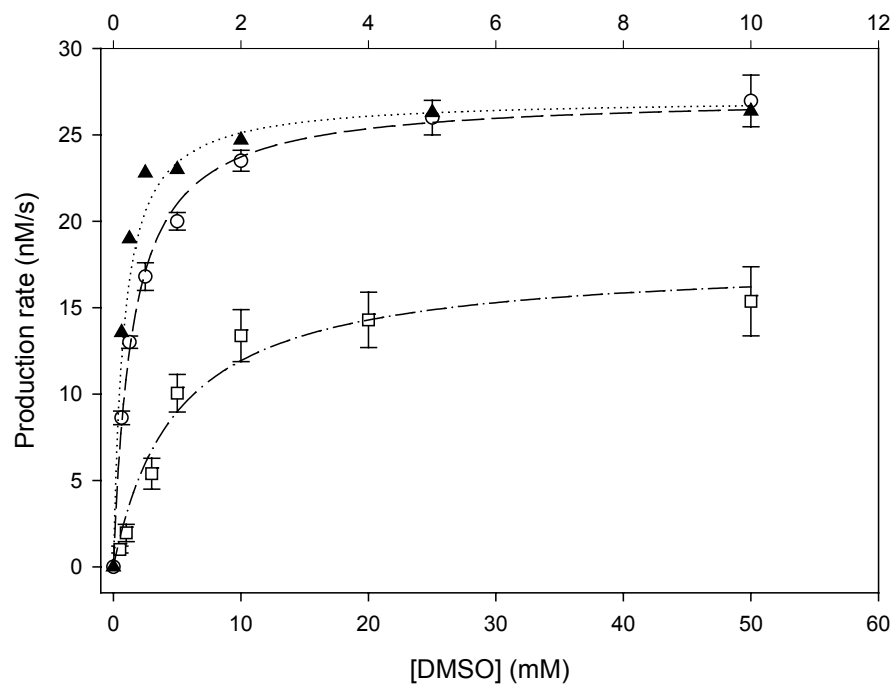- k$_{MeCN}$ = $2.2 \times 10^7\,M^{-1}.s^{-1}$

(Buxton and Greenstock 1988)

Figure III- 2. Dependence of initial III production rate on DMSO concentration during the photolysis of Cl$_4$BQ in aqueous solution.

12.5 μM Cl$_4$BQ, 30 μM 3ap, and DMSO (▲ top x axis) in the presence of 100 mM MeCN, (○ top x axis) and 5 mM BA (□ bottom x axis) were irradiated at 296 nm with 50% neutral density filter for 2 min. The lamp intensity was 3.8×10^{-4} W/cm^2.

Radical Trapping Experiment with Methane

To further test for the production of OH during photolysis of quinones, radical trapping experiments with CH_4 were conducted. The initial production rate of III (P_{CH4}) was compared to that of DMSO (P_{DMSO}) under identical conditions. The change of quinone concentration was monitored by UV spectra.

In the presence of CH_4, only trace amounts of III were detected from dimethyl-1,4-benzoquinone photolysis, indicating little or no production of OH, similar to what was observed with mBQ. Increased amounts of III was produced in the photolysis of aqueous dichloro-1,4-benzoquinone solution (**Figure III-3**).
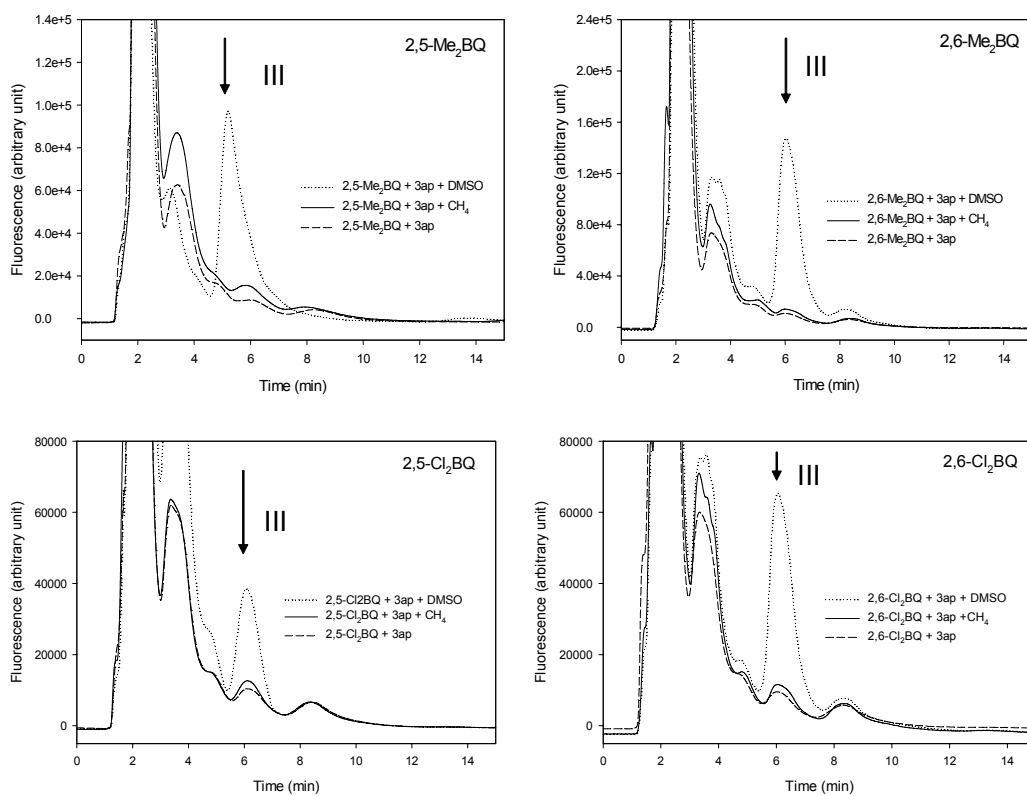
Figure III- 3. The chromatogram of III obtained from radical trapping experiments with DMSO and CH$_4$ under the same conditions in the photolysis of dimethyl and dichloro-benzoquinones in aqueous solution.

In contrast, a significant amount of III was produced during the photolysis of tetrachloro-1,4-benzoquinone in the presence of methane (**Figure III-4**). The initial production rate of III from radical trapping with methane was much greater than 5 σ of blank signal, where σ was the standard deviation of the blank signal (n=3).
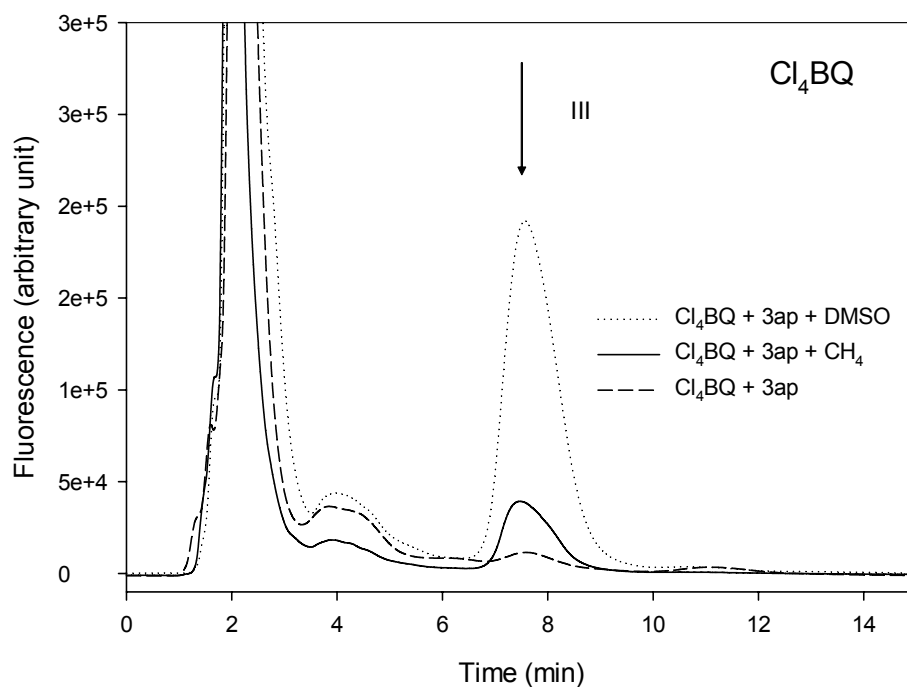

Figure III- 4. The chromatogram of III obtained in nitroxide trapping experiments with DMSO and CH_4 under the same condition for the photolysis of Cl_4BQ.

12.5 μM Cl_4BQ and 30 μM 3ap aqueous solutions were irradiated at 296 nm in the presence of 50 mM DMSO or saturated CH_4 in pH 5.0 aqueous solution.

Compared with III produced via nitroxide trapping in the presence of DMSO, the experimental initial rate ratio P_{DMSO}/ P_{CH4} for Cl_4BQ photolysis was 6, which agreed with theoretical ratio calculated on the basis of OH very well. The theoretical ratio of P_{DMSO}/ P_{CH4} can be calculated using **equation II-8** as shown below.

$R = P_{DMSO}/ P_{CH4} = 1 + \{k_{3ap}[3ap]+k_Q[Q]\}/ k_{CH4}[CH_4]$

where $k_{3ap} = 3 \sim 4\times10^9$ $M^{-1}.s^{-1}$ (this group), $k_Q =1.2 \sim 6 \times10^9$ $M^{-1}.s^{-1}$ (Adams and Michael 1967; Scheuchmann et al. 1998), and $k_{CH4} =1.2\times10^8$ $M^{-1}.s^{-1}$ (Stevens et al. 1972).

Both radical trapping experiments with DMSO and CH_4 indicate that OH radical is a major product in the photolysis of tetrachloro-1,4-benzoquinone aqueous solution, while other quinones produced no or very small amounts of OH upon irradiation.

To further test this conclusion, the photolysis of quinone was performed in the presence of benzoic acid and then analyzed for the formation of hydroxybenzoic acids, the products of OH reaction.

Only about 2~3 nanomolar of 2-OH-BA was detected during the photolysis of 10 to 20 μM dimethyl-benzoquinones in the presence of benzoic acid as shown in **Figure III-5**.
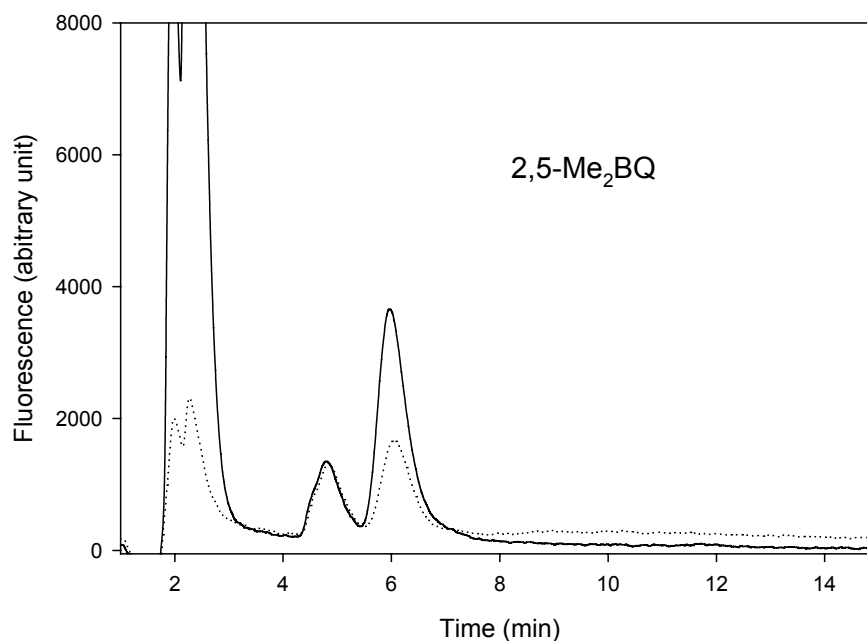
Figure III- 5.   The production of 2-OH-BA (peak at 6.2 min) in the photolysis of benzoic acid and 2,5-Me₂BQ aqueous solution.

20 µM of 2,5-Me₂BQ and 300 µM of benzoic acid was irradiated with 334 nm light for 0 sec (dotted line) and 100 sec (solid line).

Slightly increased amount of 2-OH-BA was detected in the cases of dichloro-benzoquinones (**Figure III-6**). No 3-OH-BA and 4-OH-BA was detected in the photolysis of dimethyl- and dichloro-benzoquinones, consistent with the high detection limits of these two hydroxylated acids.
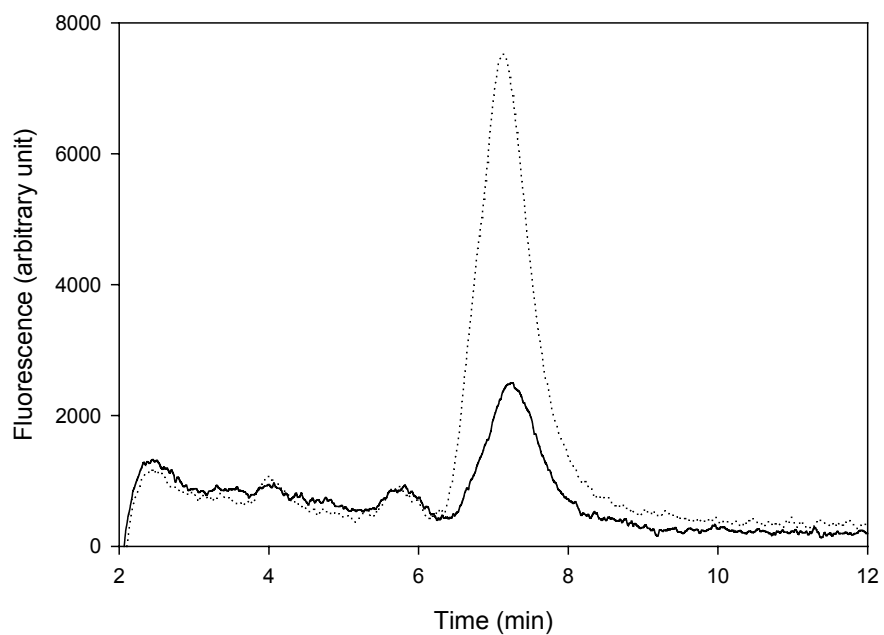
Figure III- 6.   The production of 2-OH-BA (peak at 7.3 min) from photolysis of 2,6-Cl$_2$BQ and benzoic acid aqueous solution.

30 μM of 2,6-Cl$_2$BQ and 1 mM benzoic acid was irradiated at 334 nm for 2 min (dotted line) and 0 min (solid line) with monochromatic light in aqueous solution.

The difference in 2-OH-BA retention times was due to variation in mobile phase composition. The blank signal was due to the small amount of 2-OH-BA contamination in benzoic acid sample.

For tetrachloro-1,4-benzoquinone, however, significant amounts of 2-OH-BA were detected when the sample containing 12 μM Cl_4BQ and 100 μM of benzoic acid was irradiated at 296 nm as shown in **Figure III-7**. An identical amount of 4-OH-BA was detected in the photolysis of Cl_4BQ with benzoic acid. Both 2-OH-BA and 4-OH-BA production yields increased linearly with increasing irradiation time under optically thin conditions. 3-OH-BA was not detected due possibly to the high detection limits of this hydroxylated benzoic acid.
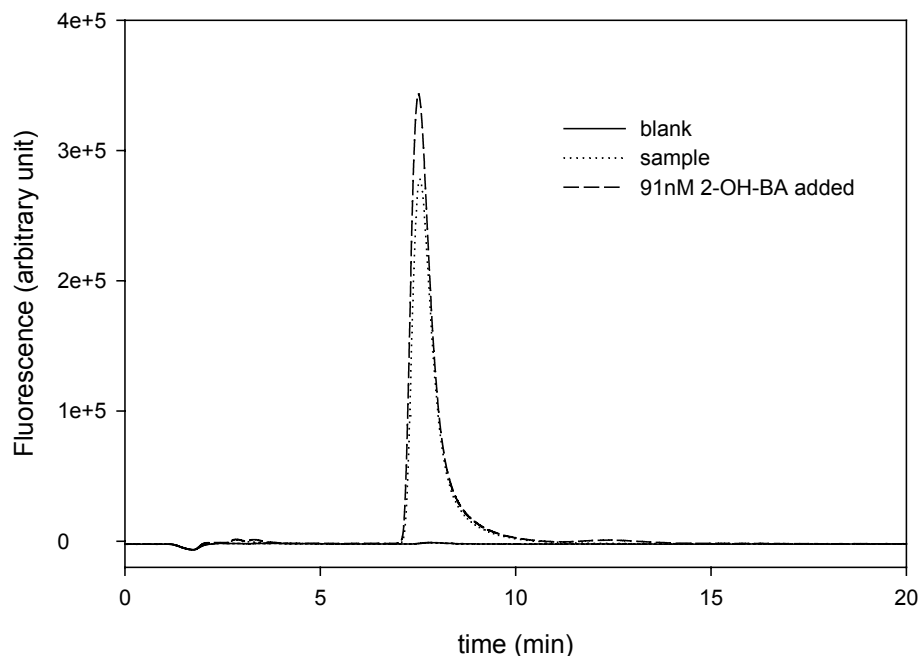
Figure III- 7.   The chromatogram of 2-OH-BA (peak at 8.0 min) produced from photolysis of Cl$_4$BQ and benzoic acid aqueous solution.

100 μM BA + 12.5 μM Cl$_4$BQ was irradiated @296 nm for 20 min with 50% transmittance ND filter during which about 20% Cl$_4$BQ was reacted. The lamp intensity was LP = 3.5×10^{-4} W/cm^2. Blank 100 μM BA was irradiated @296 nm for 20 min with ND filter   (——); 0.7 μM 2-OH-BA was produced from the sample (·····); 91 nM of standard 2-OH-BA was added to show that the species produced in the photolyed sample (– – –) was 2-OH-BA.

To compare the results of benzoic acid product analysis and radical trapping experiments, the change of quinone concentration was monitored spectroscopically and used as the basis for normalization. 3ap, DMSO, BA had no significant spectral overlap with quinones at wavelength longer than 296 nm as shown in **Figure III-8**.

No significant interference and inner filter effects in monitoring quinone concentration change or absorbing irradiation light was observed. Generally two wavelengths of the UV spectra should be monitored to ensure the accuracy of [Q] change because one wavelength may have artifacts due to the overlap of new and existing compounds spectra.
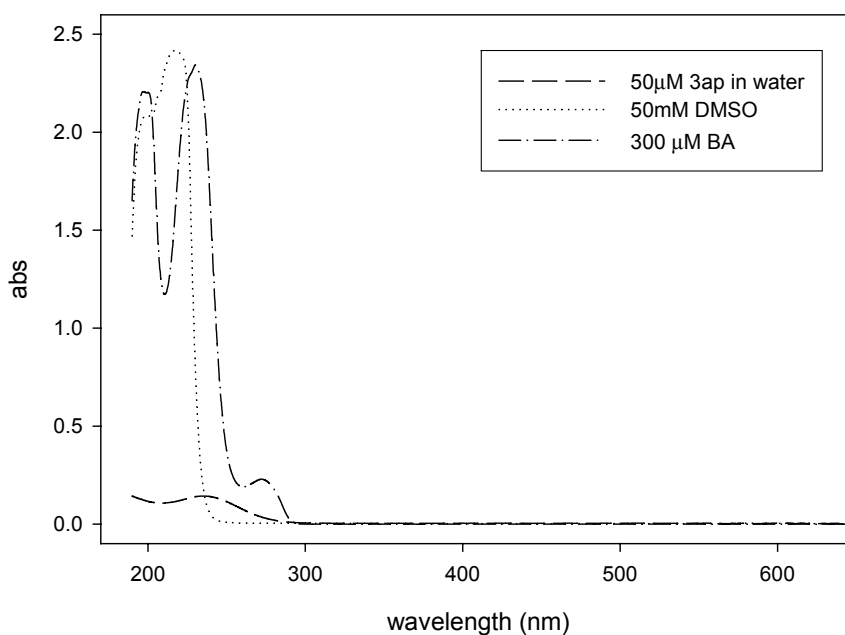

Figure III- 8.   The UV spectra of 50 μM 3ap, 50 mM DMSO, and 300 μM BA in aqueous solution.

The production of hydroxylated benzoic acids was compared with III production obtained from radical trapping experiment with 3ap in the presence of DMSO and CH$_4$ (summarized in **Table III-4**).

Table III- 4. P_{DMSO}/P_{BA} and P_{DMSO}/P_{CH4} values for quinones

	2,5-Me$_2$BQ	2,6-Me$_2$BQ	mBQ	2,5-Cl$_2$BQ	2,6-Cl$_2$BQ	Cl$_4$BQ
P_{DMSO}/P_{BA}	81 ± 5	95 ± 5	52 ± 5	22 ± 3	26 ± 4	1.5 ± 0.1
P_{DMSO}/P_{CH4}	< 100	< 100	~ 100	> 50	> 60	$6 \sim 10$

† Theoretical $P_{DMSO}/P_{BA} = 1$; and $P_{MDSO}/P_{CH4} = 4 \sim 8$. Assumes $P_{BA} = 3\, P_{2\text{-OH-BA}}$. (Oturan and Pinson 1995).

† The theoretical ratio of initial production rate P_{DMSO}/P_{CH4} can be calculated by **equation II-8** as showing below.

$$P_{DMSO}/P_{CH4} = 1 + \{k_{3ap}[3ap]+k_Q[Q]\}/ k_{CH4}[CH_4]$$

the rate constants between 3ap, quinone, CH$_4$ and OH are $k_{3ap} = 3 \sim 4\times10^9$ M^{-1}s^{-1} (this group), $k_Q =1.2 \sim 6\times10^9$ M^{-1}s^{-1} (Adams and Michael 1967; Scheuchmann et al. 1998), and $k_{CH4} =1.2\times10^8$ M^{-1}.s^{-1} (Stevens et al. 1972).
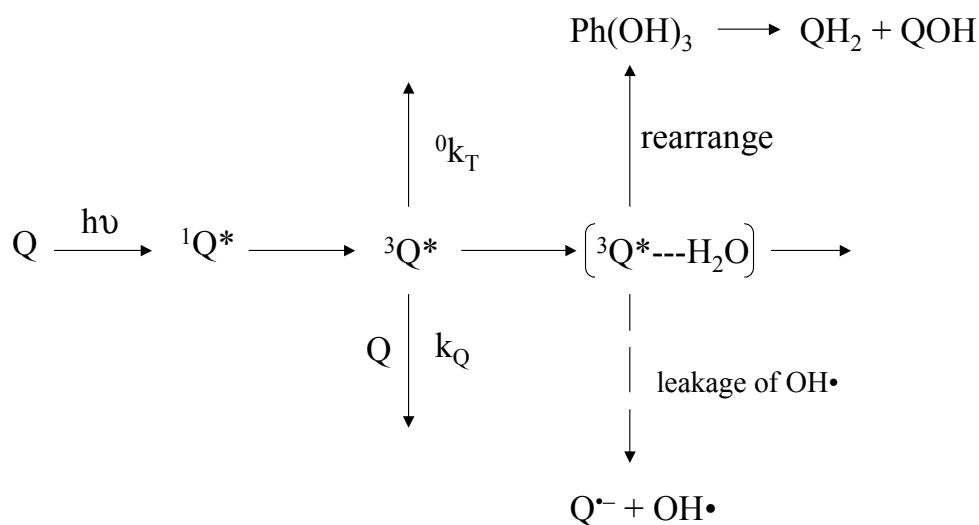
Discussion

P_{DMSO} measures the production of both strong oxidant and free OH, while P_{CH4} and P_{BA} measure the production of OH. The ratios, P_{DMSO}/P_{BA} and P_{DMSO}/P_{CH4}, indicate OH production fraction and therefore the OH production ability of different quinones. As seen in previous sections, P_{DMSO}/P_{BA} and P_{DMSO}/P_{CH4} ratios decreases with increasing number of Cl group in substituted quinones indicating that the OH production ability in the photolysis of aqueous quinones increases with increasing number of electron withdrawing group (chloro).

The radical trapping with 3ap in the presence of DMSO and CH_4 as well as product analysis of benzoic acid reaction show that OH is not a major product in the photolysis of dimethyl-, methyl-, and dichloro-1,4-benzoquinones in aqueous solution. However, trace amounts of OH were detected by the use of benzoic acid and radical trapping with 3ap in the presence of CH_4 for dichloro-benzoquinone. In the presence of 3ap and methane, the photolysis of Cl_4BQ generates substantial amounts of III. The photolysis of tetrachloro-1,4-benzoquinone with benzoic acid produces stoichiometric amounts of 2-OH-BA and 4-OH-BA. These indicate that OH is the major product of tetrachloro-1,4-benzoquinone photolysis in aqueous solution.

The above results are consistent with the suggestion of the formation of an intermediate exciplex between triplet state quinone ($^3Q^*$) and water and the "leakage" of OH from this intermediate was observed for quinones that are much better electron acceptors.

As shown in **Scheme III-2**, for dimethyl- and methyl-1,4-benzoquinones, which are not good electron acceptors, the intermediate exciplex ($^3Q^*$---H_2O) will mainly rearrange to form benzene-1,2,4-triol and then the final products.

$$Ph(OH)_3 \longrightarrow QH_2 + QOH$$

$$Q \xrightarrow{h\upsilon} {}^1Q^* \longrightarrow {}^3Q^* \longrightarrow \left[{}^3Q^*\text{---}H_2O\right] \longrightarrow$$

$$Q^{\bullet-} + OH\bullet$$

with pathways labeled: ^0k_T (upward from $^3Q^*$ to Ph(OH)$_3$), rearrange (upward from exciplex), k_Q with Q (downward from $^3Q^*$), leakage of OH• (downward from exciplex to $Q^{\bullet-} + OH\bullet$).

Scheme III - 2. Quinone photochemical pathways and the generation of OH from triplet quinone - water exciplex intermediate.

For dichloro-1,4-benzoquinone, which are better electron acceptor, increased leakage of OH from this intermediate exciplex was observed.

In the cases of tetrachloro-1,4-benzoquinone, which is an extremely good electron acceptor, free OH was produced as shown in Scheme III-3.
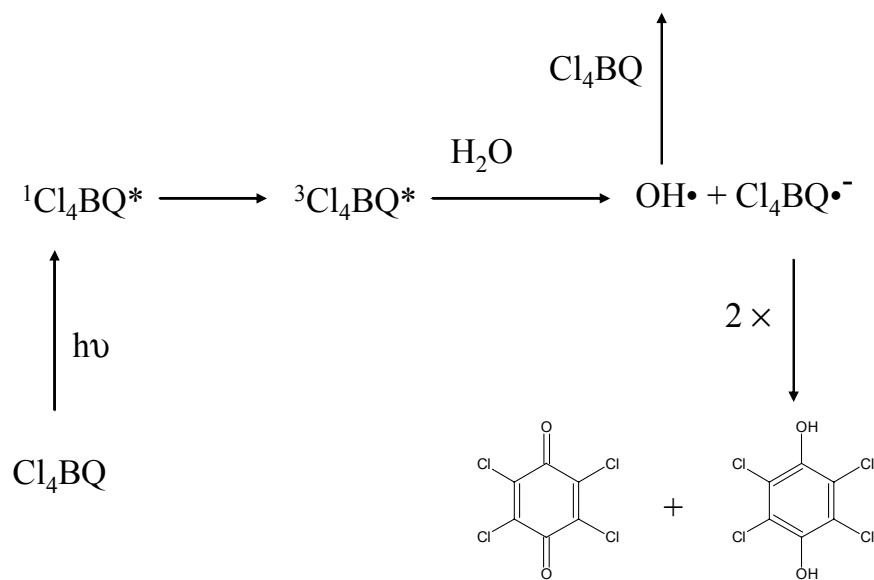
Scheme III - 3. The OH mechanism of tetrachloro-1,4-benzoquinone photolysis in aqueous solution.

The general trend that OH production ability increased with increasing number of electron withdrawing group in quinone molecule agrees with thermodynamic principles. As shown in **Table III-1**, the reduction potentials of different quinones increase with increasing number of Cl group. The free energy changes for the reaction of triplet quinone with water become more negative as calculated from **equation III-2**.

It is worth noting that in the cases of dichloro-1,4-benzoquinones, higher [DMSO]$_{1/2}$ values were obtained relative to those of dimethyl and methyl-1,4-benzoquinone. This indicated that either the intermediate formed was less reactive compared with that of dimethyl-1,4-benzoquinones or the relaxation of the intermediate was much more rapid and thus required more DMSO to compete effectively.

The investigation of this series of 1,4-benzoquinones successfully revealed the mechanisms of aqueous quinone photochemistry and demonstrated the OH production ability of different quinones with respect to the thermodynamic driving forces.

Chapter IV   Hydroxyl Radical Production in Environmental Systems

Introduction

Photo-produced reactive oxygen species (ROS) have been suggested to have a significant influence on carbon, sulfur, nitrogen, nutrient, and trace metal cycles in natural waters. To date, environmental scientists have recognized the existence of a number of reactive oxygen species including hydrogen peroxide (H_2O_2), superoxide ($O_2^{\bullet-}$), singlet dioxygen ($^1O_2$), hydroxyl radicals (OH), and organic peroxyl radicals (RO_2) in natural waters (Blough 1997; Blough and Zepp 1995). Among these reactive oxygen species, OH radicals are the most reactive and least selective in the reactions with organic and inorganic compounds. It is widely accepted that photolysis of nitrate and nitrite produces OH radicals (White et al 2003 and references therein). Further, photolysis of colored dissolved organic matter (CDOM) was suggested to be the main source for OH production over most of the oceans (Mopper and Zhou 1990). The possible organic sources of OH are thus investigated in this work. As demonstrated in previous chapters, the study of the photochemistry of quinone compounds, which were previously thought to represent the possible OH source, indicates that OH is not a major product in the photolysis of aqueous quinone solutions. A strong oxidant, thought to be an exciplex between $^3Q^*$ and H_2O, is produced upon UV irradiation. Therefore, whether the previously reported OH was truly an OH radical or another strong oxidant is open to doubt.

A number of potential problems in previous natural water photolysis studies could lead to a mistaken conclusion. First, the contribution from known OH sources, nitrite and nitrate photolysis, was not rigorously tested. Second the detection method for OH was not specific for OH radical. Methanol was used as an OH radical scavenger and the subsequent production of formaldehyde from methanol and OH reaction was monitored to indicate the presence of OH (Mopper and Zhou 1990). However, other strong oxidants such as triplet quinone could also abstract H atom from methanol and produce $\cdot CH_2OH$, which subsequently produces formaldehyde in the presence of dioxygen. Therefore, the detection of formaldehyde is not an unequivocal evidence for the involvement of OH. Third, although the authors claimed that dissolved organic matter appears to be the main source of OH in the photolysis of seawaters, no isolated organic matter was investigated to support this conclusion (Mopper and Zhou 1990).

The goal of this research is therefore to clarify whether dissolved organic matter (DOM) is a source of OH in the photolysis of natural waters.

Properties and Composition of CDOM Dissolved organic matter (DOM) in surface waters contains colored material, often called humic substance, Gelbstoffe, or colored dissolved organic matter (Blough and Del Vecchio 2002). The composition and structure of DOM are poorly characterized and the optical properties of CDOM are also not well understood. However, the absorption of CDOM in natural waters is universally similar to what is illustrated in **Figure IV-1.**
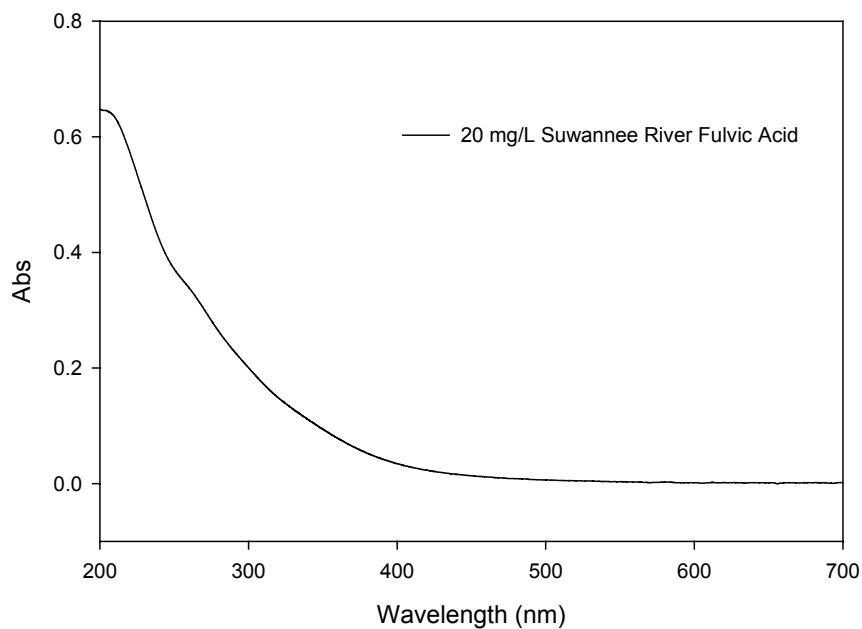
116

Figure IV- 1.   The UV/vis spectrum of Suwannee river fulvic acid.

The absorption of CDOM decreases exponentially with increasing wavelength and can be fitted to the following empirical equation (Blough 1997)

$$a(\lambda) = a(\lambda_0)e^{-s(\lambda-\lambda_0)} \qquad\qquad \text{(IV-1)}$$

$$a(\lambda) = 2.303\ A(\lambda)/r \qquad\qquad \text{(IV-2)}$$

where $a(\lambda)$ and $a(\lambda_0)$ are the absorption coefficients at wavelength λ and reference λ_0, and S is a parameter that characterizes how rapidly the absorption decreases with increasing wavelength. A is the absorbance and r is the path length.

## Sources of Hydroxyl Radicals in Natural Systems

In natural systems the identified OH radical sources are Fenton's reaction, nitrate and nitrite photolysis.

Photolysis of Nitrate and Nitrite

It has long been known that nitrate and nitrite photolysis can be a major source of OH in natural waters (Mack and Bolton 1999; Zafiriou and True 1979).

The absorption spectra of nitrite and nitrate are dominated by intense $\pi \rightarrow \pi^*$ transition at 205 nm and 200 nm, respectively. The absorption spectra also contain weak $n \rightarrow \pi^*$ transitions at 360 nm and 310 nm for NO_2^- and NO_3^-, respectively (**Figure IV-2**).

Upon irradiation, NO_2^- photolysis can produce OH through following pathway.

$$NO_2^- + h\upsilon \rightarrow [NO_2^-]^*$$

$$[NO_2^-]^* \rightarrow NO\bullet + O^{\bullet-}$$

$$O^{\bullet-} + H_2O \Rightarrow OH\bullet + OH^-$$
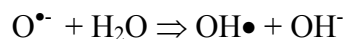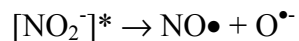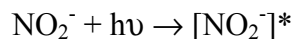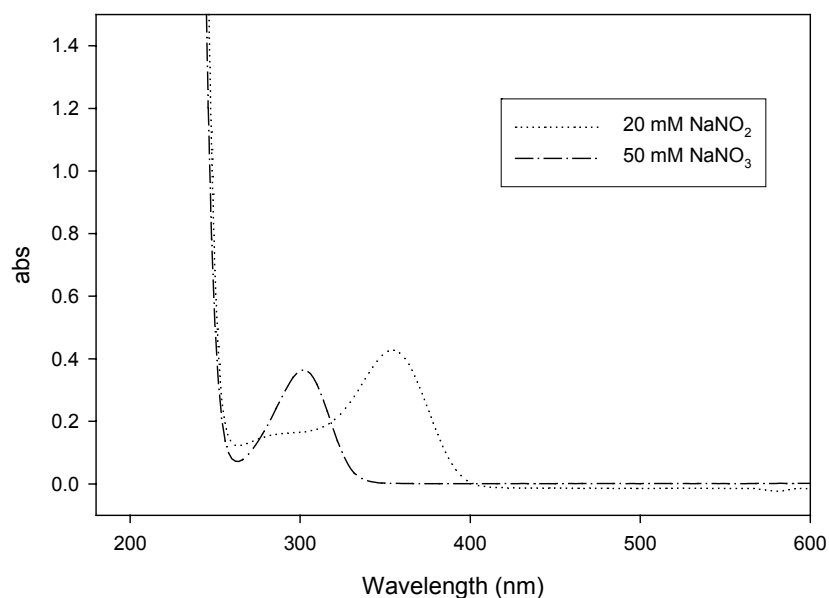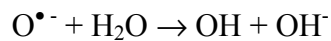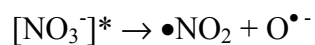
Figure IV-2.   The UV/vis spectra of nitrate and nitrite in aqueous solutions.

Unlike nitrite, which is both an OH source and sink, nitrate will not react with OH. The proposed nitrate photolysis mechanism is as follows (Mack and Bolton 1999; Mark et al. 1996).

$$[NO_3^-] + h\upsilon \rightarrow [NO_3^-]^* \rightarrow NO_2^- + O$$

$$[NO_3^-]^* \rightarrow \bullet NO_2 + O^{\bullet-}$$

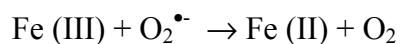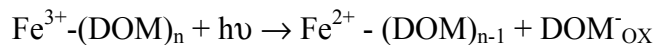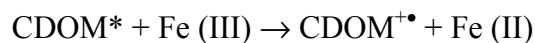$$O^{\bullet-} + H_2O \rightarrow OH + OH^-$$

Nitrite produced from nitrate photolysis might undergo secondary photolysis and produce OH (Blough, 1997).
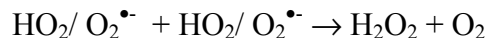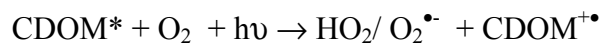
Photo-Fenton's reaction

DOM or CDOM can form complex with metals and participate in OH production through photo Fenton's reaction.

The generation of Fe(II) It has been postulated that photochemical reaction can reduce Fe (III) to Fe (II) through ligand-to-metal charge transfer (LMCT) or through direct electron transfer from photo-excited CDOM to Fe (III) as shown.

$$CDOM* + Fe (III) \rightarrow CDOM^{+\bullet} + Fe (II)$$

$$Fe^{3+}\text{-}(DOM)_n + h\upsilon \rightarrow Fe^{2+} \text{ - } (DOM)_{n-1} + DOM^-_{OX}$$

$$Fe (III) + O_2^{\bullet-} \rightarrow Fe (II) + O_2$$

The generation of H_2O_2 Hydrogen peroxide (H_2O_2) can be produced via dismutation of $HO_2/ O_2^{\bullet-}$

$$CDOM* + O_2 + h\upsilon \rightarrow HO_2/ O_2^{\bullet-} + CDOM^{+\bullet}$$

$$HO_2/ O_2^{\bullet-} + HO_2/ O_2^{\bullet-} \rightarrow H_2O_2 + O_2$$

The reaction of Fe (II) and hydrogen peroxide produces free OH radicals as follow.

$$Fe (II) + H_2O_2 \rightarrow Fe (III) + OH + OH^-$$
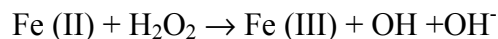
The concurrent photochemical production of Fe (II) and hydrogen peroxide in natural waters suggests that photo-Fenton's reaction may be an OH source in natural waters (Vaughan and Blough, 1998; Southworth and Voelker 2003; White et al 2003).

Direct CDOM photolysis

Direct photolysis of CDOM in the absence of oxygen and metal ions has been suggested to produce OH, although the true identity and the reaction leading to this species is not yet understood (Mopper and Zhou 1990; Vaughan and Blough 1998).

$$CDOM + h\upsilon + H_2O \Rightarrow OH$$
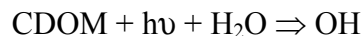
Method of Approach

Because different sources were suggested to produce OH upon UV irradiation, in order to obtain the contribution of OH production from individual source, it is important to control the experimental conditions to eliminate other potential sources. In this research we will focus on the possible OH production from direct CDOM photolysis in an oxygen independent pathway.

Our method of approach consisted of two steps. First, Suwannee river fulvic acid (SRFA), an isolated sample of CDOM that has been stripped of most of the inorganic components such as nitrite, nitrate, and metal ions was used as a model system to study the possible OH radical production from the photolysis of relatively "pure" organic source. Real natural water samples were then studied and the results were compared with model system to elucidate the OH production and mechanisms in natural systems.

Although SRFA consisted of primarily organic material, it was always possible that small amounts of nitrite, nitrate, and metals such as Fe (III) were still present in the sample. In order to eliminate the interference from oxygen related

contributions from the photo Fenton reaction, anaerobic condition was maintained and the pH was kept above 8. Nitrite and nitrate photolysis could produce OH radical upon photolysis under anaerobic condition regardless of pH and the presence of nitrite and nitrate in natural waters is unavoidable. To solve this problem, the irradiation wavelengths were carefully selected so that contribution from nitrite and nitrate photolysis can be estimated and subtracted from the experimental data.

The OH detection method employed in this research was the radical trapping method as described in previous chapters (**Scheme I-7**).

Experimental Section

Materials

HPLC grade dimethyl sulfoxide 99% (DMSO), HPLC grade acetonitrile 99.93+%, boric acid 99.999%, sodium dihydrogen phosphate 99.999%, sodium hydrogen phosphate 99.995%, sodium hydroxide 99.98%, fluorescamine (>97% TLC powder), 3-carbamoyl-proxyl free radical 97% (3-CP), activate carbon (decolorizing), KCl, $FeSO_4$, FeCl, and catalase were obtained from Aldrich. 3-amino-2,2,5,5-tetramethyl-1-pyrrolidinyloxy 99% (3ap) was obtained from Acros. Reagent grade $NaNO_3$, $NaNO_2$, HPLC grade methanol, 30% H_2O_2, 2-propanol, and chloroform were obtained from Fisher. Glacial acetic acid (99.9%) was purchased from J.T. Baker. Ultra pure nitrogen and methane were purchased from Airgas. A Millipore Milli-Q system provided water for all the experiments.

Suwannee River fulvic acid (SRFA) (IHSS standard 1s101F) was obtained from International Humic Substance Society. Thirteen natural water samples were collected at different stations in Delaware Bay, Chesapeake Bay, and Atlantic Ocean using standard natural water collection techniques during a research cruise from September 24 to September 27 2003.

Apparatus

Irradiation Systems The monochromatic irradiation system consisted of a 1000-W Hg-Xe arc lamp combined with a Spectral Energy GM 252 monochromator set to a band-pass of 10 nm. The broadband irradiation system consisted of a 300 W Xe arc lamp housed in an ILC Technology R400-2 and powered by an ILC technology PS300-1 power supply. The lamp irradiance was measured with an IL-1700 radiometer. Schott WG305, WG 325, WG 355, and KV 399 long pass filters were used, where the number indicates the wavelength of 50% transmission, to select appropriate wavelength of irradiation. A 1.0-cm and 10-cm quartz cuvettes were used for sample preparation, irradiation, and optical measurements. A Hewlett-Packard 8452A diode array and Shimadzu 2401 UV-PC spectrophotometers were used for UV and visible absorption measurements.

HPLC The reversed-phase HPLC system employed in this research and the detection of III has been previously described elsewhere (Kieber and Blough 1990; Li et al. 1997). The loop sizes was 600 μL. The chromatographic separations were performed at 27°C.

Experiment Protocol and Technique

Samples contained different concentrations of DMSO, SRFA or natural waters, and 3ap were prepared in water or borate buffer (50 mM, pH 8.0). For anaerobic experiments, the sample was degassed by bubbling with N_2 for 5 to 10 min, with the headspace then continuously purged with N_2 during irradiation. Aerobic experiments were performed with the sample cuvette open to air. Generally, the samples were irradiated with UV-vis light at appropriate wavelengths for a period of time during which 10% or less of sample was reacted under optical thin conditions (at the irradiation wavelengths). The pH of the resultant solution was adjusted to be 8 or above. To 1 ml aliquot of this solution, 200 µl of 5mM fluorescamine in acetonitrile was added and the sample was placed in dark for 2 or 3 min to produce III. The resultant solution was then loaded onto HPLC for separation and quantification.

For radical trapping experiments employing CH_4, instead of adding DMSO, the sample solution was first degassed with N_2 for 3 min and then bubbled with CH_4 for 5 min. Derivatization procedure was the same as that for DMSO.

Calibration and Identification of the Fluorescent Compound

Compound III was synthesized from an established OH source, Fenton's reaction, and was used to calibrate the response of fluorescence detector. A linear range between 5 nM and 600 nM was obtained.

For identification purposes, standard synthesized from Fenton's reaction was co-eluted with III obtained from SRFA or natural water reaction. For routine analysis,

the standard fluorescent compound was always run to find the retention time and to establish the concentration.

Natural Water Collection

The water samples were collected with increasing salinity from 0.0 to 30. Samples collected from the vessel's pumping system were filtered through a 0.2-μM nylon filter to remove particles and store at 4° C in dark until analysis.

Results and Discussion

Evidence of Photo-Fenton's Reaction at Low pH

When sample containing 20 mg/L SRFA and appropriate concentrations of 3ap and DMSO was irradiated at low pH (4.7) using polychromatic light with 399 nm long pass filter for different periods of time under **aerobic** condition, III was observed to be produced. However, significant decrease in III production rate was observed when the same sample was irradiated under **anaerobic** condition at both low and high pH. Compared with that under aerobic condition, a decrease of 70 to 80% was observed under anaerobic conditions at pH 8 as shown in **Figure IV-3**. Addition of 2 μM to 10 μM $FeSO_4$ or $FeCl_2$, the approximate concentration of Fe (II) found in many fresh natural samples, to the SRFA samples did not increase the product yields of III at 399 nm under anaerobic condition at pH 8.

When samples containing 6 or 15 mg/L of SRFA in the presence of 50 μM 3ap and 10 to 20 mM DMSO were irradiated at 310 nm using monochromatic light with 305 nm filter under anaerobic condition at pH 8.0, the addition of 50 to 100 units/mL catalse reduced only less than 20% of the III production.

These results were in good agreement with the results reported in previous literature and suggested a significant influence of photo-Fenton's reaction on OH production at low pH under aerobic conditions.

White et al studied the contribution of photo Fenton reaction to OH production in highly colored, acidic natural water (White et al 2003). Assuming that the total OX (either OH radical or strong oxidant) production rates under aerobic

condition is the sum of photo-Fenton's reaction and non-photo-Fenton's reaction, White et al. (2003) observed significant difference in OX production between aerobic and anaerobic conditions for the photolysis of this highly colored, acidic natural water and more than 70% of OX production was attributed to photo-Fenton's reaction. Because the detection method may not be able to differentiate OH and strong oxidant, OX is used to represent either free OH radicals or a strong oxidant. Similar results were previously reported by Vaughan and Blough (Vaughan and Blough 1998) as well as Southworth and Voelker (Southworth and Voelker 2003).

The above results clearly indicated that raising pH and deoxygenating of the sample removed the photo-Fenton reaction. Consistent with our results, strong pH dependence of photo-Fenton's reaction was also reported by Southworth and Voelker (2003).

The decrease in OX production caused by the addition of catalase may be attributed to 1) the inhibition of OX production by catalase; 2) the elimination of hydrogen peroxide from other sources including CDOM related H_2O_2 generation.
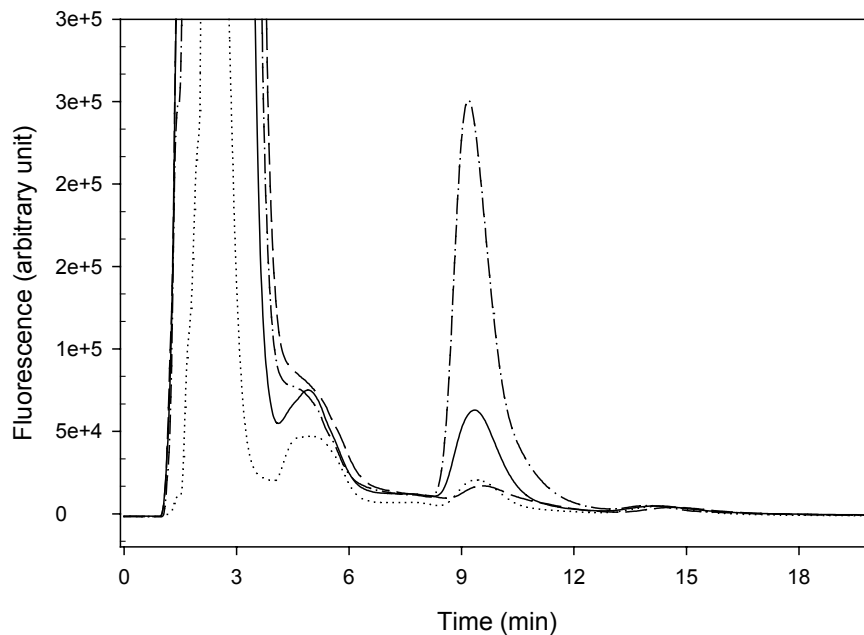
Figure IV- 3. The effects of oxygen and pH on the production of III (peak at 9.6 min).

 Samples containing 20 mg/L SRFA, 20 mM DMSO, and 250 μM or 50 μM 3ap were irradiated using the polychromatic light employing a 399 nm long pass filter for 1h under aerobic (–··–··–) and anaerobic conditions (——), respectively.

Control experiments 250 μM 3ap and 20 mM DMSO (········) or 20 mg/L SRFA + 50 μM 3ap (– – –) showed very low background signal.

All experiments were subsequently performed at pH=8.0 under anaerobic condition to avoid the interference caused by the photo-Fenton reaction.

SRFA Photolysis

The photolysis of SRFA was studied at different wavelengths or wavelength intervals in an effect to establish the sources of OX production.

The production of OX at long wavelength (>380 nm) was important in distinguishing "OH" sources because 1) it was suggested that CDOM produced OX at long wavelength (Vaughan 1999). However, monochromatic light with no filter was used and it was possible that the production of OX at long wavelength was due to an artifact; 2) there was no significant OH contribution from components other than CDOM in this range including nitrite photolysis; 3) the background signal of the radical trapping method was low and thus the sensitivity of detection was high. Photo-Fenton's reaction was eliminated at pH 8.0 under anaerobic condition as shown above. Any OX production was then most likely due to the direct photolysis of SRFA.

Filter combination

Both monochromatic and polychromatic irradiation systems were used. The polychromatic system was preferred due to its high irradiance and thus high OX formation. When monochromatic irradiation system was used, a long pass filter was used to block unwanted second order light. When polychromatic light was used a filter combination was employed to select the appropriate irradiation wavelength ranges to eliminate or estimate the interference from the photolysis of other components including nitrate and nitrite.

The production of III in different wavelength intervals can be obtained by radical trapping experiment with DMSO employing selected long pass filters. As shown in **Figure IV-4**, the production of III in 340 nm to 400 nm intervals can be calculated by subtracting the product yields obtained with 355 nm and 399 nm filters.
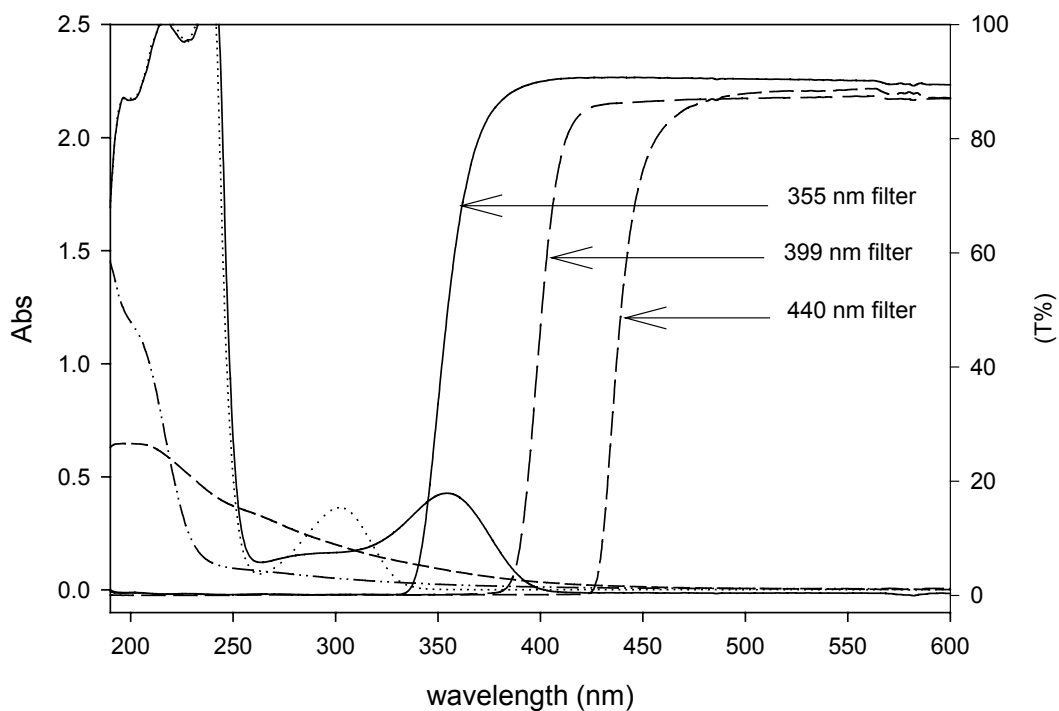

Figure IV- 4.   The transmittance of different filters and the absorption of nitrite, nitrate, SRFA, and natural waters.

The UV/vis absorbance of natural water (–··–··), 20mg/L SRFA (– – –), 20 mM $NaNO_2$ (——), 50 mM $NaNO_3$ (·····) and transmittance spectra of 355 nm, 399 nm, and 440 nm long pass filters.

Quantifying nitrite photolysis in different wavelength intervals

As stated above, for examining CDOM OX production in 380 nm to 440 nm, nitrite photolysis will have some contribution to the OX production in this range due to spectral overlap of nitrite absorption and filter transmittance as evident in **Figure IV-4**. Consider that the overall III production was low in SRFA photolysis, the contribution of nitrite photolysis in SRFA might cause misinterpretation of the results.

Because also the nitrate and nitrite concentrations in SRFA were not available from the supplier (IHSS), to estimate the contribution from nitrite photolysis, III production yields due to nitrite photolysis with 355 nm and 399 nm filters were obtained and the relative III product yields (P_{355}/P_{399}) used to estimate the contribution of nitrite photolysis to total III production in SRFA photolysis.

A series of known concentrations of nitrite were photolyzed in aqueous solutions at pH 8.0 under anaerobic conditions with 355 nm and 399 nm filters, respectively. A $P_{355}/P_{399} = 45 \pm 5$ was obtained for III production in wavelength intervals corresponding to 355 nm and 399 nm filters.

Assuming that the quantum yield of nitrite photolysis is independent of irradiation wavelength over this wavelength interval, the same ratio can be obtained by the following calculation.

$$P_{355}/P_{399} = Area_{355}/Area_{399}$$

where $Area_{355}$ and $Area_{399}$ are the overlap areas under filter transmittance and nitrite absorption. The area can be calculated (by integration or Excel) using the following

equation Area = Σ T$_i$ A$_i\Delta\lambda$. T$_i$ is transmittance and A$_i$ is absorbance at different wavelengths. $\Delta\lambda$ is the wavelength interval (1 nm).

OX production

Reasonable amounts of OX were detected in radical trapping experiments with DMSO under anaerobic condition at pH 8.0 for the photolysis of 15 to 20 mg/L SRFA aqueous solutions in 320 nm ~ 460 nm wavelength range. No long wavelength (> 500 nm) OX production was observed due possibly to 1) no production of OX from the photolysis of CDOM in this range; 2) the very weak absorption, and thus correspondingly low "OH" production.

The cumulative III product yields in the range of 300 nm to 550 nm were shown in **Figure IV-5**.
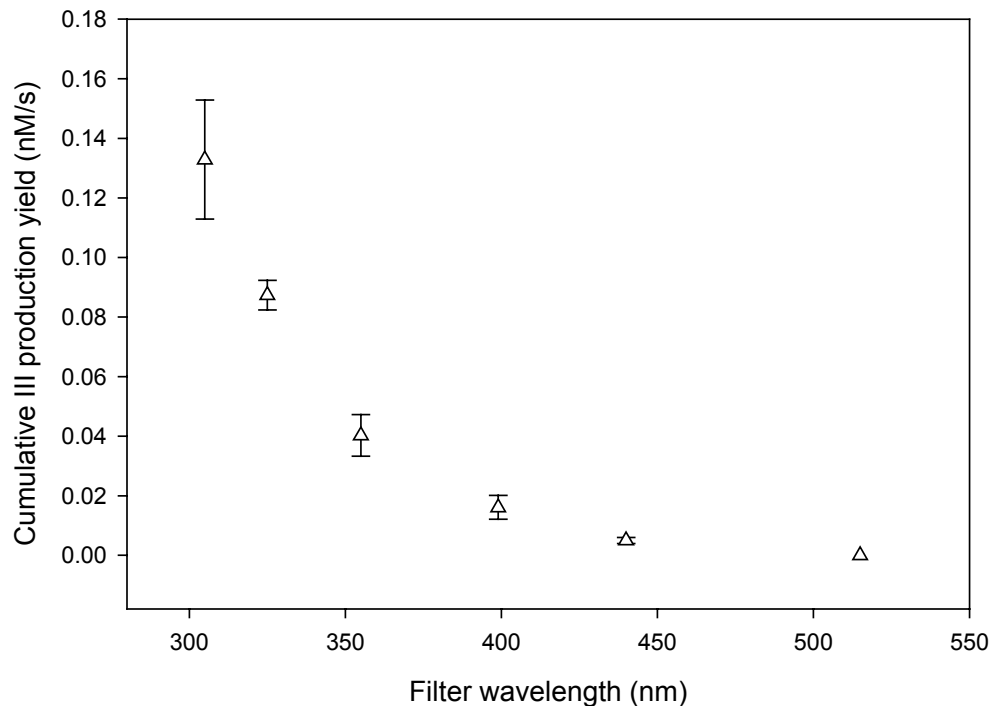
Figure IV- 5. Cumulative III production at different wavelength intervals obtained from SRFA chemical trapping experiment with DMSO.

Samples containing 15 mg/L SRFA, 50 µM 3ap, and 20 mM DMSO were irradiated with different long pass filter for 1 hr at pH 8.0 under anaerobic conditions. Each point represents III production rate using respective filter.

OX sources

The production of OX was safely assigned to an oxygen-independent photolysis of CDOM based on the comparison of III production ratios (P_{355}/P_{399}) obtained from experiment with that obtained from nitrite photolysis calibration.

According to the relative product ratio P_{355}/P_{399} obtained in nitrite photolysis, for the nitrite in SRFA to produce this much III with 399 nm filter, the same concentration of nitrite should produce 45 fold more III with 355 nm filter. However, only about two times higher III was produced when 355 nm filter was used comparing with that of 399 nm filter in SRFA photolysis. The inconsistency in III production yields between experimental and theoretical values, which was calculated on the basis of nitrite photolysis, unequivocally demonstrated that most of the III production in the photolysis of SRFA was due to sources other than nitrite photolysis. This result was in good agreement with that reported in previous literature, where the contribution of nitrite photolysis was estimated to be less than 1% [Vaughan and Blough 1998]. Photo-Fenton's reaction was eliminated by deaerating and raising pH of the samples and confirmed by the addition of Fe (II) as described above. It was then clear that direct CDOM photolysis was the only major OX source under experimental conditions.

CH$_4$ experiment

In an attempt to test if OX was indeed OH, CH$_4$ was employed. However, no signal could be observed. This may result from the low OX production rates as well as the strong competition between CDOM and CH$_4$ towards OH radicals {k_{SRFA}= 2.7 $\times 10^4$ s^{-1} (mg of C/L)$^{-1}$ and k_{SRHA}= 2.7 $\times 10^4$ s^{-1}(mg of C/L)$^{-}$1} (Goldstone et al 2002). So it is unclear at this point whether OX is OH.

OX Production from Natural Waters

Having investigated and observed the OX production from the photolysis of an isolated organic matter sample (SRFA), we further applied the methods and techniques to study the possible OH production and source in natural waters.

The photolysis of five natural waters with salinity gradient from 0.2 to 30, which were collected at different locations in Atlantic Ocean, Chesapeake Bay, Delaware Bay were tested and compared with that of SRFA. Fresh water with salinity close to 0 has a significant CDOM input from rivers. The pH value of all natural waters was above 8.0.

Optical study for fresh and coastal waters

As shown in **Figure IV-6**, exponential decay of the UV/vis absorption was observed for all natural waters. The absorption of natural water was detectable until 480 nm.
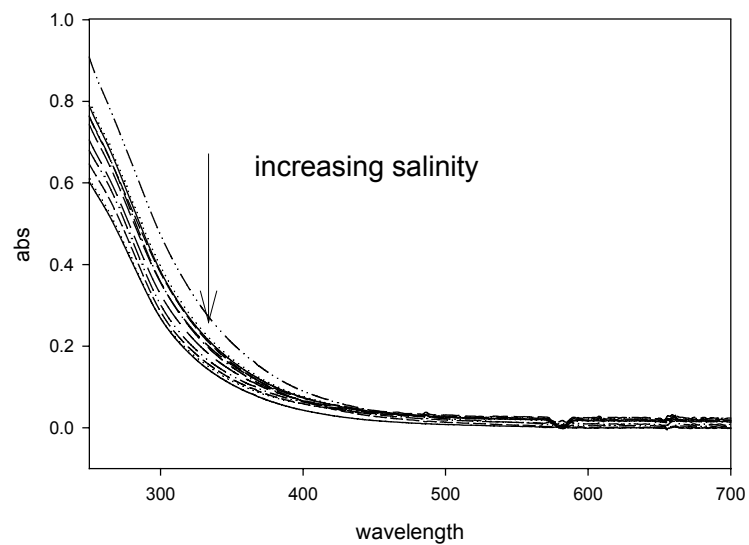
Figure IV- 6.   UV spectra of different natural waters in 10 cm cuvette prior to irradiation.

Radical trapping experiment for fresh and coastal waters

Reasonable yields of III were observed for all tested natural waters in 325 nm and 355 nm regions, while no III was detected at wavelength longer than 420 nm. The III production rates, which are identical to OX production rates, are summarized in Table IV-1 for different waters at different wavelength intervals. III production was observed to decrease with increasing salinity and the P_{355}/P_{399} ratio increases with salinity and close to that of nitrite photolysis (45).

Table IV- 1.   The OX production rates of natural waters at different wavelength intervals

Wavelength interval (nm)	Natural water 1 (nM/s)	Natural water 2 (nM/s)	Natural water 3 (nM/s)	Natural water 4 (nM/s)	Natural water 5 (nM/s)
325	0.15	0.106	0.0805	0.0765	0.0403
355	0.06	0.042	0.0318	0.0342	0.004
399	0.003	0.002	0.0012	0.00086	0
P_{355}/P_{399}	20	21	26	40	

Natural water 1, s = 0.018; Natural water 2, s = 5.52; Natural water 3, s = 10.37; Natural water 4, s =15.8; Natural water 5, s > 25. s is the salinity.

The absence of III at long wavelength (> 440 nm) might result from 1) the absorption of natural water was too low at long wavelength as seen in **Figure IV-7**. Even OX was produced upon irradiation; the concentration was below the detection limit or 2) no OX production over this wavelength interval.
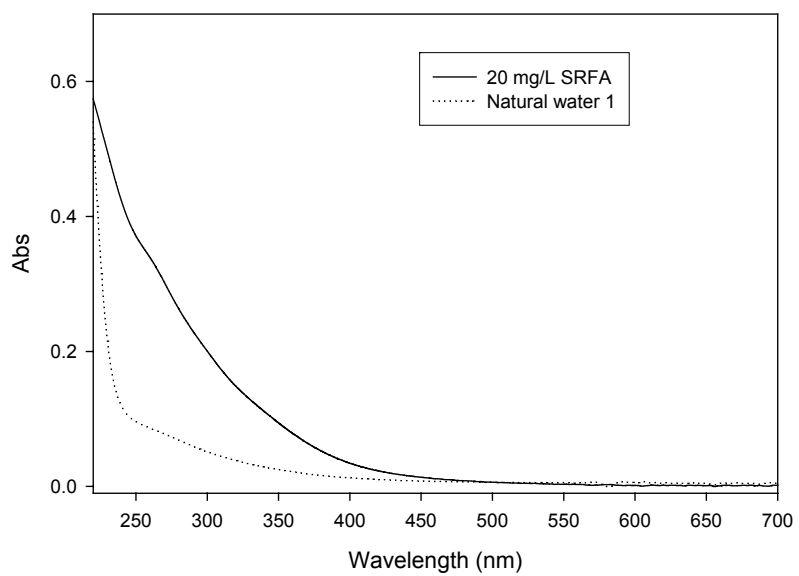
Figure IV- 7.   The UV-vis spectra of natural water and 20 mg/L SRFA in pH 8.0 borate buffer in 1 cm cell.

Discussion

Significant differences in SRFA and natural water photolysis was observed. The production of III exhibited wavelength dependence and indicated different OX sources in the photolysis of natural waters as shown in **Figure IV-8**.

In 250 nm to 500 nm range, 20 mg/L SRFA absorbed much stronger than that of natural water (**Figure IV-7**). With 399 nm filter, the production of III from SRFA was much higher than that from natural waters. With 440 nm filter, small quantities of III was still observed in the photolysis of 20 mg/L SRFA while no III was detected in the irradiation of natural water. In general the production yields of III in 380 nm to 450 nm range were consistent with relative UV absorbance of SRFA and natural waters. Therefore, CDOM was the species responsible for III production in this long wavelength range. 20 mg/L SRFA contained more CDOM than natural water and thus produced more OX upon irradiation.
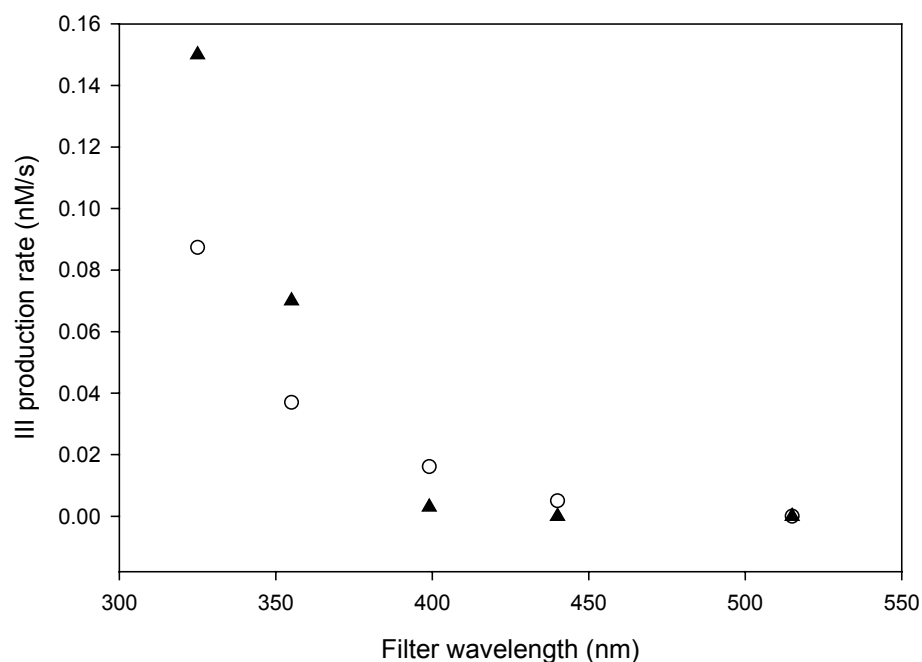
Figure IV- 8.   Comparison of III production yields from the photolysis of SRFA and natural water.

20 mg/L SRFA (○) or natural water 1 (▲), 50 μM 3ap, and 20 mM DMSO in pH 8.0 aqueous solution were irradiated using broadband light with 325 nm, 355 nm, 399 nm, 440 nm, and 515 nm filters.

However, when 325 nm and 355 nm filters were used, the production of III from natural water photolysis was much higher than that from 20 mg/L SRFA although the UV spectra showed that natural water had much lower absorption in 250 nm to 380 nm ranges. This clearly demonstrated that SRFA and natural waters follow different OX production patterns in these wavelength intervals.

The inconsistency between UV absorption and III production in 320 nm to 355 nm wavelength interval may be explained by the participation of nitrite and

nitrate photolysis. In long wavelength ranges (> 390 nm), no nitrite photolysis contributed to OH production and the only possible major OX source was CDOM. Because natural waters contained much lower concentration of CDOM, the III product yield was lower in natural waters than that of SRFA photolysis.

On the other hand, when 355 nm and 325 nm filters were used, the nitrite and nitrate in natural waters can absorb strongly (**Figure IV-2**) and produce OH. This was consistent with the observation of more III formed in natural water photolysis in this range. Detailed examination of III production yields with 355 nm and 399 nm filters clearly showed that the relative ratio (P_{355}/P_{399}) obtained from experiment was close to the theoretical values on the basis of nitrite photolysis (see Table IV-1). The production of OX in 325 nm to 355 nm wavelength intervals appears to result from a combination of nitrate and nitrite photolysis.

The investigation of the OX production from isolated CDOM sample and natural waters revealed the following:

1. The experiments provided evidence for the production of an oxidant by the photolysis of colored dissolved organic matter in natural systems, though the true identity of OX is not yet known.

2. For estuarine water, however, a substantial fraction of OX production appears to be OH arising from nitrite and nitrate photolysis.

Chapter V   Summary and Future Work

Summary

Radical trapping employing 3ap in conjunction with DMSO and CH_4 was successfully applied to the study of a series of 1,4-benzoquinones and a long-standing debate about the mechanism of quinone photolysis in aqueous solution was clarified.

The aqueous photochemical mechanism of 2-methyl-1,4-benzoquinone was extensively investigated at both low and high concentrations in the presence of different substrates. At low quinone concentrations, the triplet quinone and water reaction was the major pathway and an oxidizing intermediate, which was derived but distinct from the triplet state quinone, was produced upon UV irradiation. The existence of this intermediate was confirmed by radical trapping with 3ap employing DMSO in the presence of chloride and other substrates. Ground state quinone was involved in the reaction with the triplet in a competitive fashion and the ground – triplet quinone reaction was the major pathway at high concentrations of quinone.

OH as a major product in the photolysis of aqueous mBQ solution was eliminated based on the results obtained in radical trapping experiments with methane and benzoic acid product analysis. Kinetics obtained in radical trapping experiments with 3ap in the presence of DMSO provided further evidence for this conclusion.

Because significant decrease in relative III production yields was observed in the radical trapping experiment for high concentrations of mBQ, any intermediate produced from the photolysis of high concentrations of mBQ was not reactive towards DMSO to produce methyl radicals.

An intermediate mechanism was also proposed for the photolysis of dimethyl- and dichloro-1,4-benzoquinones in aqueous solutions based on the results obtained from radical trapping with DMSO and CH_4 as well as benzoic acid product analysis.

Consistent evidence was obtained from radical trapping with DMSO, methane, and benzoic acid product analysis experiments to conclude an OH mechanism for the photolysis of tetrachloro-1,4-benzoquinone in aqueous solution.

A general relationship between OH production capability and quinone redox potentials was suggested.

Organic matter as sources of strong oxidant was confirmed based on the results obtained from the photolysis of isolated CDOM (SRFA) at long wavelengths. The identity of this intermediate is not known for certain. However, quinone photochemistry study suggested that the strong oxidizing intermediate produced from CDOM photolysis might not be OH. It could be the OX, which was previously described as OH radical.

The dependence of OX production rates on the irradiation wavelength indicated that different OX sources were presented in SRFA and natural waters. For SRFA, the major OX source is organic matter. For natural waters collected from Delaware Bay, Chesapeake Bay, and Atlantic Ocean, nitrite and nitrate photolysis appears to be responsible for OX production. However, the possibility of a different dissolved organic matter, which produced OX with a wavelength distribution different from that of SRFA, can not be eliminated for certain.

Future Work

Although the existence of an oxidizing intermediate that was distinct from triplet quinone and OH radical was confirmed in the photolysis of low concentrations of mBQ, the structure, reactivity, and lifetime of this intermediate was not known for certain. Future work may be directed to the study of this intermediate with emphasis on the structure and reactivity.

The production, reactivity, and structure of the intermediate or stable radical anion and cation, which was produced in the photolysis of high concentrations of mBQ might be another topic of future investigation.

For the production of OX from CDOM photolysis, further research is needed to identify this strong oxidant although quinone photochemical mechanism suggested that OH radical was not the major product.

Although the production of OX from dissolved organic matter under anaerobic and basic pH was studied, the contribution of dissolved organic matter to OH production under aerobic condition in the presence of different metal ions at different pH will be a valuable future research topic.

Appendices 1

The EPR spectra listed in this section were part of the spectra obtained from relative 3ap consumption measurement (see **Table II-3**) for different concentrations of mBQ. The EPR spectra for 20 μM and 500 μM of mBQ as shown in **Figure II-4** were not presented.

The 3ap concentrations can be calculated either from low field 3ap peak heights or double integration of three EPR peaks. The experimental conditions have been described in corresponding sections. The common EPR settings are as the followings.

Receiver:

Gain: depends on the concentration of 3ap, the gain is either 1×10^4 or 1×10^5. Phase: 10.0 deg; Mod Frequency: 100. 00 kHz;   Mod Amplitude: 0.952 G.

Signal Channel:
Conversion: 81.92 ms; Time Constant: 40.96 ms; Sweep Time: 83.886 s.

Field:
Center Field: 3480.00 G; Sweep Width: 80.00 G; Resolution: 1024 points.

Microwave:
Power: 6.32 E-2.
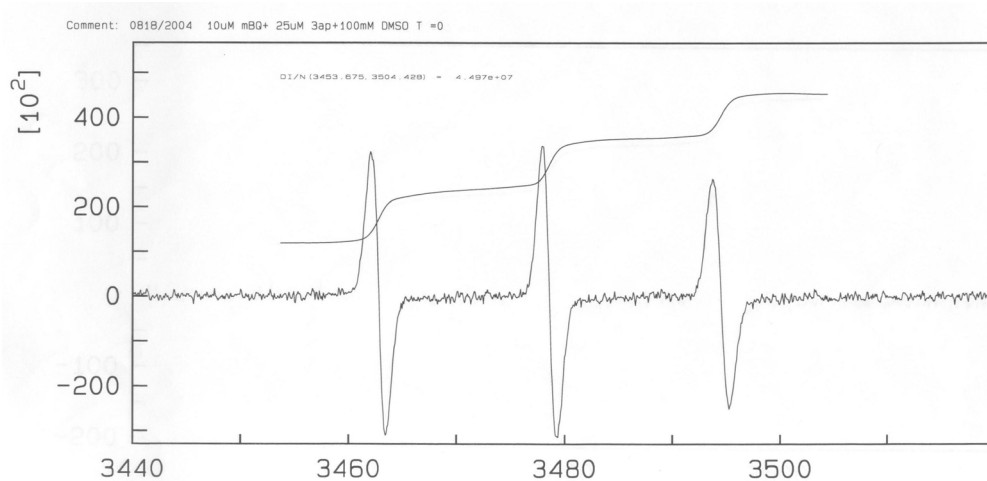
Figure 1.   The EPR spectrum of sample containing 10 μM mBQ, 25 μM 3ap, and 100 mM DMSO before irradiation (T = 0). The receiver gain is 1×10^5.
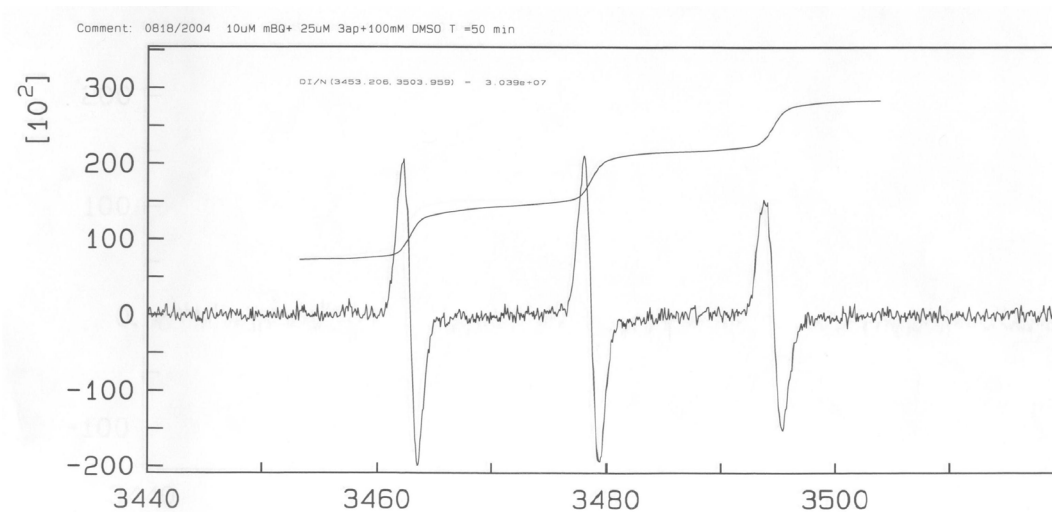
Figure 2.   The EPR spectrum of sample containing 10 μM mBQ, 25 μM 3ap, and 100 mM DMSO, which was irradiated with polychromatic light until complete consumption of mBQ (T = 50 min). The receiver gain is 1×10^5.
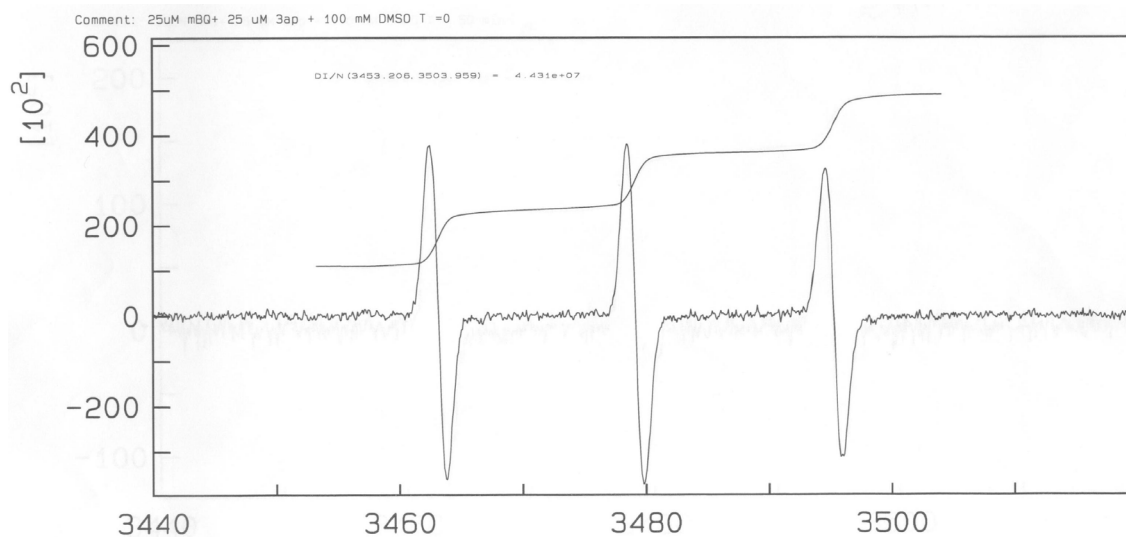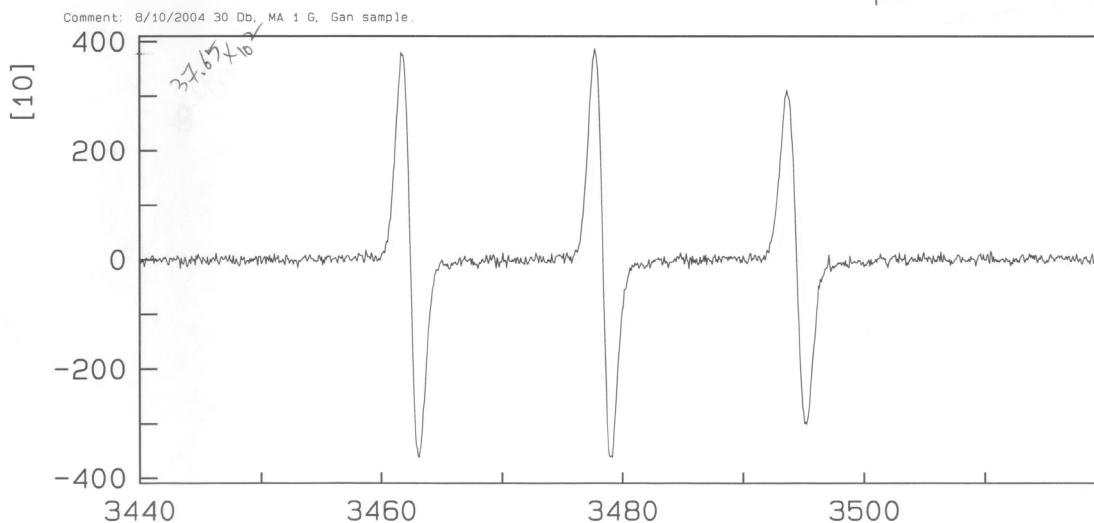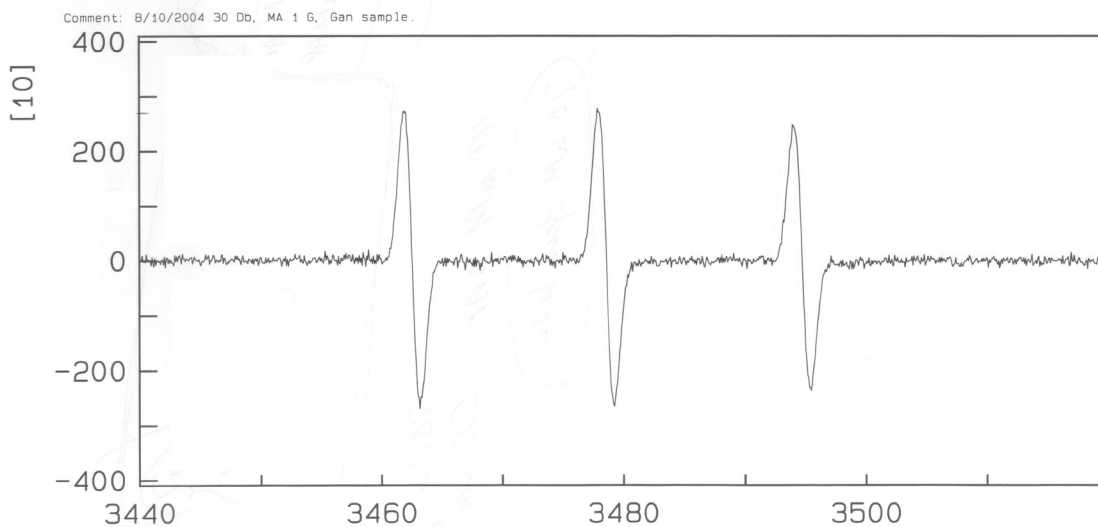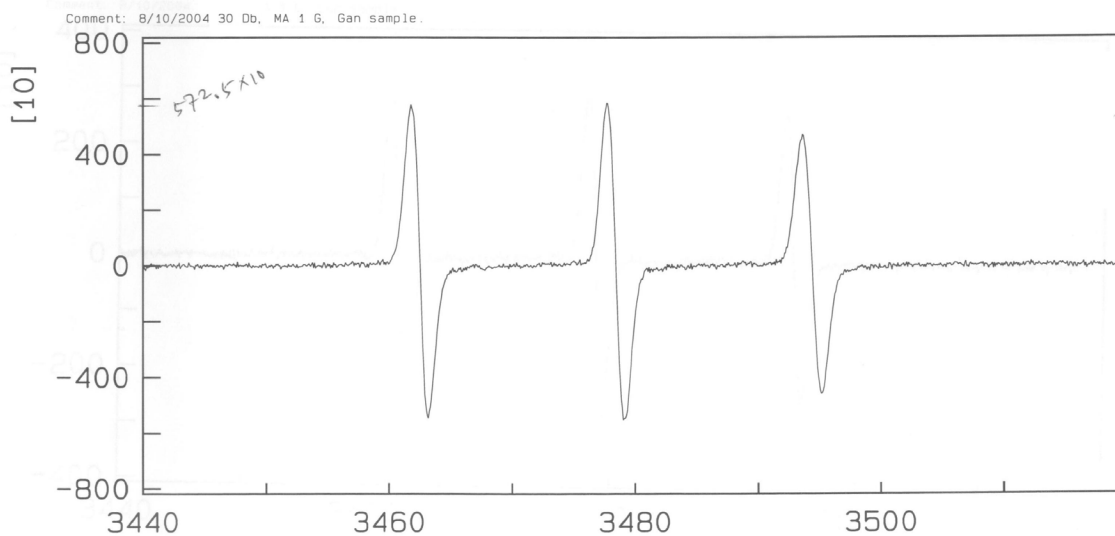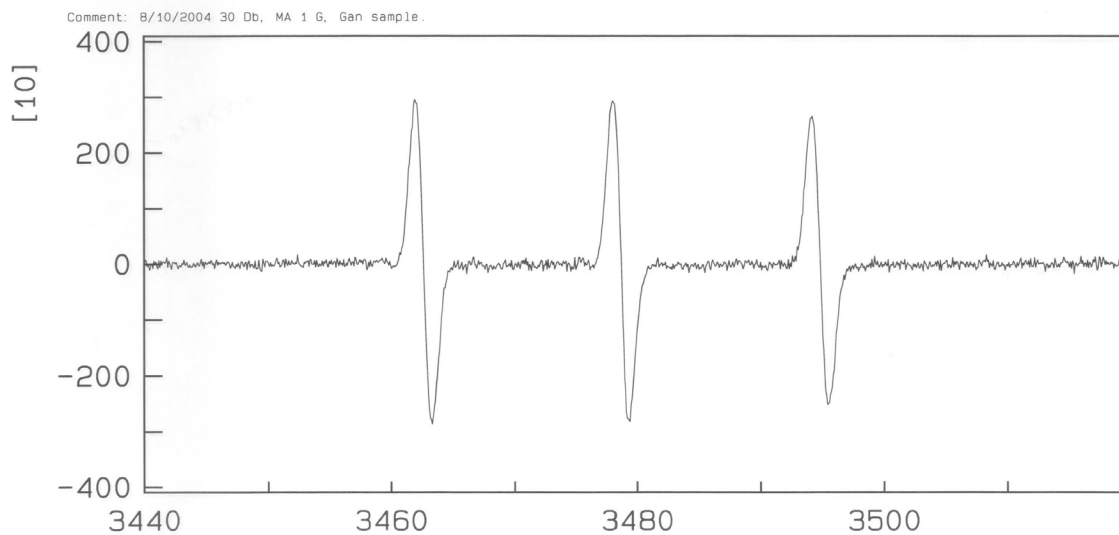
Figure 3. Sample containing 25 μM mBQ, 25 μM 3ap, and 100 mM DMSO before irradiation (T = 0). The receiver gain is 1×10^5.
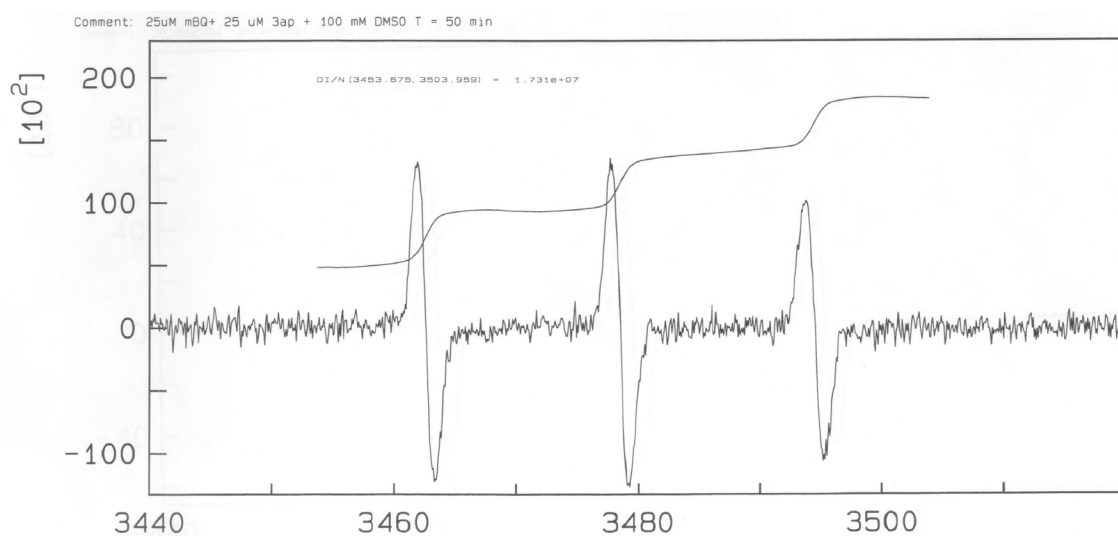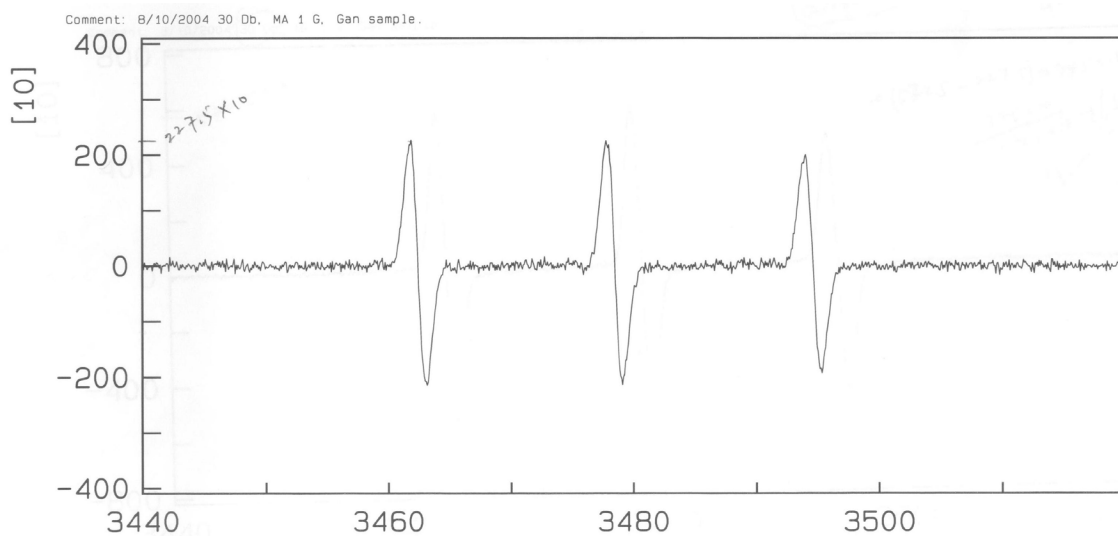

Figure 4. The EPR spectrum of sample containing 25 μM mBQ, 25 μM 3ap, and 100 mM DMSO, which was irradiated with polychromatic light until complete consumption of mBQ (T = 50 min). The receiver gain is 1×10^5.

Comment: 8/10/2004 30 Db, MA 1 G, Gan sample.
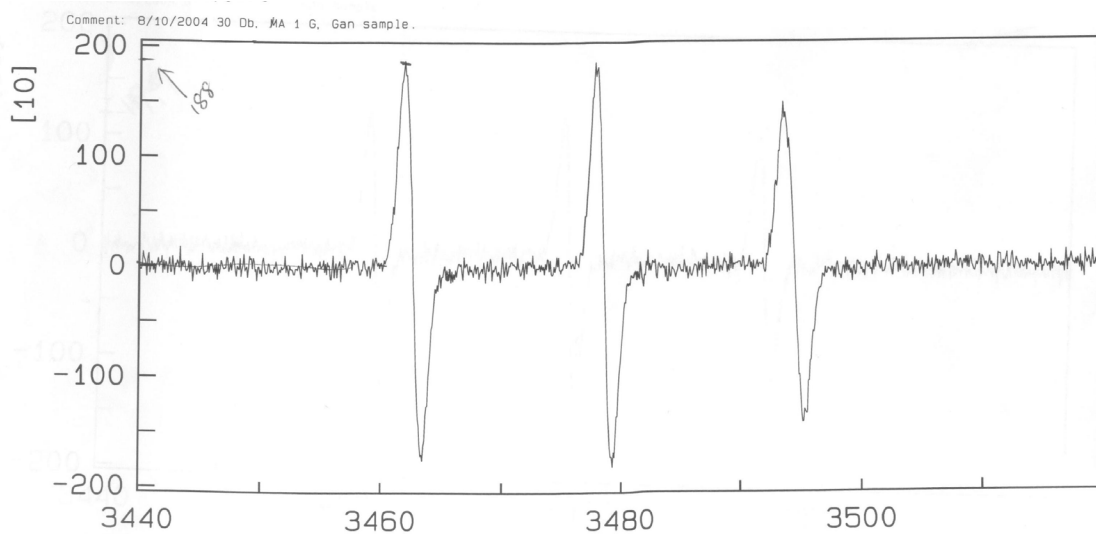
Figure 5.   The EPR spectrum of sample containing 50 µM mBQ, 50 µM 3ap, and 100 mM of DMSO before irradiation (T = 0). The receiver gain is 1× 10^4.

Comment: 8/10/2004 30 Db, MA 1 G, Gan sample.
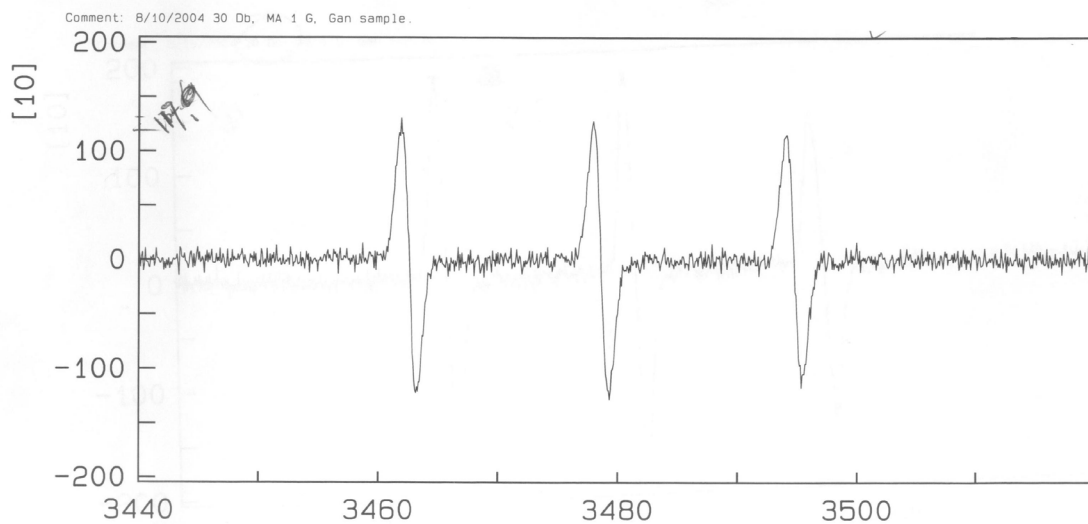
Figure 6.   The EPR spectrum of sample containing 50 µM mBQ, 50 µM 3ap, and 100 mM DMSO, which was irradiated with polychromatic light until complete consumption of mBQ (T = 50 min). The receiver gain is 1×10^4.
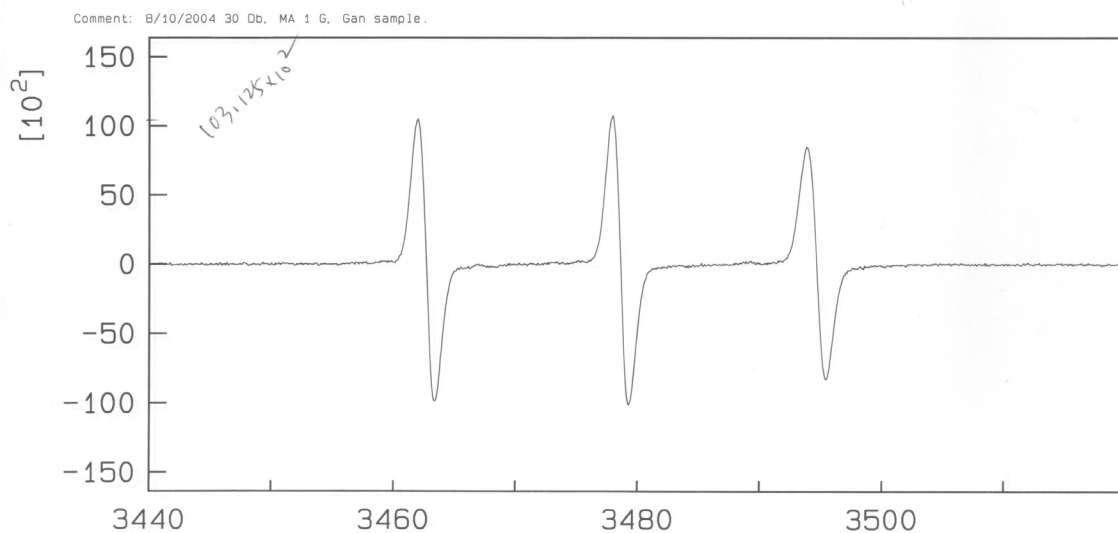
149

Figure 7. The EPR spectrum of sample containing 100 μM mBQ, 100 μM 3ap, and 100 mM DMSO before irradiation (T= 0). The receiver gain is 1×10^4.
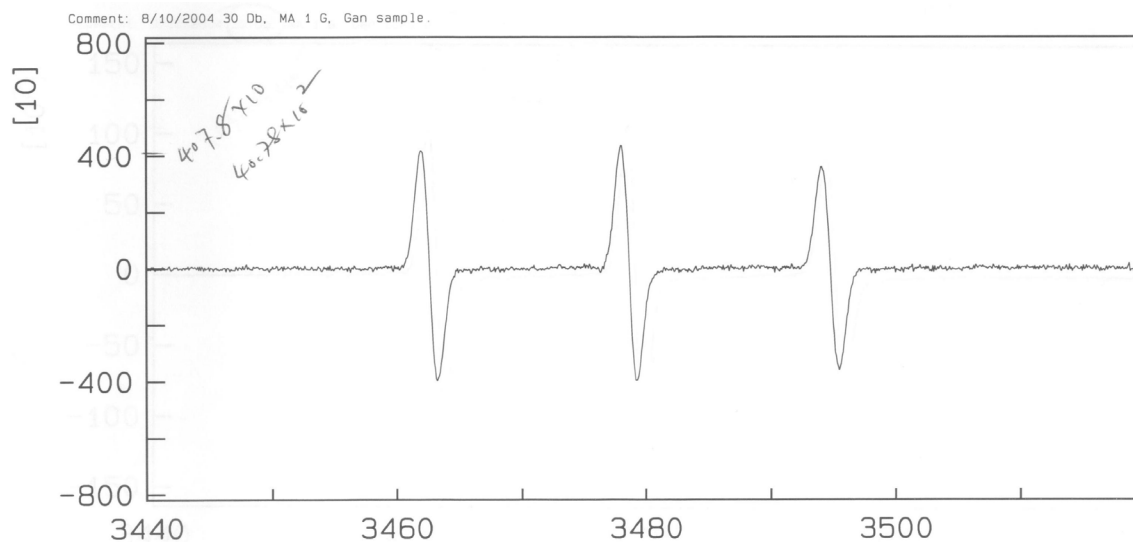

Figure 8. The EPR spectrum of sample containing 100 μM mBQ, 100 μM 3ap, and 100 mM DMSO, which was irradiated with polychromatic light until complete consumption of mBQ (T = 50 min). The receiver gain is 1×10^4.
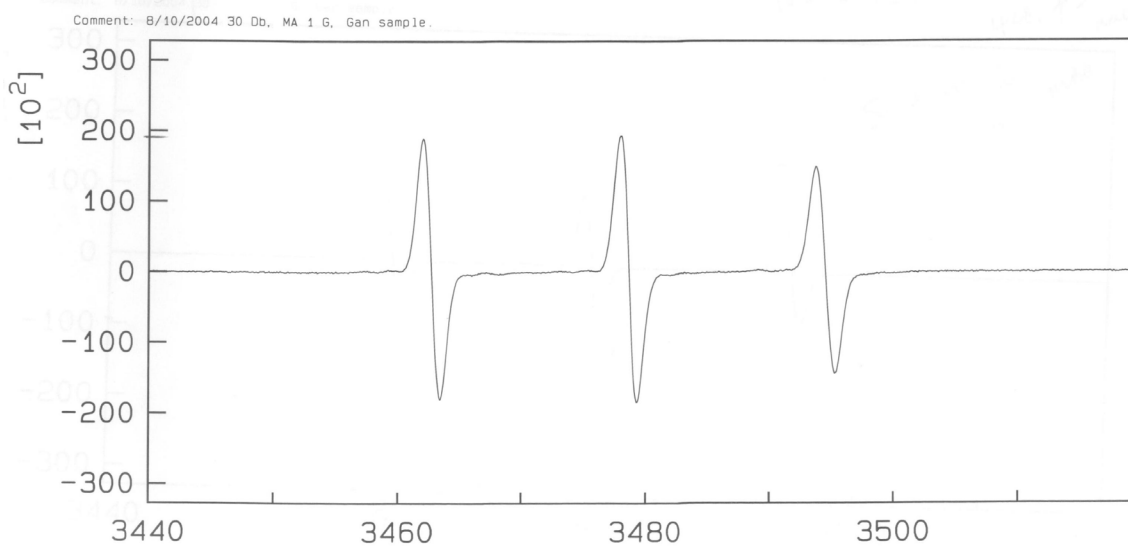
Figure 9. The EPR spectrum of sample containing 300 μM mBQ, 150 μM 3ap, and 100 mM DMSO before irradiation (T= 0). The receiver gain is 1×10^4.
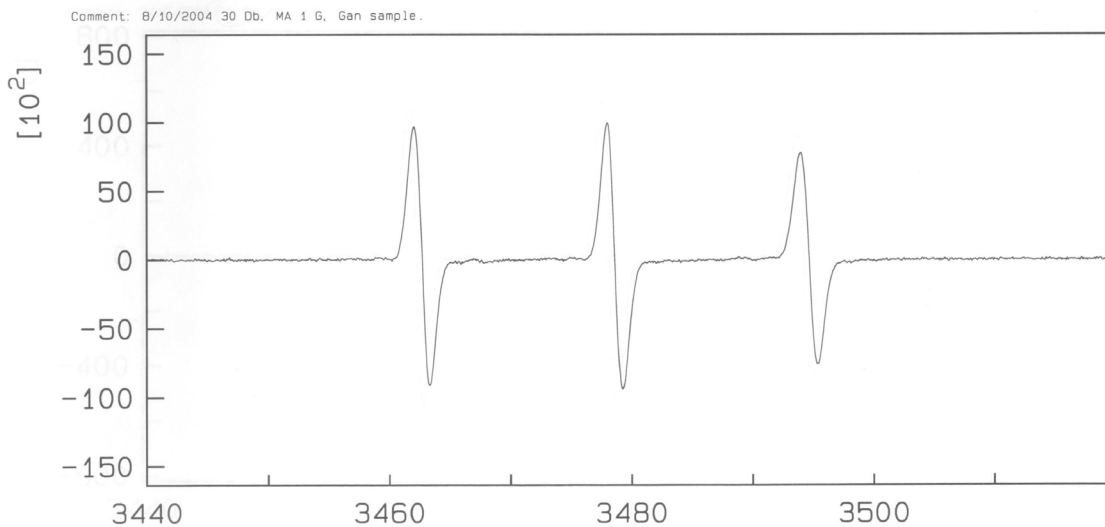

Figure 10. The EPR spectrum of sample containing 300 μM mBQ, 150 μM 3ap, and 100 mM DMSO, which was irradiated with polychromatic light for 34 min. The receiver gain is 1×10^4.
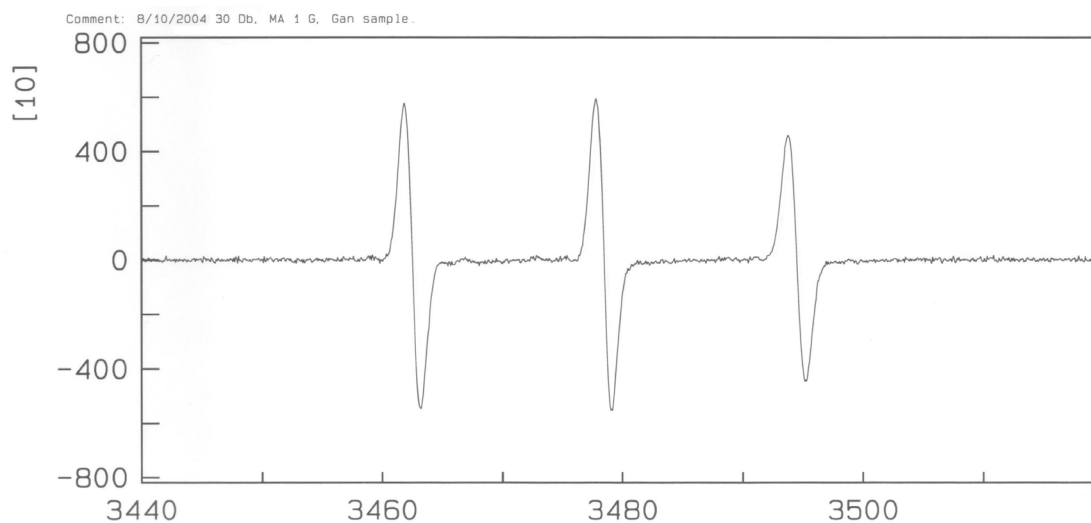
Figure 11.   The EPR spectrum of sample containing 300 μM mBQ, 150 μM 3ap, and 100 mM DMSO, which was irradiated with polychromatic light until complete consumption of mBQ (T= 56 min). The receiver gain is 1×10^4.

Figure 12.   The EPR spectrum of sample containing 1 mM mBQ, 300 μM 3ap, and 100 mM DMSO before irradiation (T= 0 min).

Figure 13. The EPR spectrum of sample containing 1mM mBQ, 300 μM 3ap, and 100 mM DMSO, which was irradiated with polychromatic light until complete consumption of mBQ (T= 40 min). The receiver gain is 1×10^4.

Figure 14. The EPR spectrum of sample containing 5 mM mBQ, 500 μM 3ap, and 100 mM DMSO before irradiation (T= 0).
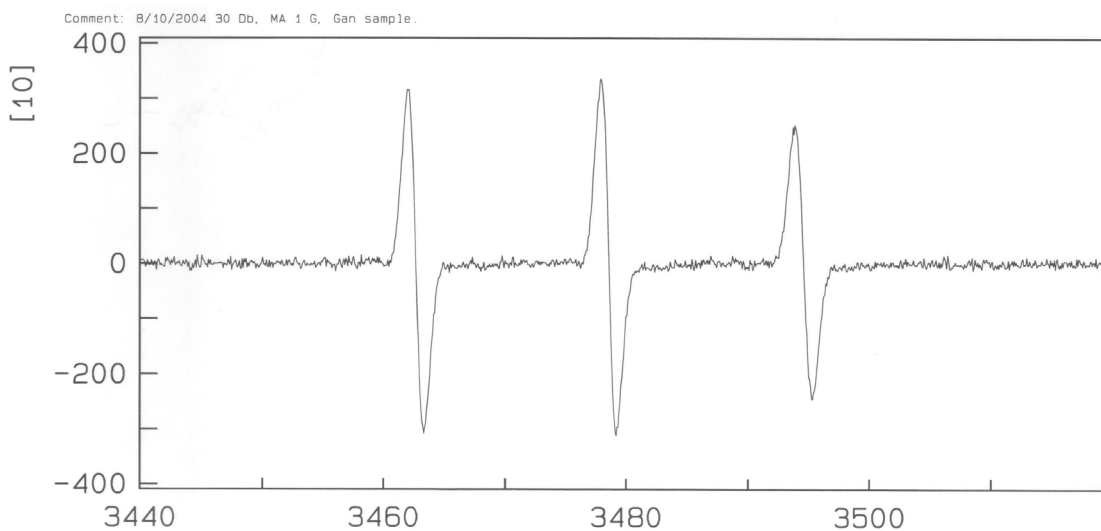
Figure 15. The EPR spectrum of sample containing 5 mM mBQ, 500 μM 3ap, and 100 mM DMSO, which was irradiated with polychromatic light for 6 min. The receiver gain is 1×10^4.

Figure 16. The EPR spectrum of sample containing 5 mM mBQ, 500 μM 3ap, and 100 mM DMSO, which was irradiated with polychromatic light for 15 min. The receiver gain is 1×10^4.

Figure 17. The EPR spectrum of sample containing 5 mM mBQ, 500 μM 3ap, and 100 mM DMSO, which was irradiated with polychromatic light for 45 min. The receiver gain is 1×10^4.
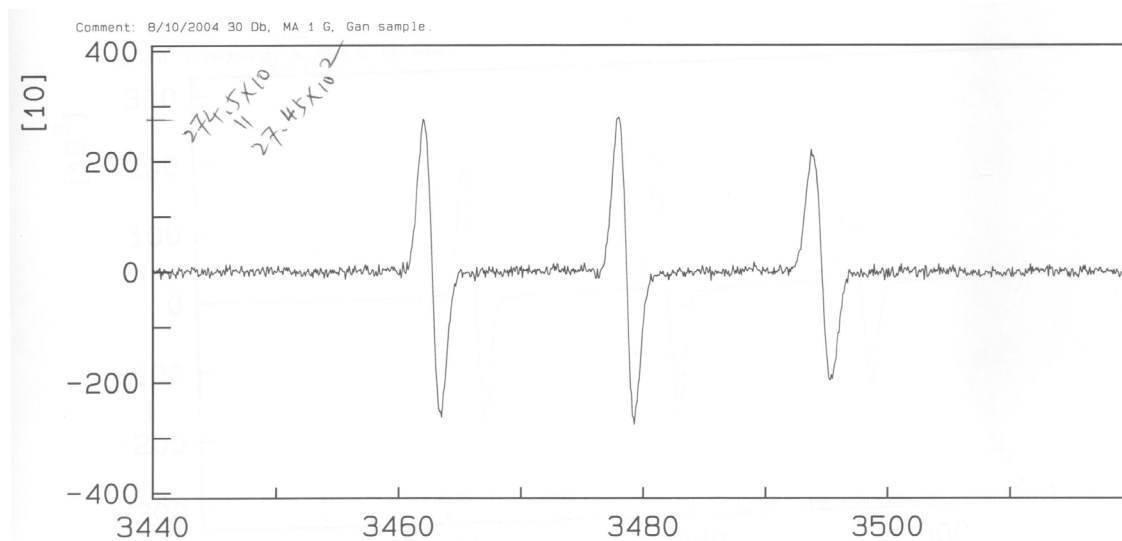

Figure 18. The EPR spectrum of sample containing 5 mM mBQ, 500 μM 3ap, and 100 mM DMSO, which was irradiated with polychromatic light until complete consumption of mQB (T= 65 min). The receiver gain is 1×10^4.
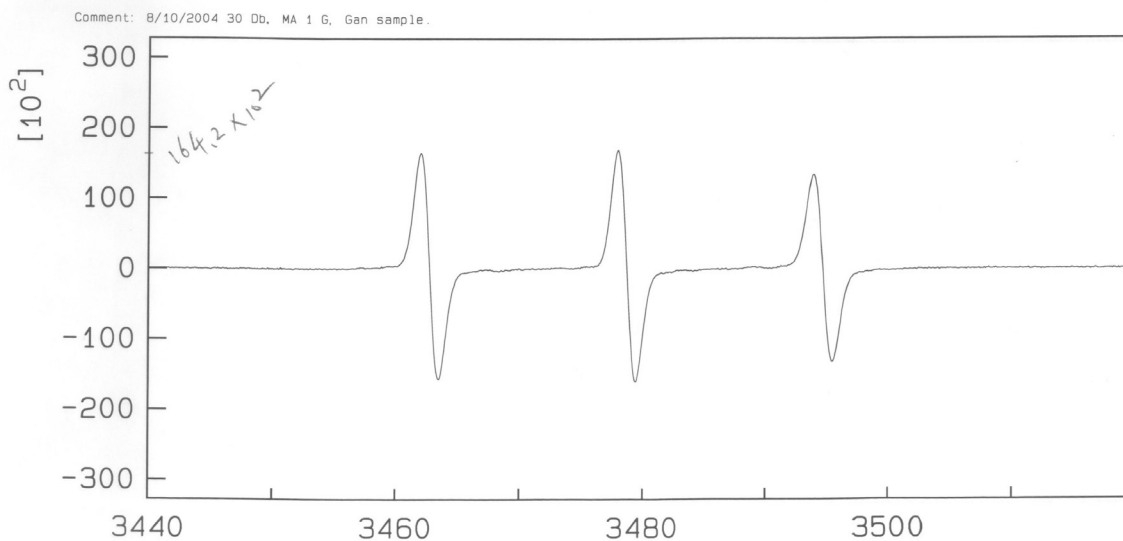
Figure 19. The EPR spectrum of sample containing 10 mM mBQ, 500 μM 3ap, and 100 mM DMSO before irradiation (T= 0).
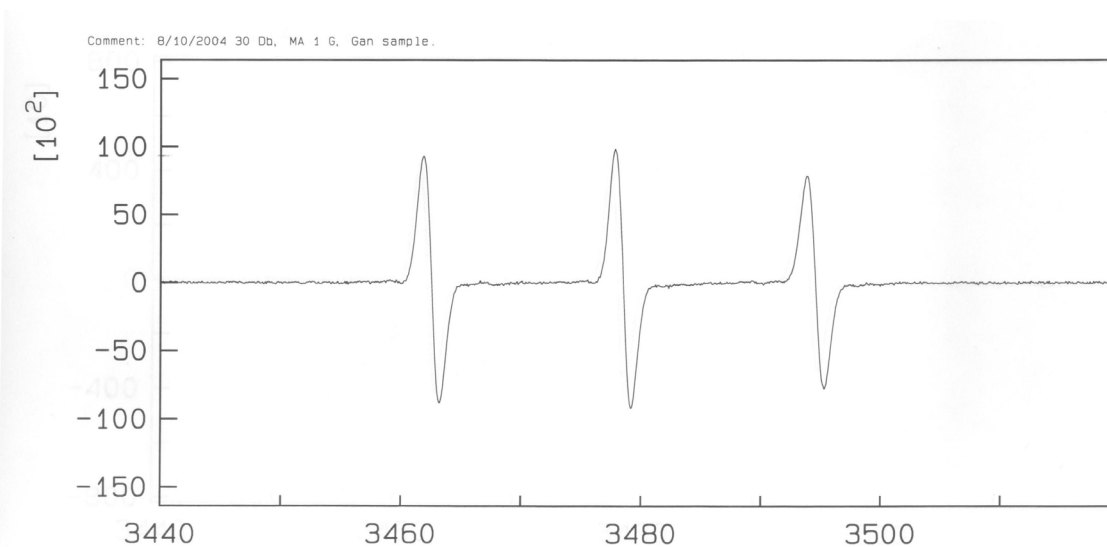

Figure 20. The EPR spectrum of sample containing 10 mM mBQ, 500 μM 3ap, and 100 mM DMSO, which was irradiated with polychromatic light for 6 min. The receiver gain is 1×10^4.
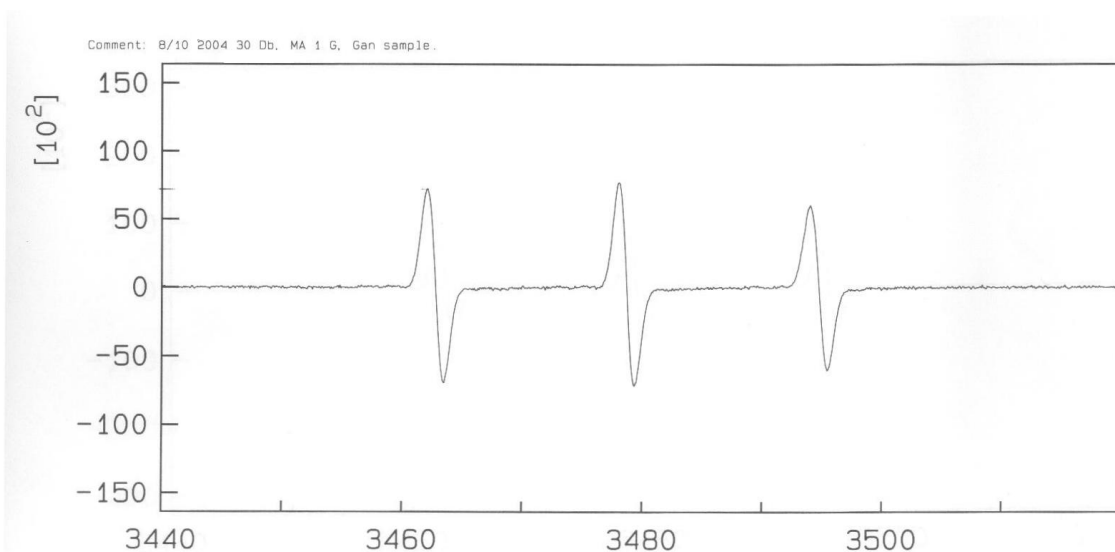
156

Figure 21. The EPR spectrum of sample containing 10 mM mBQ, 500 μM 3ap, and 100 mM DMSO, which was irradiated with polychromatic light for 12 min. The receiver gain is 1×10^4.
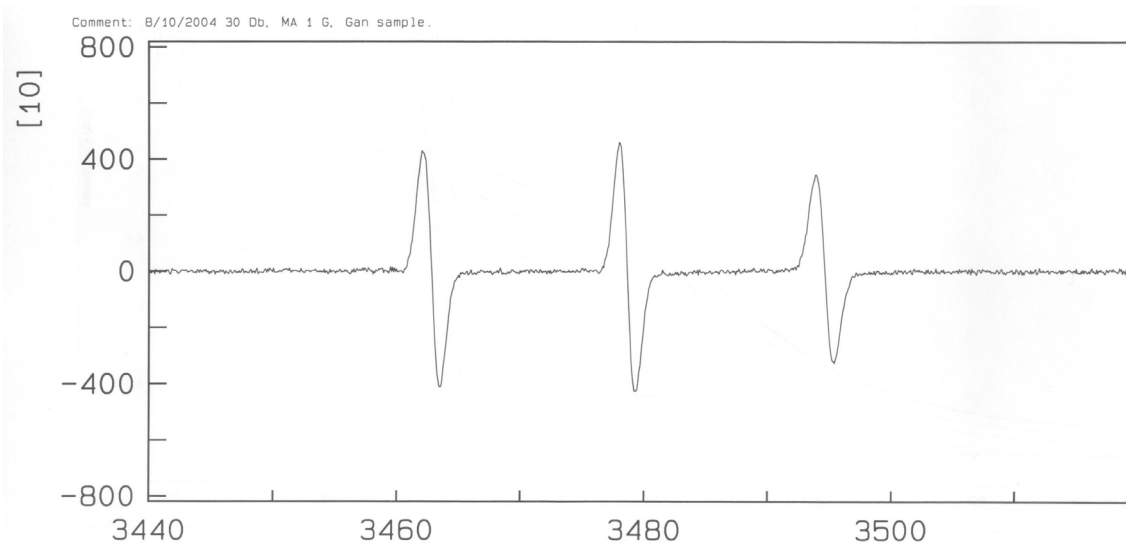

Figure 22. The EPR spectrum of sample containing 10 mM mBQ, 500 μM 3ap, and 100 mM DMSO, which was irradiated with polychromatic light for 24 min. The receiver gain is 1×10^4.

Figure 23. The EPR spectrum of sample containing 10 mM mBQ, 500 μM 3ap, and 100 mM DMSO, which was irradiated with polychromatic light for 40 min. The receiver gain is 1×10^4.
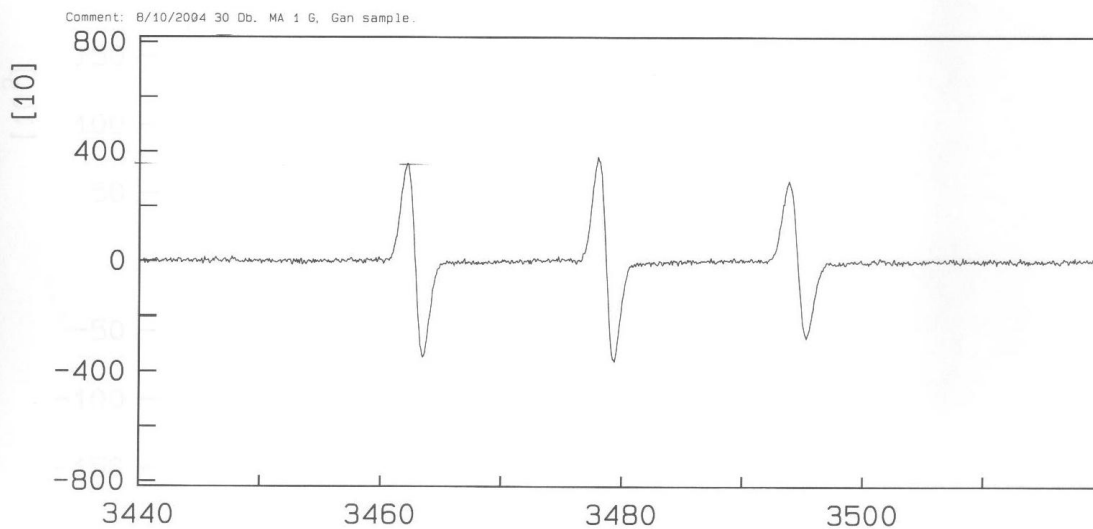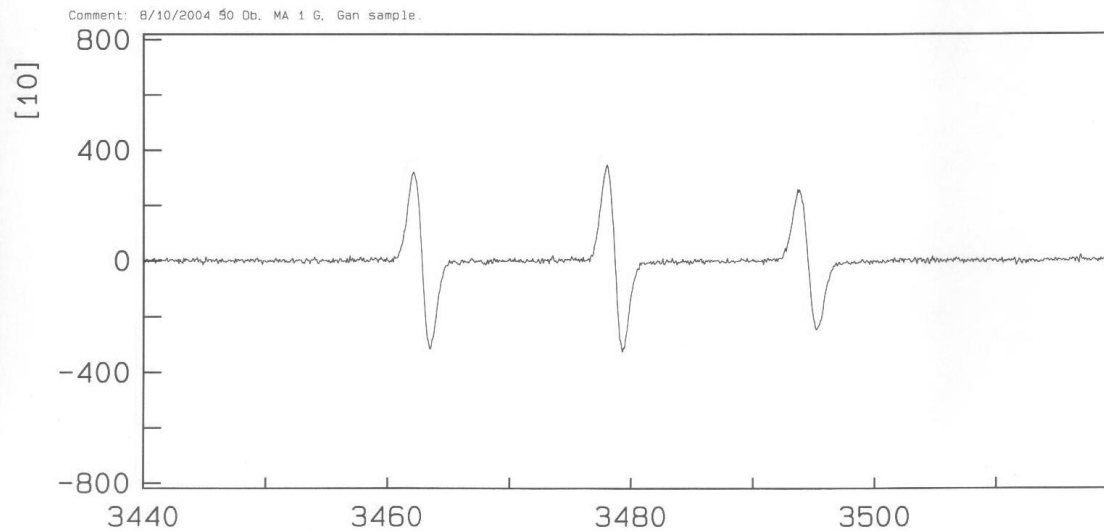

Figure 24. The EPR spectrum of sample containing 10 mM mBQ, 500 μM 3ap, and 100 mM DMSO, which was irradiated with polychromatic light for 50 min. The receiver gain is 1×10^4.
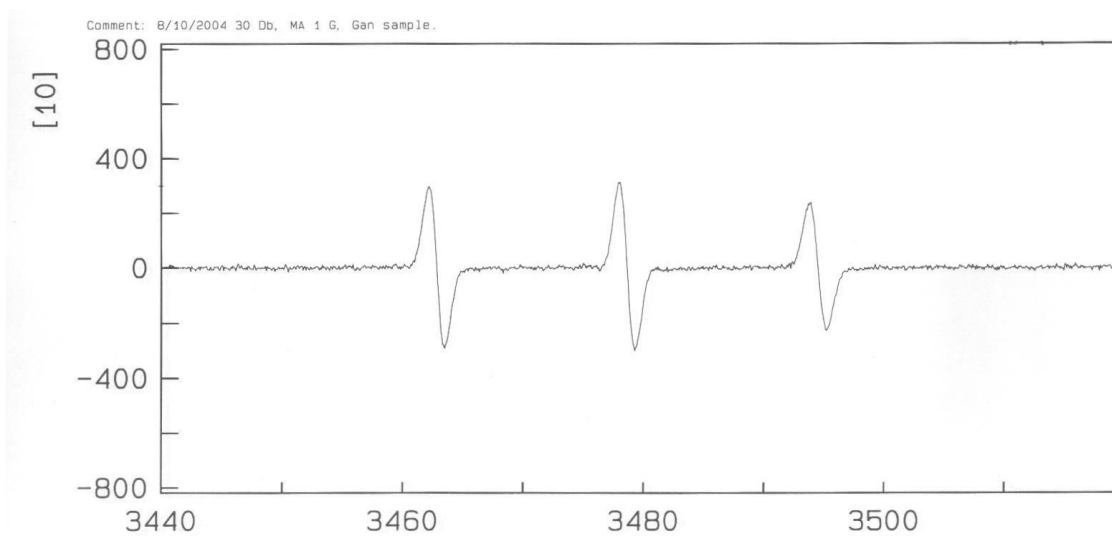
Figure 25.   The EPR spectrum of sample containing 10 mM mBQ, 500 μM 3ap, and 100 mM DMSO, which was irradiated with polychromatic light until complete consumption of mBQ (T= 65 min). The receiver gain is 1×10^4.

Appendices 2

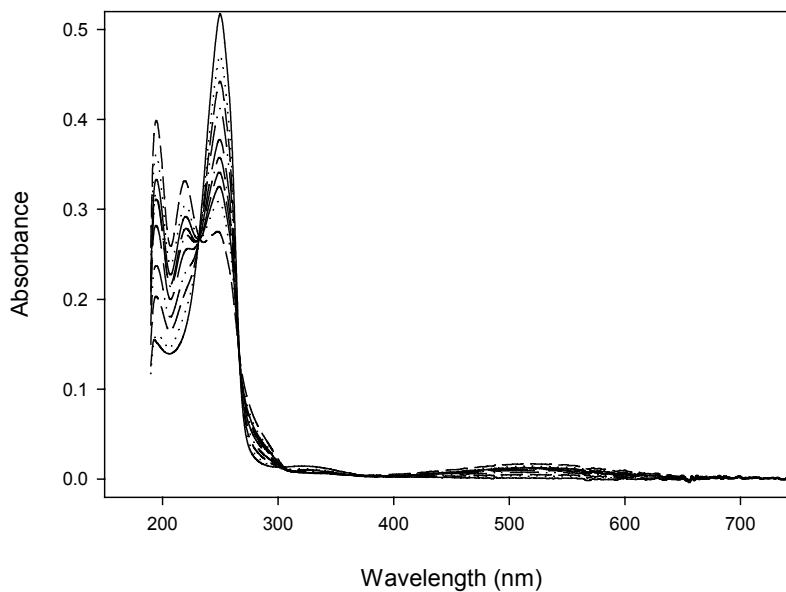The optical study data for mBQ and other 1,4-benzoquinones.

Figure 1. 20 µM mBQ + 50 µM 3ap was irradiated @ 320 nm with monochromatic light in 12 mM pH 7.0 phosphate buffer under anaerobic conditions. The lamp intensity was 1.0×10^{-3} W/cm^2. Total irradiation time was 5 min.

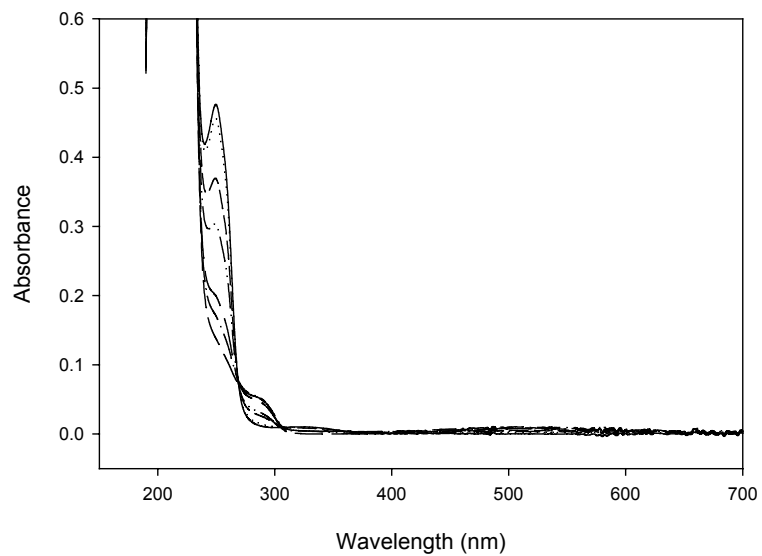**Figure 2.**   20 µM mBQ + 50 µM 3ap + 50 mM DMSO was irradiated @ 320 nm with monochromatic light in 12 mM pH 7.0 phosphate buffer under anaerobic conditions for 40 min. The lamp intensity was 1.0×10^{-3} W/cm^2.
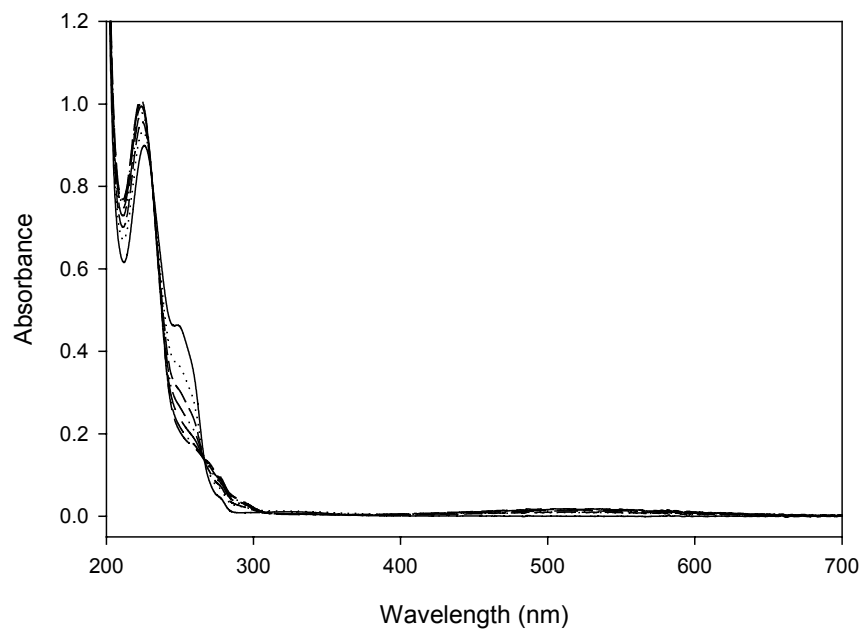
Figure 3. 20 µM mBQ + 100 µM Benzoic acid in pH 7.0 phosphate buffer was irradiated at 320 nm for 6 min under anaerobic conditions. The lamp intensity was 1.05×10^{-3} W/cm^2.
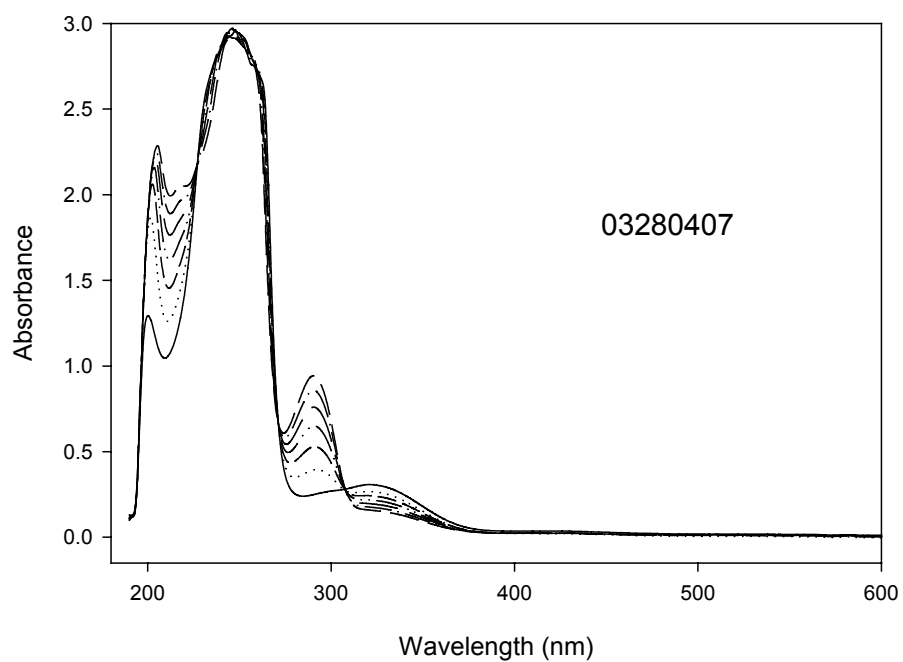
Figure 4.   500 µM mBQ was irradiated at 320 nm in 1:1 pH = 7.0 phosphate buffer and 2-propanol solution for 6 min under anaerobic conditions with monochromatic light. The lamp intensity was 1.1×10^{-3} W/cm^2.
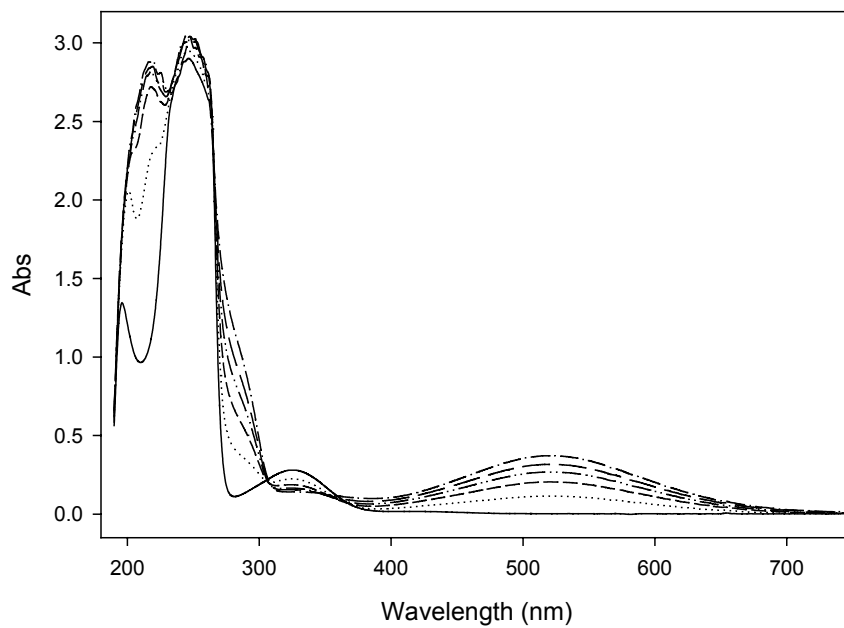
Figure 5.   500 µM mBQ + 50 µM 3ap was irradiated at 320 nm in pH = 7.0 phosphate buffer for 6 min The lamp intensity was 1.0×10^{-3} W/cm^2.
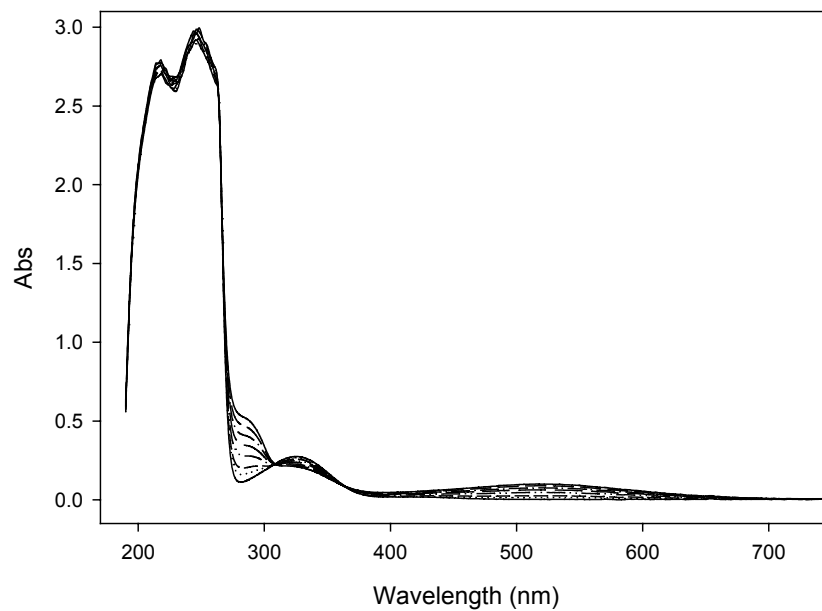
Figure 6.　　500 µM mBQ + 50 µM 3ap + 50 mM DMSO was irradiated at 320 nm in pH = 7.0 phosphate buffer for 12 min under anaerobic conditions with monochromatic light. The lamp intensity was 1.0×10^{-3} W/cm^2.
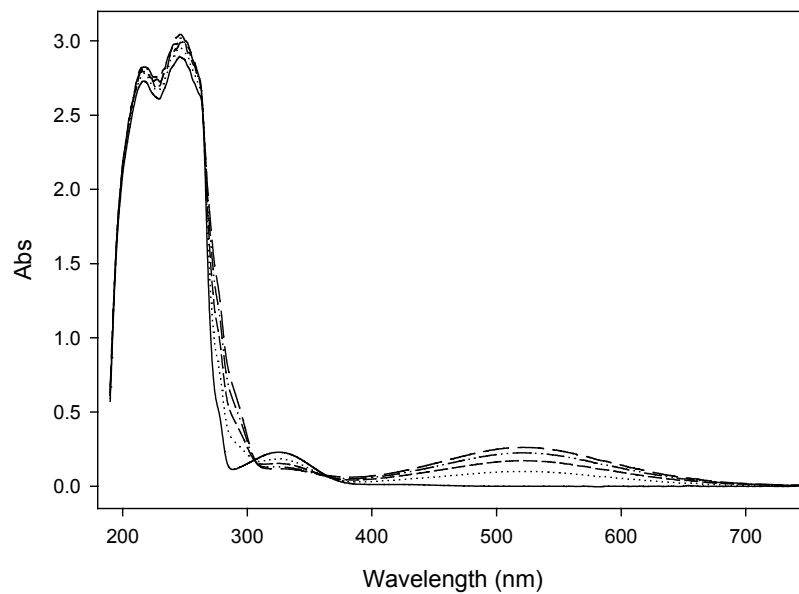
Figure 7.   500 μM mBQ + 1 mM Benzoic acid was irradiated @ 320 nm in pH 7.0 phosphate buffer for 5 min under anaerobic conditions with monochromatic light. The lamp intensity was 1.0×10^{-3} W/cm^2.
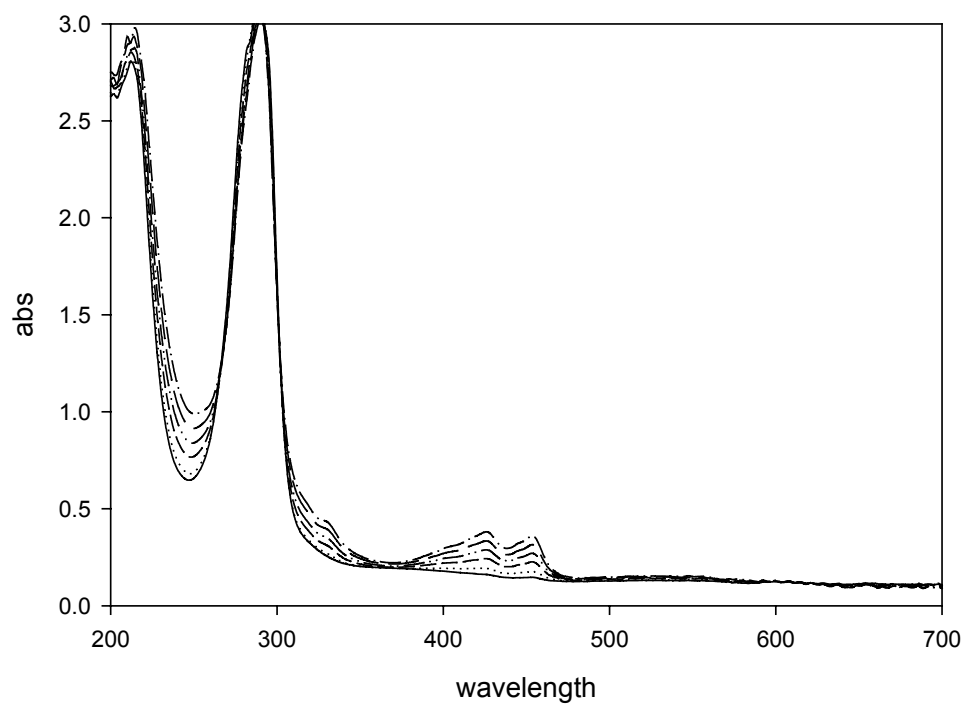
**Figure 8.** 100 μM Cl$_4$BQ in 1:3 MeCN and 12 mM phosphate buffer solution after irradiated @296 nm using monochromatic light and a 50% neutral density filter. The lamp intensity was 5.5×10^{-4} W/cm^{-2}.
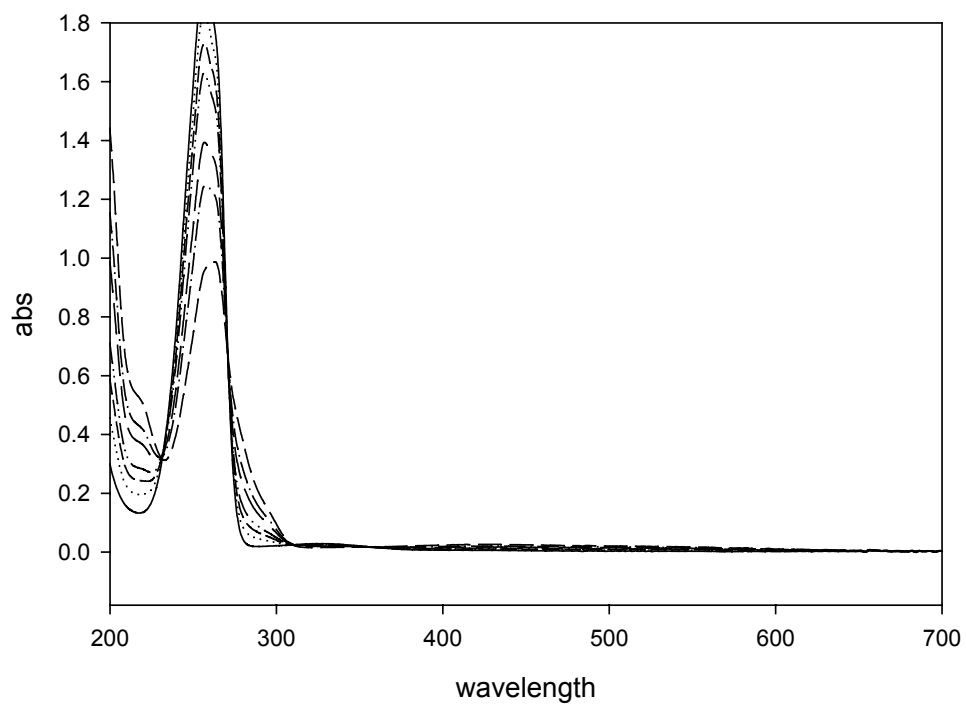
Figure 9. 100 µM 2,5-Me$_2$BQ in aqueous solution was irradiated at 334 nm with monochromatic light. The light intensity was 6.0×10^{-4} W/cm^2.
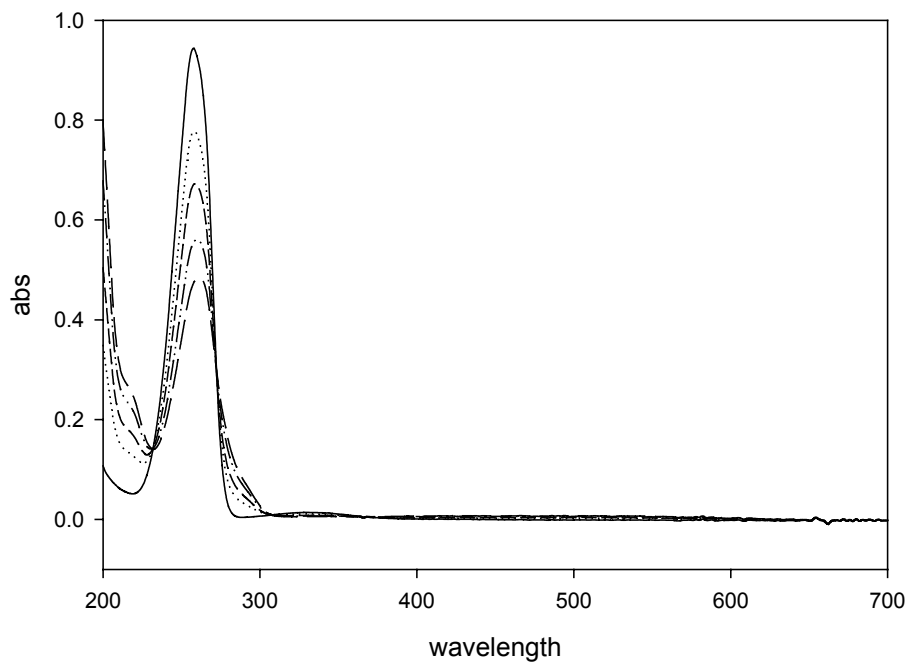
Figure 10. 100 µM 2,6-Me$_2$BQ in aqueous solution was irradiated at 334 nm with monochromatic light. The light intensity was 6.0×10^{-4} W/cm^2.
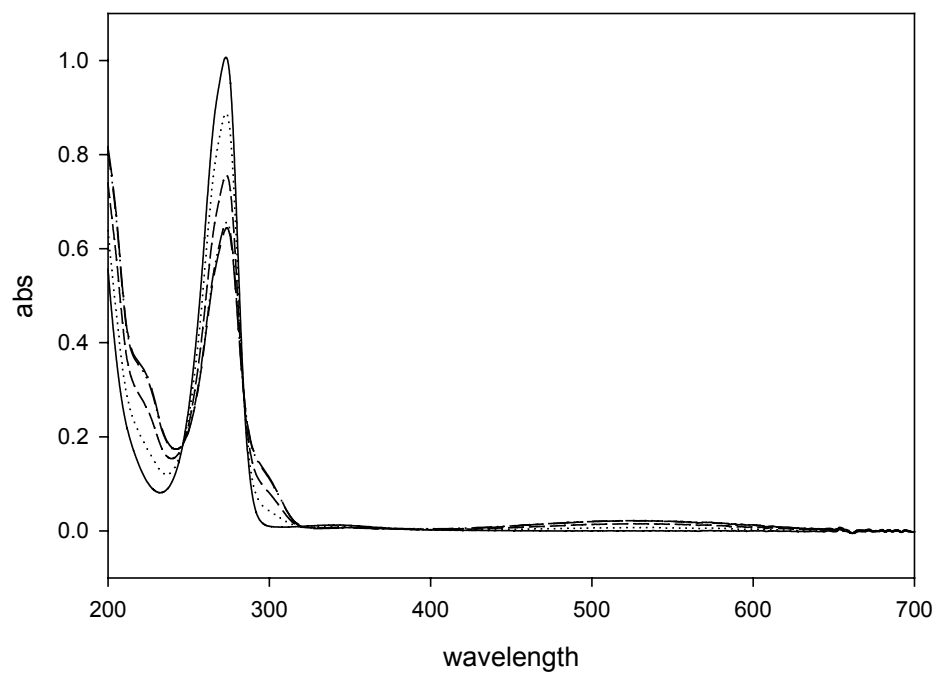
Figure 11.   100 µM 2,5-Cl$_2$BQ in aqueous solution was irradiated at 334 nm with monochromatic light. The light intensity was 6.0×10^{-4} W/cm^2.

Figure 12. 100 µM 2,6-Cl$_2$BQ in aqueous solution was irradiated at 334 nm with monochromatic light. The light intensity was 6.0×10^{-4} W/cm^2.

Bibliography

Adams, G. E. and B. D. Michael. "Pulse radiolysis of benzoquinone and hydroquinone." *Trans.of the Farad. Soc.* **1967**, 63, 1171-1180.

Alegría, A. E.; Ferrer, A. and E. Sepúlveda. "Photochemistry of water-soluble quinones. Production of a water-derived spin adduct." *Photochem. Photobiol.* **1997**, 66, 436 – 442.

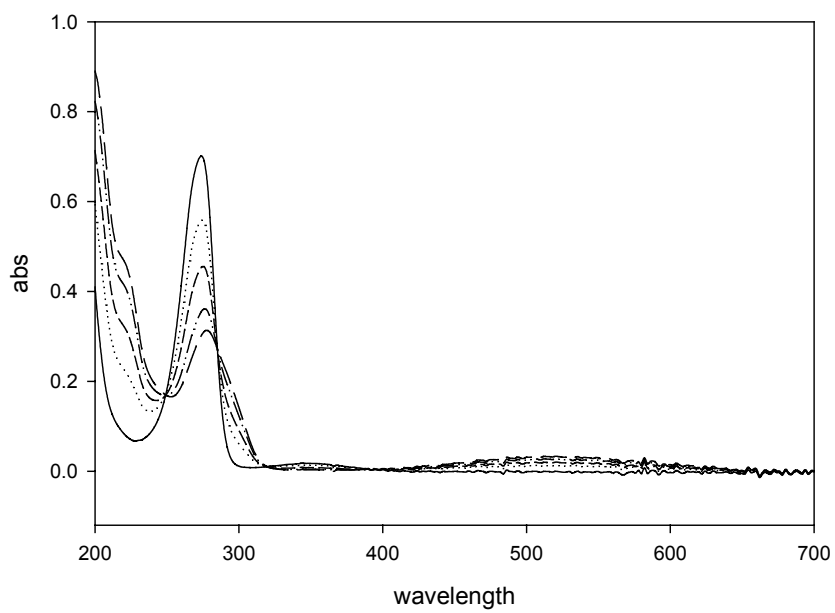Alegría, A. E.; Ferrer, A.; Santiago, G.; Sepúlveda, E. and W. Flores "Photochemistry of water-soluble quinones. Production of the hydroxyl radical, singlet oxygen and the superoxide ion." *J. Photochem. Photobiol. A: Chem.* **1999**, 127, 57 – 65.

Beck, S. M.and L. E. Brus. "Photooxidation of water by p-benzoquinone." *J. Am. Chem. Soc.* **1982**, 104, 1103 – 1104.

Beck, S. M.and L. E. Brus. "Transient Raman Scattering Study of the Initial Semiquinone Radical Kinetics following Photolysis of Aqueous Benzoquinone and Hydroquinone." *J. Am. Chem. Soc.* **1982**, 104, 4789 – 4792.

Bishop, C.A. and L. K. J. Tong. "Equilibra of Substituted Semiquinone at High pH." *J. Am. Chem. Soc.* **1965**, 87, 501 – 505.

Blough, N.V. Photochemistry in sea-surface microlayer. <u>The Sea Surface and Global Change</u>. P. S. Liss and R. A. Duce. Cambridge, Cambridge University Press. **1997**, 13: 383-424.

Blough, N. V. and R. Del Vecchio "Chromophoric dissolved organic matter (CDOM) in the coastal environmental." In: Hansell, D., Carlson, C. (Eds.), *Biogeochemistry of Marine Dissolved Organic Matter*. Academic Press, San Diego, pp. 509 – 546.

Blough, N. V. and S. A. Green "Spectroscopic characterization and remote sensing of nonliving organic matter" *Environ. Sci. Res. Rep.* **1995**, 16: 23 – 45.

Blough, N.V. and R. G. Zepp. Reactive Oxygen Species in Natural Waters. Active Oxygen in Chemistry. C. S. Foote, J. S. Valentine, A. Greenberg and J. F. Liebman. New York, Chapman and Hall: **1995**, 280-333.

Bruce, J. M. Photochemistry of quinones. The chemistry of quinonoid compounds. Patai, S. Ed. New York, John Wiley and Sons. 1. **1974**, 465 – 538.

Buettner, G. R. Spin Trapping: ESR parameters of spin adducts. *Free Radic. Biol. Med.* 3, **1987**, 259 –303.

Buxton, G.V. and C.L. Greenstock. "Critical review of rate constants for reactions of hydrated electrons, hydrogen atoms, and hydroxyl radicals (OH/O-) in aqueous solution." *J. Phys. Chem. Ref. Data.* **1988**, 17(2): 513-886.

Clark, K. P. and H. I. Stonehill, "Photochemistry and Radiation Chemistry of 9, 10-Anthraquinone-2-sodium-sulphonate in Aqueous Solution, Part. 1." *J. Chem. Soc. Faraday Trans.* I. **1972**, 68, 577 – 590.

Clark, K. P. and H. I. Stonehill, "Photochemistry and radiation chemistry of 9, 10-anthraquinone-2-sodium-sulphonate in aqueous solution, Part. 2." *J. Chem. Soc. Faraday Trans.* I. **1972**, 68, 1676 – 1686.

Eberson, L. and O. Persson "Generation of acyloxyl spin adducts from N-tert-butyl-α-phenyl-nitrone (PBN) and 4,5-dihydro-5,5-dimethylpyrrole 1-oxide (DMPO) via nonconventional mechanisms." *J. Chem. Soc. Perkin Trans.* 2 **1997**, 1689 – 1696.

EI'tsov, A. V.; Studzinskii, O.P. and V. M. Grebenkina "Photoinitiation of the Reactions of Quinones." *Russ. Chem. Rev.* **1977**, 46 (2) 93 –114.

Flyunt, R.; Makogon, O.; Schuchmann, M. N.; Asmus, K.D. and C. von Sonntag. " OH-Radical-induced oxidation of methanesulfinic acid. The reactions of methansulfonyl radial in the absence and presence of dioxygen." *J. Chem. Soc. Perkin Trans.* 2, **2001**, 787 – 789.

Goldstone, J. V.; Pullin M. J.; Bertilsson, S. and B. M. Voelker. "Reactions of Hydoxyl Radical with Humic Substances: Bleaching, Mineralization, and Production of Bioavailable carbon Substrates." *Environ. Sci. Techol.* **2002**, 36, 364-372.

Görner, H. "Photoprocesses of p-Benzoquinones in Aqueous Solution." *J. Phys.Chem. A*. **2003**, 107, 11587 – 11595.

Green, S.A.; Simpson, D. J.; Zhou, G.; Ho, P.S. and Blough, N.V. "Intramolecular quenching of excited singlet states by stable nitoxyl radicals." *J. Am. Chem. Soc.* **1990**, 112 (20), 7337 –7346.

Grigor'ev, A. E.; Makarov, I. E.; Pikaev, A. K. "Formation of Cl_2^- in the bulk solution during the radiolysis of concentrated aqueous solution of chlorides." *High Energy Chem.* 1987, 21, 99 –102.

Harriman, H. and A. Mills. "Photochemistry of anthraquinone-2,6-disodium sulphnate in aqueous solution." *Photochem. Photobiol.* **1981**, 33, 619 – 625.

Hubig, S. M. and J. K. Kochi. "Electron-Transfer Mechanisms with Photoactivated Quinones. The Encounter Complex versus the Rehm-Weller Paradigm." *J. Am. Chem. Soc.* **1999**, 121, 1688 –1694.

Ilan, Y.; Czapski, G. and D. Meisel. "The one-electron transfer redox potentials of free radicals." *Biochim. Biophys. Acta.* **1976**, 430, 209-224.

Jankowski, J. J.; kieber, D. J. and K. Mopper. "Nitrate and Nitrite Ultroviolet Actinometers." *Photchem & photobiology,* **1999**, 70(3), 319-328.

Janzen, E. G. and D. L. Haire. "Two decades of spin trapping." In *Advances in Free Radical Chemistry*, Vol. 1 (D. D. Tanner, Ed.), pp. 253 –295. JAI press, Greenwich, CT, **1990**.

Jayson, G. G.; Parsons, B. J.; Swallow, A. J. "Some simple, highly reactive, inorganic chlorine derivatives in aqueous solution. Their formation using pulses of radiation and their role in the mechanism of the Fricks dosimeter." *J. Chem. Soc., Faraday Trans.* 1, **1973**, 69, 1597-1607.

Johnson,C.G.; Caron, S. and N. V. Blough. "Combined Liquid Chromatography/Mass Spectrometry of the Radical Adducts of a Fluresceamine-Derivatized Nitroxide." *Anal.Chem.* **1996**, 68, 867-872.

Joschek, H,-I. and S. I. Miller "Photooxidation of Phenol, Cresole, and Dihydroxybenzenes." *J. Amer. Chem. Soc.* **1966**, 88, 3273 – 3281.

Kavarnos, G.J. Ed. <u>Fundamentals of Photoinduced Electron Transfer</u>, Wiley, New York. **1993**.

Kieber, D.J. and N.V. Blough. "Determination of carbon-centered radicals in aqueous solution by liquid chromatography with fluorescence detection." *Anal. Chem.* **1990**, 62 (21), 2275-2283.

Kieber, D.J.; Johnson, C.G. and N.V. Blough. "Mass spectrometric identification of the radical adducts of a flurescamine-derivatized nitroxide." *Free Radical Res. Comm.* **1992**, 16 (1): 35-39.

Kurien, K.C. and P. A. Robins, "Photolysis of Aqueous Solutions of p-Benzoquinones: a Spectrophotometric Investigation." *J. Chem. Soc. (B),* **1970**, 855 – 859.

Leighton, P.A. and G.S. Forbes. "The photochemical decomposition of benzoquinone in water and in alcohol." *J. Amer. Chem. Soc.,* **1929**, 51, 3549.

Lewis, F. D.; Liu, X.; Liu, J.; Miller, S. E.; Hayes, T. R. and M. R. Wasielewski. "Direct measurement of hole transport dynamics in DNA." *Nature* **2000**, 406, 51 – 53.

Li, B.; Gutierrez, P. L. and N. V. Blough. "Trace Determination of Hydroxyl Radical in Biological Systems." *Anal. Chem.* **1997**, 69, 4295-4302.

Li, B.; Gutierrez, P.L. and N. V. Blough. Trace Determination of Hydroxyl Radical using Fluorescence Detection." *Method in enzymology,* **1998**, vol, 300, 202.

Loeff, I.; Treinin, A. and H. Linschitz. "Photochemistry of 9,10- anthraquinone-2-sodium-sulphonate in solution. Part 1." *J. Phys. Chem.* **1983**, 87, 2536 – 2544. (Loeff et al 1983 A)

Loeff, I.; Treinin, A. and H. Linschitz. "Photochemistry of 9,10- anthraquinone-2-sodium-sulphonate in solution. Part 2." *J. Phys. Chem.* **1983**, 88, 4931 − 4937. (Loeff et al 1983 B)

Loeff, I.; Treinin, A. and H. Linschitz, "Interactions of NO2 and SO3 with Organic Triplets. Charge Transfer versus Rnergy Transfer: The Role of Reorganization Energy in Triplet-Anion Interactions and Spectroscopic Methods for Its Evaluation." *J. Phys. Chem.* **1992**, 96, 5264 −5272.

Loeff, I.; Rabani, J.; Treinin, A. and H. Linschitz, "Charge Transfer and Reactivity of nπ* and ππ* Organic Triplets, Including Anthraquinonesulfonates, in Interactions with Inorganic Anions: A Comparative Study Based on Classical Marcus Theory." *J. Am. Chem. Soc.* **1993**, 115, 8933 − 8942.

Logager, T and K. Sehested. "Formation and decay of peroxynitrous acid: A pulse radiolysis study." *J. Phy. Chem.* **1993**, 97, 6664 − 6669.

Lovley, D. R.; Coates, J. D.; Blunt-Harris, E. L.; Phillips, E. J. and J. C. Woodward "Humic substances as electron acceptors for microbial respiration." *Nature* **1996**, **382**, 445 − 448.

Mack, J. and J. R. Bolton. "Photochemistry of nitrite and nitrate in aqueous solution: a review." *J. Photochem. Photobio. A: Chemistry* 128 (**1999**) 1 −13.

Mark, G.; Korth, H. G.; Schuchmann, H. P. and C. von Sonntag. "The photochemistry of aqueous nitrate ion revisited." *J. Photochem. Photobio. A: Chemistry* 101 (**1996**) 89 −103.

Marquardt, R.; Grandjean, S. and R. Bonneau. "Competition between intersystem crossing and intramolecular electron transfer in substituted benzoquinones." *J. Photochem. Photobiolo. A. Chem.*, **1992**, 69, 143 − 153.

Meisel, D. and R. W. Fessenden. "Electron exchange and electron transfer of semiquinones in aqueous solutions." *J. Am. Chem. Soc*. **1976**, 98, 7505-7510.

176

Mopper. K. and X. Zhou. "Hydroxyl radical photoproduction in the sea and its potential impact on marine processes." *Science*, **1990**, 250, 661-664.

Morton, R. A. Ed. Biochemistry of Quinones. Academic Press, London and New York, **1965**.

Neta, P. "Redox Properties of free Radicals." *J. Chem. Edu.* **1981**, 58, 110 –113.

Ononye, A. I.; MacIntosh, A. R. and J. R. Bolton. "Mechanism of the photochemistry of p-benzoquinone in aqueous solutions. 1. Spin trapping and flash photolysis electron paramagnetic resonance studies." *J. Phys. Chem.* **1986**, 90, 6266 – 6270.

Ononye, A. I. and J. R. Bolton. "Mechanism of the photochemistry of p-benzoquinone in aqueous solutions. 2. Optical flash photolysis studies." *J. Phys. Chem.* **1986**, 90, 6270 – 6274.

Oturan, M. A. and J. Pinson. "Hydroxylation by Electrochemically Generated OH Radicals. Mono- and Polyhydroxylation of Benzoic Acid: Products and Isomers' Distribution." *J. Phys. Chem*. **1995**, 99, 13948 – 13954.

Patai, S. Ed. The Chemistry of Quinoid Compounds, **1974,** Wiley, London.

Patel, K. B. and R.L. Willson. "Semiquinone free radicals and oxygen." *J. Chem. Soc., Farad. Trans. I.* **1973**, 69, 814 – 825.

Pochon, A.; Vaughan, P. P.; Gan, D.; Vath, P.; Blough, N. V. and Daniel E. Falvey. "Photochemical Oxidation of Water by 2-Methyl-1,4-benzoquinone: Evidence against the Formation of Free Hydroxyl Radical." *J. Phys. Chem. A.* **2002**, *106*, 2889-2894.

Pou, S.; Hassett, D. J.; Britigan, B. E.; Cohen, M. S.; and G. M. Rosen "Problems associated with spin trapping oxygen-centered free radicals in biological systems." *Anal. Biochem.* **1989**, 177, 1 – 6.

Poupe, F. "A polarographic investigation of photochemical changes in quinones." *Coll. Czech. Chem. Comm.,* **1947**, 12, 225.

Raymond, K.S.; Grafton, A. K. and R.A. Wheeler. "Calculated one-electron reduction potentials and solvation structures for selected p-benzoquinones in water." *J. Phys. Chem. B*. **1997**, 101, 623-631.

Ronfard –Haret, J. – C.; Bensasson, R. V. and E. Amouyal. J. Chem. Soc. Faraday Trans. 1 **1980**, 76, 2432 – 2436.

Rossetti, R.; Beck, S. M. and L. E. Brus. "Resonance Raman Investigation of the π* Antibonding Distribution in Excited Triplet Aqueous p-Benzoquinone." J. Phy. Chem. **1983**, 87, 3058 – 3061.

Schuchmann, M. N.; Bothe, E.; von Sonntag J. and C. von Sonntag. "Reaction of OH radicals with benzoquinone in aqueous solutions. A pulse radiolysis study." *J. Chem. Soc., Perkin Trans*. 2, **1998**, 791 – 796.

Schwarz, H.A. "Free radicals generated by radiolysis of aqueous solutions." *J. Chem. Edu*. **1981**, 58(2), 101-105.

Scott, D.T.; Mcknight, D.M.; Blunt-Harris, E. L.; Kolesar, S. E. and D. R. Lovley "Quinone Moieties Act as Electron Acceptors in the Reduction of Humic Substances by Humics-Reducing Microorganisms." *Environ. Sci. Technol.* **1998**, 32, 2984 – 2989.

Senesi, N. and C. Steelink "Application of ESR Spectroscopy to the study of humic substances." In *Humic Substances II In Search of Structure*; Hayes, M.; MacCarthy, P.; Malcolm, R.; Swift, R. Eds.; John Wiley and Sons: New York, **1989**; PP 373 – 408.

Shirai, M; Awatsuji, T. and M. Tanaka. "Photolysis of p-Benzoquinone in Aqueous Solution. Possibility of a polar Mechanism in the Primary Process." *Bull. Chem. Soc. Japan*, **1975**, 48(4), 1329-1330.

Southworth, B. A. and B. M. Voelker. " Hydroxyl Radical Production via the Photo-Fenton Reaction in the Presence of Fulvic Acid." *Environ Sci. Technol*, **2003**, 37, 1130-1136.

Stevens, G. C.; Clarke, R. M. and E. J. Hart "Radiolysis of aqueous methane solutions." *J. Phy. Chem.* **1972**, 76, 3863 – 3867.

Stevenson, J. <u>Humus Chemistry: Genesis, Composition, Reactions</u>; John Wiley and Sons: New York, **1994**.

Thorn, K. A.; Arterburn, J. B. and M. A. Mikita "15N and 13C NMR investigation of hydroxylamine – derivatized humic substances." *Environ Sci. Technol*, **1992**, 26, 107 –116.

Turro, N. J. <u>Modern Molecular Photochemistry</u>. **1991**, University Science Books, Sausalito, California.

Vaughan, P.P and N. V. Blough. "Photochemical Formation of Hydroxyl Radical by Constituents of Natural Waters." *Environ Sci. Technol*, **1998**, 32, 2947-2953.

Vaughan, P. P. "Photochemical Formation of Hydroxyl Radical by Constituents of Natural Waters and by Quinones." PhD dissertation, **1999**.

Veltwisch, D. and K.-D. Asmus "The reaction of methyl and phenyl radicals with p-benzoquinone in aqueous solution. *J. Chem. Soc. Perkin Trans.* 2 **1982**, 1147-1152.

Veltwisch, D.; Janata, E. and K.-D. Asmus "Primary processes in the reaction of OH-radical with sulphoxides." J. Chem. Soc. Perkin Trans. 2, **1980**, 146 –153.

von Sonntag, J.; Mvula, E.; Hildenbrand, K.; von Sonntag, C. "Photohydroxylation of 1,4-Benzoquinone in Aqueous Solution Revisited." *Chem.Eur. J.* **2004**, 10, 440 – 451.

Weil, J. A.; Bolton, J. R. and J. E. Wertz "Electron Paramagnetic Resonance: Elementary Theory and Practical Applications." New York: Wiley, **1994**.

White, E. M. Vaughan, P. P. and R. G. Zepp "Role of the photo-Fenton reaction in the production of hydroxyl radicals and photobleaching of colored dissolved organic matter in a coastal river of the southeastern United States." *Aquat. Sci.* **2003**, 65, 402-414.